POLYAMINES AND ALVEOLAR MACROPHAGE APOPTOSIS DURING *PNEUMOCYSTIS* PNEUMONIA

Chung-Ping Liao

Submitted to the faculty of the University Graduate School
in partial fulfillment of the requirements
for the degree
Doctor of Philosophy
in the Department of Pathology and Laboratory Medicine,
Indiana University

August 2009

Accepted by the Faculty of Indiana University, in partial
fulfillment of the requirements for the degree of Doctor of Philosophy.

_____

Chao-Hung Lee, Ph.D., Chair

_____

Mark E. Lasbury, Ph.D.

Doctoral Committee

_____

Thomas E. Davis, M.D., Ph.D.

July 10, 2009

_____

Richard L. Gregory, Ph.D.

DEDICATION

To my parents, wife, and lovely kids, I cannot thank you enough for your unconditional support throughout my research. Your precious gifts have helped me to achieve this milestone in my life.

ACKNOWLEDGEMENTS

First, I would like to appreciate my mentor Dr. Chao-Hung Lee. Thank you for providing this valuable research opportunity to work with you and for all you have taught me in science and in writing. I would also like to thank Dr. Mark Lasbury, your assistance and many great ideas have substantially helped this study. To Dr. Richard Gregory and Dr. Thomas Davis, I acknowledge your beneficial comments to this research. To Dr. Diane Leland, thank you very much for guiding me through the entire graduate study.

I would also like to thank all of my colleagues who have helped this study. To Dr. Chen Zhang, thank you for sharing your pathology expertise and all of your assistance in life. To Pam Durant, thank you for your help with animal surgeries, technical support and proofreading manuscripts. To Dr. Shao-Hung Wang, thank you for your valuable advice on my experiments. I also thank Dennis Tschang, Dr. Shoujin Shao, and Jinghong Wang for their technical assistance.

ABSTRACT

Chung-Ping Liao

POLYAMINES AND ALVEOLAR MACROPHAGE APOPTOSIS

DURING *PNEUMOCYSTIS* PNEUMONIA

Pneumocystis pneumonia (PCP) is the leading opportunistic disease in immunocompromised individuals, particularly in AIDS patients. The alveolar macrophage (AM) is the major type of cell responsible for the clearance of *Pneumocystis* organisms; however, they undergo a high rate of apoptosis during PCP due to increased intracellular polyamine levels. This study examined the mechanism of this polyamine mediated apoptosis and investigated an alternative therapy for PCP by targeting this mechanism. The elevated polyamine levels were determined to be caused by increased polyamine synthesis and uptake. Increased polyamine uptake was found to be AM-specific, and recruited inflammatory cells including monocytes, B cells, and CD8+ T cells were found to be a potential source of polyamines. The expression of the antizyme inhibitor (AZI), which regulates both polyamine synthesis and uptake, was found to be greatly up-regulated in AMs during PCP. AZI overexpression was confirmed to be the cause of increased polyamine synthesis and uptake and apoptosis of AMs during PCP by gene knockdown assays. *Pneumocystis* organisms and zymosan were found to induce AZI overexpression in AMs, suggesting that the β-glucan of the *Pneumocystis* cell wall is responsible for this AZI up-regulation. In addition, levels of mRNA, protein, and activity of polyamine oxidase (PAO) were also found to be increased in AMs during PCP, and its substrates N1-acetylspermidine and N1-acetylspermine were found to induce its up-regulation. These results indicate that the H_2O_2 generated during PAO-mediated

polyamine catabolism caused AMs to undergo apoptosis. Since increased polyamine uptake was demonstrated to be a pathogenic mechanism of PCP in this study, the potential therapeutic activity of five putative polyamine transport inhibitors against PCP was tested. Results showed that compound 44-Ant-44 significantly decreased pulmonary inflammation, organism burden, and macrophage apoptosis, and prolonged the survival of rats with PCP. In summary, this study demonstrated that *Pneumocystis* organisms induce AZI overexpression, leading to increased polyamine synthesis, uptake, and apoptosis rate in AMs and that targeting polyamine transport is a viable therapeutic approach against PCP.

Chao-Hung Lee, Ph.D., Chair

TABLE OF CONTENTS

LIST OF FIGURES

INTRODUCTION

Chapter 1: *Pneumocystis* Organisms and *Pneumocystis* Pneumonia

Discovery

Pneumocystis pneumonia (PCP) is caused by infection of the organism *Pneumocystis*. *Pneumocystis* was first discovered by Carlos Chagas in 1909 in a Trypanosome infection guinea pig model (30). Chagas mis-identified it as a novel morphologic form of *Trypanosoma cruzi*. In 1910, Antonio Carinii found *Pneumocystis* in rat lungs and also considered it a new type of trypanosome (27). In 1912, Delanoe and Delanoe at the Pasteur Institute recognized that the organism identified by both Chagas and Carinii was a new species (43) and named the organism *Pneumocystis carinii* to highlight its lung tropism, cyst-like morphology and to give credit to Carinii.

Taxonomy

Since the time of discovery until the late 1980s, *Pneumocystis* was widely thought to be a protozoan on the basis of its morphological features and susceptibility to antimicrobial drugs. Histological examination reveals that *Pneumocystis* exhibits trophic and cyst forms which are almost exclusively present in protozoa, such as *Entamoeba* and *Giardia*. In addition, *Pneumocystis* is susceptible to anti-protozoan drugs, such as pentamidine, trimethoprim, and sulfamethoxazole, but resistant to anti-fungal agents including imidazole and amphotericin B. In 1988, DNA sequencing analysis of the

Pneumocystis small subunit ribosomal RNA gene (16S-like rRNA) demonstrated that *Pneumocystis carinii* and *Saccharomyces cerevisiae* are more closely related to than *Pneumocystis carinii* and *Trypanosoma brucei* (49). Therefore, *Pneumocystis* was reclassified as an ascomycetous fungus. *Pneumocystis* species are now taxonomically placed in the phylum *Ascomycota*, class *Pneumocystidomycetes*, order *Pneumocystidales*, and family *Pneumocystidaceae*.

Nomenclature

Pneumocystis carinii was the only species in the genus *Pneumocystis*. In 1993, *Pneumocystis* isolates from different hosts were proven to exhibit stringent host specificity. For example, *Pneumocystis* organisms from humans do not infects rats and vice versa (62). To recognize this host specificity, a trinominal naming system was then implemented. For example, *Pneumocystis* infecting human and mice were named *Pneumocystis carinii* f.sp. *hominis* and *Pneumocystis carinii* f.sp. *murina*, respectively. This naming system has proven to be very cumbersome to use; therefore, the *Pneumocystis* naming system was further changed. Human *Pneumocystis* is now called *Pneumocystis jirovecii* (197) in honor of the Czech parasitologist Otto Jirovec who first described *Pneumocystis* in humans (195). Mouse *Pneumocystis* was renamed as *Pneumocystis murina*. *Pneumocystis carinii* now refers to the rat-derived *Pneumocystis* organisms.

Life cycle

Pneumocystis has two major morphological forms in its life cycle: trophic and cyst forms. During *Pneumocystis* infection in the lung, the trophic forms predominate over the cyst forms by 10 fold. DNA analysis reveals that most trophic forms are haploid (241). The sizes of *Pneumocystis* trophic and mature cyst forms range from 1 to 4 μm and 8 to 10 μm in diameter, respectively. *Pneumocystis* can be reproduced through both sexual and asexual cycles. Sexual reproduction begins from the conjugation of two trophic organisms to form a precyst. There are three precyst stages, including early, intermediate, and late stages with 2, 4, and 8 intracystic nuclei, respectively. Mature *Pneumocystis* cysts may rupture to release the trophs which can undergo vegetative growth or conjugate to reform a new cyst. In addition to sexual reproduction, *Pneumocystis* also undergoes asexual reproduction by binary fission like most prokaryotic cells, although *Pneumocystis* is a eukaryotic organism. The events of *Pneumocystis* life cycles described above are solely established from microscopic observations of organisms from infected animals, since *Pneumocystis* organisms cannot be cultured continuously.

Cell Wall

Pneumocystis cell wall is composed of complex carbohydrates and proteins. The main component is β-1,3-glucan. It is a linear glucose polymer with 1,3-linked carbohydrate core and side chains of 1,6- and 1,4-linked glucose residues (47). The main function of *Pneumocystis* β-glucan is to provide rigid structural stability for the organisms. Since β-glucan is not present in mammalian cells, *Pneumocystis* β-glucan is a

pathogen associated molecular pattern (PAMP) for host cells, particulary inflammatory cells (222). Chitin is another structural carbohydrate on the *Pneumocystis* cell wall, but its levels are much lower than those of β-glucan.

In addition to carbohydrate meshes, *Pneumocystis* cell wall also contains abundant surface proteins. These proteins are highly glycosylated with hundreds of mannose residues. The major surface glycoprotein (MSG) (also known as glycoprotein A) is the most abundant mannoprotein on *Pneumocystis*. MSG has been shown to be a target of the mannose receptor of AMs (158).

Pneumocystis MSG genes are located on all *Pneumocystis* chromosomes, determined by pulsed field gel electrophoresis hybridization (198). All MSG genes were found to reside at the ends of chromosomes (199), and they are organized as a cluster of 2 - 4 genes in each chromosomal ends. Therefore, there are a total of approximately 100 MSG genes in the *Pneumocystis* genome. Since they are located at the ends of chromosomes, the MSG genes are associated with telomeric sequences (216) and are sensitive to exonuclease digestion (199).

Although there are about 100 MSG genes in the *Pneumocystis* genome, only a single form of MSG is expressed at a time (198). This serves as a pathogenic mechanism allowing *Pneumocystis* to evade host immune defenses. The single MSG gene expression is controlled by a 429 bp conserved DNA sequence located upstream of an expressing MSG gene termed upstream conserved sequence (UCS) (226) and a common 23 bp sequence called the conserved recombination junction element (CRJE) (226). An active MSG gene requires an UCS to be present at its 5' end in order to be transcribed. Since there is only one UCS in the *Pneumocystis* genome, only one MSG gene can be expressed at one time and most MSG genes remain silent. The change in MSG expression

is mediated by a reciprocal recombination. A silent MSG gene must be translocated downstream of UCS through a homologous recombination at the CRJE site present in all MSG genes to become active. This recombination only happens one way in that a MSG gene translocates to the UCS locus, but not vise versa.

Culture

Animals with *Pneumocystis* infection have long been the only reliable source to obtain a large number of *Pneumocystis* organisms for study. Continuous depletion of CD4+ cells by steroid or anti-CD4 antibody is a necessary requirement to render the animals susceptible to *Pneumocystis* infection. *Pneumocystis* organisms are often introduced by transtracheal instillation one week after initiation of immunosuppression, and PCP usually develops after four weeks of infection. Untreated animals usually die within 6 - 10 weeks due to servere respiratory failure. The organism burden is increased over time and reaches the maxium levels right before the host's death.

Although long-term culture is not possible, short-term cultures with feeder cells have been achieved using African green monkey kidney epithelial cells (170), human embryonic lung fibroblasts (108), and rat alveolar epithelial cells (2). In general, these cell-based *Pneumocystis* culture systems increase the number of organisms approximately 6 - 10 fold within the first 3 - 4 days. The organism number stays constant for 7 - 14 days and then decreases rapidly. The speed of *Pneumocystis* growth is decreased over passage, and the growth is stopped after 2 - 3 passages (7).

In 1999, Merali et al. reported an axenic *Pneumocystis* culture system (136). This method grows *Pneumocystis* organisms in Minimal Essential Medium (MEM) with

Earle's salts supplemented with horse serum, S-adenosylmethionine sulfate, aminobenzoic acid, putrescine, ferric pyrophosphate, cysteine, glutamine, N-acetyl-D-glucosamine, penicillin, and streptomycin. *Pneumocystis* organisms are cultured at 31°C in normal atmosphere on 0.4 μM pore size, collagen-coated Transwell inserts. Medium is changed twice daily. The doubling time of *Pneumocystis* organisms in this culture system ranges from 35 to 65 hours. The culture can be maintained up to 96 days with a total of 12 subcultures. The cultured organisms can be frozen for reculture. Unfortunately, this method has remained an isolated success as no other laboratory has been able to reproduce it (25).

S-adenosylmethionine (SAM), a key molecule in methylations and polyamine biosynthesis, is a controversial molecule in this *Pneumocystis* culture system. Merali et al. described that SAM is a critical supplement in *Pneumocystis* culture since *Pneumocystis* lacks the SAM synthetase (SAMS) activity and must rely on exogenous SAM supply (137). However, a contradictory study demonstrated the presence of a functional *Pneumocystis* SAMS gene by cloning the gene and expressing the recombinant protein (100). The role of SAM in supporting *Pneumocystis* growth is also controversial, as an independent group found that addition of SAM to *Pneumocystis* culture dramatically decreased the viability rather than increased the growth of *Pneumocystis* organisms (42).

Strains

There are multiple strains in each *Pneumocystis* species. Owing to the lack of a reliable *in vitro* culture system, typing of different *Pneumocystis* strains is practically impossible to perform by conventional microbial typing methods such as biochemical

reactions or serotypings since these methods require large numbers of organisms. Current *Pneumocystis* typing is achieved by determining the number and size of chromosomes or certain nucleotide variations. Each rat *Pneumocystis* strain has 13 - 15 linear chromosomes ranging from 300 to 700 kb (196). The nucleotide sequences of human *Pneumocystis* strains differ in the internal transcribed spacer (ITS) regions of nuclear rRNA (121) or mitochondrial large subunit rRNA (227) genes. At least 60 different types of *P. jirovecii* have been identified (109).

Clinical Features

Pneumocystis infection only occurs in immunocompromised individuals, particularly when the number of CD4+ T cells is lower than 200 per millimeter of blood (168). Patients with AIDS have the highest risk of developing PCP since CD4+ T cells are the target cells for HIV, and the number of CD4+ T cells is further decreased as HIV infection progresses. Patients with cancers, transplants, rheumatoid arthritis, and systemic lupus erythematosus are also susceptible to PCP (190) due to the administration of immunosuppressive drugs resulting in a decrease in CD4+ T cell number. Such drugs may include steroids, dactinomycin (a chemotherapeutic agent for cancers), and adalimumab (an anti-TNF-α drug).

Pneumocystis has a high lung tropism; therefore nearly all *Pneumocystis* infections occur in the lung. However, some clinical reports have described cases of *Pneumocystis* infections in the thyroid (246), spleen (53), liver (53), and eyes (177). These extrapulmonary *Pneumocystis* infections usually occur on individuals with critically low immunity, such as patients at the very late stage of AIDS or cancer.

Clinical features of PCP include subtle onset of progressive dyspnea, nonproductive cough, and low-grade fever. Pneumothorax may develop when acute dyspnea and pleuritic chest pain appear. Lung auscultation is usually normal, but tachypnea and tachycardia normally occur (210). Chest radiography typically reveals bilateral perihilar interstitial infiltrates that become increasingly homogeneous and diffuse as PCP progresses (44). The mortality rate of PCP ranges from 10 to 20% in patient with AIDS and 30 to 60% in patients without AIDS (210).

Pulmonary Pathology

The histopathology of PCP is characterized by eosinophilic foamy exudates and *Pneumocystis* organisms in the alveoli (95). The protein-rich alveolar exudates contain abundant fibronectin, vitronectin, and surfactant proteins A and D (157, 255). *Pneumocystis* organisms are usually embedded in these exudates and attached on the alveolar epithelium in groups without cell invasion. Common pathological changes of PCP include a moderate level of interstitial fibrosis and alveolar septal thickening (124). Severe PCP is characterized by extensive pulmonary inflammation due to recruitment of inflammatory cells, particularly neutrophils and CD8+ T cells. Overwhelmed lung inflammation is more likely a direct cause of respiratory failure and death than the levels of *Pneumocystis* burden (118).

Epidemiology

In the early 1980s, PCP rapidily became the leading opportunistic disease in HIV-infected patients (130), and approximately 75% of HIV-infected patients developed PCP during that time period (70). The incidence of PCP was significantly decreased due to PCP prophlaxis that began in 1989 (52) and highly active antiretrovial therapy (HAART) which started in 1992 (85). However, there is still a 0.4% PCP incidence rate among all population (144).

Animal experiments showed that *Pneumocystis* organisms can be transmitted through the airborne route (80). However, it is still unknown whether *Pneumocystis* can survive outside mammalian hosts and remain infective, although there are evidences showing the presence of *Pneumocystis* DNA in natural environment (29). Clinical studies suggest that person-to-person spread is an important transmission route and individuals with normal immunity could be asymptomatic reservoirs of *Pneumocystis* (123, 140, 220). Serology studies of anti-*Pneumocystis* antibody in healthy infants reveal that the seropositive rate is 16% at the age of two months and gradually increases to 85% at the age of 20 months (219), showing that *Pneumocystis* infection is common in humans since early life and is usually asymptomatic unless immunocompromised.

Althogh *Pneumocystis* infection is usually asymptomatic in immunocompetent people, it may cause a low level of pulmonary inflammation in associated with other pulmonary diseases. Recenly studies have suggested the association between *Pneumocystis* residence and other lung diseases, such as chronic obstructive pulmonary disease (COPD), cystic fibrosis (CF), and lung cancers. Patients with these lung diseases appear to have a higher rate of *Pneumocystis* colonization (145).

Diagnosis

Pneumocystis organisms must be determined to be present in clinical samples to diagnose PCP. Bronchoalveolar lavage fluid (BALF) from bronchoscopy is the preferred diagnostic sample with a sensitivity ranging from 89 to 98% (78). Induced sputum or oropharyngeal wash are alternative samples; however the sensitivity and specificity of diagnosis using these samples are significantly lower than using BALF (236).

Pneumocystis organisms in BALF, induced sputum, oropharyngeal wash, or lung tissue can be visualized with several staining methods. *Pneumocystis* trophs can be detected by using Papanicolaou, Gram-Weigert, or modified Wright Giemsa stains, and cysts can be visualized with Grocott-Gomori methenamine silver (GMS), cresyl echt violet, toluidine blue O, or calcofluor white fungal stains. GMS and Gram-Weigert are preferred staining methods for *Pneumocystis* diagnosis in clinical laboratories. In addition to conventional stains, immunofluorescent assay (IFA) using monoclonal antibodies against *Pneumocystis* organisms, is also commonly used. IFA is capable of detecting both trophic and cyst forms of *Pneumocystis*. While IFA is more sensitive than conventional stains, it is more expensive, time consuming, and less specific (174).

Serum testing is being developed to help in the diagnosis of PCP. The levels of serum β-glucan, lactate dehydrogenase, KL-6 (a mucinous high-molecular weight glycoprotein, expressed on type II pneumonocytes), and C-reactive protein are changed during PCP. However, none of them is a specific marker for PCP. Among, these, β-glucan seems to be the most reliable serum marker for PCP (207).

Advances in molecular biology continue to add new tools for diagnosis of PCP. Molecular diagnosis of PCP is performed by determining the presence of *Pneumocystis*

DNA in clinical specimens. The latest technology uses real-time PCR to detect *Pneumocystis* DHFR, DHPS, HSP70, or CDC2 genes (99).

Prophylaxis and Therapy

The first-line drug for treatment of PCP is a combination of trimethoprim and sulfamethoxazole (TMP/SMZ). TMP and SMZ inhibits *Pneumocystis* dihydrofolate reductase (DHFR) and dihydropteroate synthase (DHPS), respectively (77). TMP/SMZ is also commonly used for PCP prophylaxis. However, TMP/SMZ may cause adverse effects, such as rash, fever, and leucopenia (191). Approximately 60% of HIV(+) patients have TMP-SMZ hypersensitivity reactions (191). Furthermore, TMP/SMZ-resistant *Pneumocystis* strains have emerged (138). Molecular analyses revealed that a point mutation at amino acid 55 or 57 of the DHPS gene renders *Pneumocystis* organisms resistant to SMZ (77, 218). Mutations at amino acid codons 23, 60, 111, 171 of the *Pneumocystis* DHPS gene have also been reported, but their associations with SMZ resistance remains uncertain (180). DHPS mutants that are resistant to SMZ are also resistant to dapsone which is a sulfone drug and also targets DHPS (77).

A number of studies have examined the effects of DHPS mutations on clinical outcomes such as treatment failure and death rate; however, the results from these studies are inconsistent. Some studies found that DHPS mutations are associated with increased treatment failure with TMP/SMZ or TMP/Dapsone (87) and increased death rates and that the death rate in patients infected with DHPS mutants is 3 fold higher than those infected with the wild-type (73). However, another study reported contradictory results

with no statistical differences between patients infected with wild-type and DHPS mutants in both treatment failure and death rate (150).

The combination of clindamycin and primaquine is an alternative choice for PCP therapy. Clindamycin interferes with protein synthesis of the organism by preferentially binding to its ribosome (94). The target of primaquine remains unknown. Clindamycin/primaquine combination shows comparable efficacy to TMP/SMZ on mild to moderate PCP (211) and is an alternative regimen for patients who fail or cannot tolerate TMP/SMZ therapy. Another alternative drug for PCP is atovaquone, an analog of ubiquinone (coenzyme Q). It inhibits mitochondrial respiration in *Pneumocystis* by specifically binding to the ubiquinol oxidation site of the cytochrome bc_1 complex. Atovaquone resistant *Pneumocystis* strains have also emerged, and mutations in the *Pneumocystis* cytochrome *b* gene have been shown to confer this resistance (89). Pentamidine is another PCP drug targeting mitochondrial function (253). Although it is commonly used to treat PCP, it is highly toxic and has significant adverse effects such as hypoglycemia and nephrotoxicity (155).

Chapter 2: Macrophage Receptors That Recognize *Pneumocystis* Organisms

Pattern Recognition Receptor and Pathogen Associated Molecular Pattern

The major surface antigens on *Pneumocystis* cell wall are mannoproteins and β-glucan, which are recognized as foreign antigens by immune cells. Since these molecules are shared among microorganisms, particularly fungi, these antigens are also named a pathogen associated molecular pattern (PAMP). Cell receptors recognizing a PAMP are termed pattern recognition receptors (PRRs). All *Pneumocystis* receptors that have been identified belong to PRRs. These receptors include mannose receptor (MR), Toll-like receptors (TLRs), dectin-1, and scavenger receptor (SR). The downstream signaling mediated by these receptors usually leads to activation of the transcription factor NF-κB which activates immune responses, such as phagocytosis and cytokine production.

Mannose Receptor (MR)

MR is a sugar binding protein and is classified as a C-type lectin. MR is primarily expressed on the surface of macrophages and dendritic cells. The extracellular region of MR contains an N-terminal cysteine-rich (CR) domain, a fibronectin type II (FNII) domain, and eight tandemly arranged C-type lectin-like carbohydrate recognition domains (CTLDs). The CR domain has sugar binding activity and binds to sulfated sugars terminating in SO_4-3-Gal or SO_4-3/4-GalNAc (209). The FNII domain binds to collagen I, II, III, and IV (149). The CTLDs bind to sugars terminating in mannose,

fructose, or N-acetyl glucosamine (209). The function of the MR cytoplasmic region is relatively unknown and no signaling motif has been identified. MR is also classified as a PRR and has been shown to bind *P. carinii* (51), *Candida albicans* (129), and *Mycobacterium tuberculosis* (84). The most well characterized ligand for MR on *Pneumocystis* organisms is the mannose-rich major surface glycoprotein (MSG) (158). One study found that soluble mannan (a ligand of MR) can reduce *Pneumocystis* β-glucan-induced TNF-α release (222), suggesting *Pneumocystis* β-glucan can also interact with MR, probably through the cooperation with TLR2 (205).

The binding activity (97) and expression levels (96) of MR are found to be decreased in AMs during HIV infection, indicating that MR function is impaired during PCP. *Pneumocystis* is also shown to evade immune surveillance by stimulating AMs to increase the production of soluble MR thus decreasing phagocytosis (55).

MR is involved in *Pneumocystis*-mediated AM activation, including NF-κB translocation, oxidant production, and cytokine release. *Pneumocystis* organisms stimulate AM NF-κB p50 and p65 nuclear translocation in a time- and MOI-dependent manner, and this activation is diminished by competitive inhibition of MR with mannan or siRNA (250). Likewise, *Pneumocystis* stimulated H_2O_2 burst is decreased by 63% when AMs are treated with the MR competitive inhibitor mannosyl-BSA (98). The release of chemotactic cytokine IL-8 from AMs after *Pneumocystis* stimulation is decreased after MR siRNA knockdown, and this *Pneumocystis*-mediated IL-8 production is dependent on coexpression of TLR2 (205).

Although previous results have suggested the importance of the MR in host defense during *Pneumocystis* infection, a study using MR-knockout (MR-KO) mice found that deficiency of MR does not cause increased *Pneumocystis* susceptibility (203); this is

similar to the results found in MR-KO mice infected with *Candida albicans* (110). These results reveal that the role of the MR in host defense is dispensable and may be compensated by other signaling pathways.

Toll-Like Receptor (TLR)

In 1996, a protein termed Toll was found with antifungal activity in *Drosophila* (112). A human homologue of *Drosophila* Toll protein (now known as TLR4) was later found to mediate immune signaling and responses, including NF-κB activation, the production of inflammatory cytokines IL-1, IL-6, IL-8, and the expression of the costimulatory molecule B7.1 for naive T cell activation (132). A number of human membrane proteins sharing structural similarity to Toll have been identified and classified into a family named Toll-like receptor (TLR) (181). The progress in genome projects has led to the identification of at least 10 TLRs in vertebrates (59).

TLRs are type I transmembrane glycoproteins (59). The extracellular domains of TLRs have leucine-rich repeat (LRR) modules and are responsible for the binding of PAMPs. For example, lipoproteins or lipopeptides are recognized by TLR2; lipopolysaccharide, a major component on Gram(-) bacteria, is recognized by TLR4; viral double-stranded RNA is recognized by TLR3; bacterial flagellin is recognized by TLR5; single-stranded RNA virus is recognized by TLR7 or TLR8; and microbial unmethylated CpG DNA is recognized by TLR9 (212). The cytoplasmic domain of TLRs shares high similarity to that of IL-1 receptor family and is referred to as Toll/IL-1 receptor (TIR) domain which is composed of 150 amino acid residues. Binding of ligands induces the

dimerization of TLRs and then recruits adaptor proteins to the TIR domains to initiate intracellular signaling.

The adaptor proteins for TLR signaling include MyD88, MAL, TRIF, TRAM, and SARM. These TLR adaptors also contain TIR domains (156), and the TIR-TIR interactions between receptor-receptor, receptor-adaptor, and adaptor-adaptor play a critical role in TLR signalings (163). MyD88 is the most commonly used TLR adaptor by TLRs. MyD88 plays a critical role in the immune responses against microbial infections as MyD88-deficient mice produce less cytokines and are more susceptible to microbial infections (156).

MyD88 is composed of two major domains: a TIR domain at the C-terminal end and a death domain at the N-terminal end. The death domain of MyD88 interacts with the death domain of IL-1 receptor-associated kinase 4 (IRAK4) which recruits and phosphorylates IRAK1, leading to its activation (201). Activated IRAK1 in turn activates tumour necrosis factor receptor-associated factor 6 (TRAF6). Activated TRAF6 forms a complex with transforming growth factor-β-activated kinase-1 (TAK1) via the associations with the proteins TAK1 binding protein 1 (TAB1) and TAB2. Formation of TRAF6/TAK1 complex leads to the activation of TAK-1 (154). TAK-1 then phosphorylates the inhibitory κB (IκB) kinase complex, leading to NF-κB activation. Transcription factor NF-κB plays a central role in immune responses by controlling the production of a variety of cytokines and chemokines.

TLR2 recognizes the most numerous ligands among all TLRs. Parts of this diversity are due to its ability to form heterodimers with many other receptors, such as TLR1, TLR6, MR (205), and Dectin-1 (58). Ligands that are recognized by TLR2 include

zymosan on fungi, peptidoglycan and lipoteichoic acid on Gram(+) bacteria, lipoarabinomannan on *Mycobacteria*, and lipoproteins on most organisms (59).

TLR2 mediates immune reactions in response to *Pneumocystis* infection. An *in vivo* study shows that TLR2 is involved in *Pneumocystis*-induced production of the proinflammatory cytokine tumor necrosis factor α (TNF-α) and chemokine macrophage inflammatory protein 2 (MIP-2) (247). *In vivo* study of *Pneumocystis*-infection in TLR2-deficient mice shows less inflammation, TNF-α production, and NF-κB activation than in wild-type mice with PCP. These results confirm the inflammatory role of TLR2 in PCP. However, TLR2-deficient mice show increased severity in symptoms and organism burden and decreased levels of inducible nitric oxide synthase, NADPH oxidase p47phox, amd nitric oxide in the lungs, indicating the important roles of TLR2 in host defense against *Pneumocystis* (234). In addition, TLR2 has also been shown to mediate the release of IL-8 from macrophages when coexpressed with MR during *Pneumocystis* challenge (205).

TLR4 has also been shown to mediate host responses during PCP. TLR4-deficient mice showed exacerbated pulmonary damage compared to wild type mice with PCP. TLR4-deficiency results in increases in the levels of TNF-α and IL-6, but decreases in those of IL-10, IL-12, and MIP-2 in response to *Pneumocystis* infection. TLR4 seems to play no role in controlling organism burden since the numbers of *Pneumocystis* organisms were nearly the same in TLR4-deficient and wild type mice with PCP (46).

Dectin-1

Dectin-1 (also known as C-type lectin domain family 7 member A, CLEC7A) is a 33 kDa type II transmembrane protein. The N-terminal domain of Dectin-1 is located in the cytoplasmic region. It has a motif similar to the short immunoreceptor tyrosinase-based activation motif (ITAM) and works as a signaling tail. The C-terminal end of dectin-1 is exposed to extracellular space for antigen binding by the carbohydrate recognition domain (CRD). Unlike most C-type lectin members, Dectin-1 binds to ligands in a calcium-independent manner. Dectin-1 is predominantly expressed on the surface of myeloid cells, including macrophages, monocytes, and neutrophils. Dendritic cells and some T cells also express Dectin-1, but at lower levels. AMs have been shown to express the highest levels of surface dectin-1 (208).

In 2001, Dectin-1 was first reported as a receptor for β-1,3-glucan (24), a major component on fungal and some bacterial cell walls. Engagement of Dectin-1 by β-glucan induces a variety of cellular responses including endocytosis, phagocytosis, reactive oxygen species (ROS) production, and the synthesis of cytokines and chemokines, such as TNF, IL-6, IL-10, IL-23, and CXCL2 (23). Dectin-1 directs intracellular signaling alone or in cooperation with other membrane receptors, such as TLR4 (58) or DC-SIGN (217). This feature is cell-type dependent. For example, Dectin-1 signaling alone induces TNF production in dendritic cells (111), but this response requires TLR2 costimulation in macrophages (45). Evidence has suggested that this difference is, at least partly, caused by cytokines, such as GM-CSF and IFN-γ (64).

Dectin-1 is the first non-TLR PRR found to be capable of inducing its own intracellular signaling (23). The most well studied Dectin-1 signaling is through the

canonical NF-κB activation pathway. Dectin-1 signaling begins from the phosphorylation of its cytoplasmic ITAM-like motif by spleen tyrosine kinase (Syk) (215). Biding of Sky to the target tyrosine residues on Dectin-1 is mediated by the two SH2 domains on Syk. Although both Syk SH2 domains are involved in Dectin-1 phosphorylation, only the proximal tyrosine is required for signaling (56). Caspase recruitment domain 9 (CARD9) is an essential downstream adaptor protein for Syk-coupled receptors. CARD9 assembles with B-cell CLL/lymphoma 10 (BCL10), mucosa associated lymphoid tissue lymphoma translocation 1 (MALT1), and TNF receptor associated factor 6 (TRAF6). TRAF6 interacts with UBE2N/UBC13 and UBE2V1/UEV1A which ubiquitinate IκB kinase (IKK). Activated IKK phosphorylates IκB and results in IκB degradation. NF-κB released from IκB then translocates to the nucleus and activates gene expressions. Dectin-1 signaling through Syk-independent pathway (67), non-canonical NF-κB activation pathway (67), CARD9-independent pathway (64), or Nuclear factor of activated T-cells (NFAT) activation (65) has also been reported. Dectin-1 appears to be the first PRR found to activate non-canonical NF-κB pathway (67).

Dectin-1 also induces intracellular signals via collobration with other membrane receptors. In macrophages, TLR2 plays a necessary role in Dectin-1 signaling in the induction of TNF production (45). This was the first demonstration of interactions between a TLR and a non-TLR receptor (23).

In 2003, Dectin-1 was first shown to be a phagocytosis receptor for *Pneumocystis* (193), mediating organism killing and the production of MIP-2 in response to *Pneumocystis* challenge *in vitro*. Another study found that anti-Dectin-1 antibody blocked the production of TNF-α in dendritic cells challenged with purified *Pneumocystis*

β-glucan (28). These results demonstrated the role of Dectin-1 in organism recognization and clearance and cytokine productions in response to *Pneumocystis* infection.

Taken the property of β-glucan/Dectin-1 binding, a Dectin-1-Fc fusion protein was generated and used as an immunomodulating molecule against *Pneumocystis*. *Pneumocystis* organisms pre-opsonized with Dectin-1-Fc are more readily phagocytosed and killed by AMs (178). SCID mice transduced by a Dectin-1-Fc-containing adenovirus have decreased *Pneumocystis* burden and pulmonary damages (178).

Dectin-1-deficient mice were used to clarify the role of Dectin-1 in defense against *Pneumocystis* infection. These mice had increased *Pneumocystis* burden and decreased ROS levels. However, the levels of cytokine TNF-α and IL-12 were not significantly changed, suggesting the existence of a compensatory mechanism for Dectin-1 in the induction of cytokine productions during PCP. (184).

Scavenger Receptor (SR)

SR is a membrane protein principally expressed on myeloid cells such as macrophages and dendritic cells. SRs can bind to a variety of ligands such oxidized or acetylated low density lipoproteins, lipopolysaccharide on Gram(-) bacteria, lipoteichoic acid on Gram(+) bacteria, intracellular bacteria, and CpG-rich DNA (165). SRs mediate the internalization and cleaning (scavenging) of these exogenous molecules or organisms. There are three categories of SRs: classes A, B, and C, differentiated by their structural characteristics. Class SR A (SR-A) is mainly expressed on macrophages and plays a major role in inflammatory responses. SR-A knockout mice are more susceptible to bacterial infections (200), showing the role of SR in the deference against microbial

infections. However, SR-A knockout mice infected with *Pneumocystis* showed decreased organism burden compared to wild-type mice; this is likely due to elevated numbers of activated CD4+ cells in SR-A deficient micc. SR-A deficiency also caused increased productions of TNF-α, IL-12, and IL-18 during PCP, but AM phagocytosis was not affected. In contrast to its role in bacterial infections, SR-A seems to be a negative inflammatory regulator during PCP (76).

NF-κB

Nuclear factor kappa-light-chain-enhancer of activated B cells (NF-κB) is a complex of proteins acting as a transcription factor in nearly all cell types. NF-κB is involved in cellular responses to various stimuli such as cytokines, microorganism, viruses, free radicals, UV, and hypoxia.

There are five NF-κB family members in mammalian cells: NF-κB1, NF-κB2, RelA (p65), RelB, and c-Rel. All members in the NF-κB family share a Rel homology domain (RHD) in their N-terminus. The Rel subfamily of NF-κB, including RelA, RelB, and c-Rel, has a transactivation domain (TAD) in their C-termini. In contrast, the C-termini of immature NF-κB1 (p105) and NF-κB2 (p100) are composed of ankyrin repeats which have transrepression activity. p105 and p100 are processed by the ubiquitin/proteasome pathway which selectively degrads the C-terminal ankyrin repeats to form mature NF-κB1 (p50) and NF-κB2 (p52) subunit. A mature NF-κB complex is a homodimer or a heterodimers of these proteins. Since the NF-κB subunits p50 and p52 do not contain TAD in their C-terminals, the homodimer or heterodimer of p50 and p52 do not activate

gene expression. Therefore, p50 and p52 must dimerize with other TAD-containing subunit to form a functional NF-κB transcription complex.

NF-κB is one type of the "rapid-acting" transcription factors which are mostly present in an inactive state in cells; when receiving stimulus, NF-κB can be quickly activated without new NF-κB protein synthesis. Without stimulation, NF-κB is normally retained in the cytoplasmic area by inhibitors of NF-κB (IκBs). Activation of NF-κB is typically initiated from the phosphorylation of IκB by IKK, which consequently results in IκB degradation. Released NF-κB is then translocated to the nucleus to bind to promoters to activate gene expression.

NF-κB is commonly activated in response to infections and is a key transcription factor in immune responses. Nearly all *Pneumocystis* receptor signaling pathways converge at NF-κB, including TLR (247), Dectin-1 (50), MR (250), and SR (113).

NFAT

Nuclear factor of activated T-cells (NFAT) is a family of transcription factors involved in immune response and is commonly expressed in immune cells. There are five members in the NFAT family: NFATc1, NFATc2, NFATc3, NFATc4, and NFAT5 (40). The activation of NFATc1, NFATc2, NFATc3, and NFATc4 is regulated by the calcium sensor protein calmodulin. Calmodulin activates a serine/threonine phosphatase termed calcineurin. Activated calcineurin rapidly dephosphorylates the serine rich region and serine-proline repeats in the amino termini of NFAT proteins, resulting in a conformational change. Dephosphorylated NFAT exposes a nuclear localization signal which leads NFAT to the nucleus to active gene expression by acting as a transcription

factor. The nuclear translocation of NFAT is inhibited by kinases present in cytoplasm and nucleus. NFAT alone has weak DNA binding ability; therefore, cooperation with other nuclear resident transcription factors is required for effective binding to DNA by NFAT (125). NFAT has recently reported to be activated by *Candida albicans* or zymosan through Dectin-1 signaling, suggesting that NFAT may be a transcription factor involved in immune responses during PCP.

Chapter 3: Host Responses during PCP

The host immune response during PCP involves complex interactions among inflammatory cells, including lymphocytes (CD4+ T cells, CD8+ T cells, and B cells), neutrophils, and AMs. These interactions are communicated by complex cytokine and chemokine networks, particularly IFN-γ and TNF-α.

CD4+ T Lymphocytes

CD4+ T cells play a crucial role in host defense against PCP, as patients with CD4+ cells lower than 200 per microliter of the peripheral blood have a higher risk of PCP. CD4+ T cells can be classified into three categories by their functions: effector T cells secrete cytokines to activate or recruit other immune cells; memory T cells retain the same antigen affinity as originally activated T cell for a rapid response during reinfections; regulatory T cells are responsible for negative regulation of immune responses. CD4+ cells mainly secret IFN-γ and IL-2 to activate macrophage and promote the proliferation of CD8+ cells. Insufficient IFN-γ levels have been shown to be a consequence of low CD4+ cell number and contribute to the immunosuppressive status to allow *Pneumocystis* infection (92).

CD8+ T Lymphocytes

CD8+ T cells are substantially infiltrated into the lung in the severe stage of PCP. The major type of cytokine secreted by CD8+ T cells during PCP is IFN-γ which

activates other immune cells such as AMs. The role of CD8+ cell in the disease progress of PCP is controversial. CD8+ cells have been shown to play a role in host defense against this infection, as depletion of both CD8+ and CD4+ cells in animals results in a more severe PCP than those with depletion of only CD4+ cells (15). An increase in the number of CD8+ cells can lead to PCP recovery (92). These results demonstrate the protective role of CD8+ cells in the host defense against PCP (194). However, CD8 cells have also been shown to be responsible for the pulmonary damage during PCP, as *Pneumocystis*-infected SCID mice reconstituted with wild-type CD8 T cells showed more severe lung injury than those that were not immune reconstituted (133). This type of damage has been shown to be dependent on MHC class I (133). This CD8+ cells mediated pulmonary injury has been proposed to be the direct cause of impaired gas exchange and respiratory failure in PCP, since respiratory impairment and death seem to be more closely related to the extent of pulmonary inflammation than to the *Pneumocystis* burden (118).

B Lymphocytes

B cells are involved in humoral immunity. The presence of B cell is very important in host defense against PCP since B cell-deficient mice are naturally susceptible to *Pneumocystis* infection (122). This susceptibility is due to the requirement of B cells in the generation of effector and memory CD4+ T cells, which are the key cell types against PCP as described above.

Neutrophils

Neutrophils are largely recruited into the lungs in an advanced stage of PCP. The main function of neutrophils is to perform non-specific phagocytosis and release microorganism-killing materials such as proteases and oxidants. The recruitment of neutrophils is mediated by a potent neutrophil chemoattractant IL-8, whose levels in BALF were reported to be a good predictor of severe respiratory compromise and death in patients with PCP (20). Neutrophils were thought to be responsible for the pulmonary injury during PCP due to its potent protease and oxidative activity. However, a recent study using neutrophil-depleted mice model found that pulmonary damage caused by PCP is independent of neutrophils, but is highly associated with CD8+ T cells (204).

Alveolar Macrophages (AMs)

AM is differentiated from its precursor cell monocyte in the blood. When an infection occurs in the lung, monocytes are recruited from the blood by chemokines, such as monocyte chemoattractant protein-1 (MCP-1). There are several types of macropahges in the lung, including alveolar, interstitial, intravascular and airway macrophages. AMs are the most predominant population. The maturation of AMs is mainly regulated by the granulocyte macrophage colony-stimulating factor (GM-CSF).

AMs produce TNF-α and MIP2 during PCP. Production of these cytokines are induced by *Pneumocystis* β-glucan (68, 107) with the assistance of glucan binding proteins vitronectin and fibronectin (221). Membrane receptor TLR2, but not TLR4, and transcription factor NF-κB are involved in the production of these cytokines (247).

AM is the major cell type responsible for the clearance of *Pneumocystis* organisms (117). Phagocytosis is initiated when *Pneumocystis* organisms bind to membrane receptors on AMs. The organisms are then internalized into AMs to form a phagosome which can fuse with lysosome to become a phagolysosome. The organisms are killed by free radicals and degraded by various proteolytic enzymes in phagolysosome. As described above, some AM receptors have been found to bind *Pneumocystis*; however, not all of them are involved in phagocytosis. MR (51) and Dectin-1 (193) have the ability to mediate AM phagocytosis of *Pneumocystis* organisms, whereas TLR2 (248), TLR4 (46), and SR (76) are not known to trigger phagocytosis.

Although being an important organism clearance process, AM phagocytic activity is decreased during PCP. The downregulation of MR (96) and transcription factor GATA-2 (106) have been shown to cause defects in AM phagocytosis.

In addition to reduced phagocytosis, the number of AMs is decreased during PCP in both humans (54) and animals (101, 105) due to the increased rate of apoptosis (103) and decreased GM-CSF production (104), which may cause less maturation of macrophages from monocytes in the lung. Inhibition of AM apoptosis by treating with caspase-9 inhibitor significantly prolonges animal survival, increases AM number and phagocytic activity, and decreases organism burden in rodents with PCP, demonstrating that AM apoptosis correlates with the disease progress of PCP (103).

Alveolar Epithelial Cells

There are two types of alveolar epithelial cells (also know as pneumocytes). Type I alveolar epithelial cells (also called squamous alveolar cells) are the main cell type that

forms the structure of alveolar walls. Type II alveolar epithelial cells (also called great alveolar cells) secrete surfactant proteins to lower the surface tension in the lung, allowing the alveolar membrane to separate and increasing the capacity of gas exchange.

Pneumocystis infects type I alveolar epithelial cells. This infection is facilitated by some host matrix proteins such as fibronectin and vitronectin which allow tight adherence of *Pneumocystis* to type I alveolar epithelial cells (228). Fibronectin and vitronectin bind to both *Pneumocystis* and the integrin receptors on the alveolar epithelium to enhance organism and host cell interactions (119). Histopathology analysis showed that *Pneumocystis*-infected epithelial cells are vacuolated and eroded (19). An *in vitro* study showed that *Pneumocystis* dose not cause any disruptions in the metabolism, structure, and barrier function of epithelial cells and suggested that inflammatory cells are responsible for the damage of epithelial cells during *Pneumocystis* infection (16). Another study showed that *Pneumocystis* inhibits cyclin-dependent kinase (CDK) activity in lung epithelial cells; this may serve another mechanism causing epithelial cell damages (116).

Although not a major source of chemokines and cytokines, alveolar epithelial cells also produce TNF-α (50), MIP2 (50), IL-8 (18), IL-6 (172), and MCP-1 (18) in response to *Pneumocystis* infection. Activated NF-κB is involved in the production of TNF-α and MIP2 (50, 249), and JNK participates in the induction of MCP-1 production (233).

Interferon-γ (IFN-γ)

IFN-γ is a cytokine predominately secreted by CD4+ and CD8+ T cells, and its main target is macrophages. IFN-γ activates phagocytosis, cytokine productions, antigen presentation, and lysozyme activity in macrophages. Transfer of IFN-γ gene by

adenovirus-mediated gene delivery (92) or aerosolized recombinant IFN-γ protein (14) showed significantly improved organism clearance, demonstrating the essential role of IFN-γ against *Pneumocystis* infection.

Tumor Necrosis Factor α (TNF-α)

TNF-α is a cytokine mainly produced by activated AMs in *Pneumocystis*-infected lungs. It recruits other inflammatory cells, including neutrophils, lymphocytes, and monocytes in order to establish an optimal environment for organism clearance. TNF-α also induces the generation of other cytokines and chemokines, particularly IFN-γ from T cells and IL-8 from lung epithelial cells. TNF-α has been demonstrated to play a critical role in the immune response against *Pneumocystis* infection, as the clearance of *Pneumocystis* is significantly reduced when TNF-α is neutralized by antibodies (33) or inhibitors (93). Although playing an important role in the clearance of *Pneumocystis* organisms, TNF-α-mediated inflammatory response is considered a major cause of lung damages during PCP (175). Several substances have been found to induce TNF-α production during PCP, including *Pneumocystis* cell wall components β-glucan (75) and MSG (17) and IFN-γ (48).

Macrophage Inflammatory Protein 2 (MIP-2)

MIP-2 is a chemokine produced by AMs and lung epithelial cells. The main function of MIP-2 during PCP is to recruit neutrophils into the lungs. The production of MIP-2 can

be induced by isolated *Pneumocystis* β-glucan (68). *Pneumocystis* mediated MIP-2 production has been shown to be mediated by TLR2 (247) and TLR4 (46) signaling.

Surfactant Protein (SP)

SP is a type of protein secreted by alveolar epithelial cells and reduces the surface tension at the alveolar air spaces. SP also modulates immune responses in the defense of *Pneumocystis* infection. Different types of SPs are formed as foamy exudates in the alveoli in the lungs with PCP. The expression levels of SP-A and SP-D are increased, whereas those of SP-B and SP-C are decreased during PCP (6).

SP-A enhances the binding between *Pneumocystis* and AMs (239). MSG has been shown to be a ligand of SP-A (255). SP-A-deficient mice with PCP showed enhanced lung injury and delayed organism clearance due to attenuated cytokine and oxidative responses (5). SP-D mediates aggregation of *Pneumocystis* and impairs AM phagocytosis (245). SP-D-overexpressing mice with PCP showed markedly increased *Pneumocystis* burden (225). This surfactant mediated pathology seems to be a result of the inflammatory responses, rather than a direct effect from *Pneumocystis* organisms (240).

Chapter 4: Polyamines and Macrophage Apoptosis

Polyamines and Their Metabolism Enzymes

Polyamines are polycationic amines present in all cells and are involved in the regulation of many cellular functions, such as cell cycle progression (160), differentiation (223), oncogenesis (61), and apoptosis (187). The most common biological polyamines are putrescine, spermidine, and spermine (Fig. 1). Polyamine metabolism pathway is shown in Fig. 2. Ornithine decarboxylase (ODC) is the rate-limiting enzyme in polyamine biosyntheses. ODC decarboxylates ornithine to putrescine which is converted to spermidine by spermidine synthase (SRM). Spermidine is then converted to spermine by spermine synthase (SMS). Polyamine catabolism is activated in response to the excessive intracellular polyamine levels. This catabolism is mediated by spermidine/spermine N1-acetyltransferase (SSAT), polyamine oxidase (PAO), and spermine oxidase (SMO). SSAT acetylates spermidine to N1-acetylspermidine and spermine to N1-acetylspermine. N1-acetylspermine and N1-acetylspermidine are excreted from cells or converted back to spermidine and putrescine, respectively by PAO, while spermine can be back converted to spermidine by SMO. A mechanism which controls the level of ODC is degradation. ODC antizyme (OAZ) targets ODC to the 26s proteasome for degradation, whereas antizyme inhibitor (AZI) inhibits this degradation by binding to OAZ.

Intracellular polyamine homeostasis is critical for normal cellular functions and cell survival. Several polyamine regulatory mechanisms exist in cells in response to altered intracellular polyamine levels. When cellular polyamine levels are high, the mechanisms

of increased ODC degradation, polyamine catabolism, and polyamine export are activated. In contrast, mechanisms of increased ODC synthesis and polyamine import and decreased ODC degradation and polyamine catabolism are activated in response to insufficient polyamine levels.

Ornithine Decarboxylase (ODC)

ODC, the key enzyme for polyamine biosynthesis, is crucial for cell survival as homozygous ODC knockout mice are lethal (166). In mammalian cells, ODC is the only source for cells to acquire putrescine from *de novo* biosynthesis. However, ODC is abscent in some microorganisms and plants due to the existence of a similar enzyme arginine decarboxylase which can convert arginine to putrescine (91). A functional ODC protein is a homodimer with active site between the N-terminal domain of one subunit and the C-terminal domain of the other (3). Pyridoxal phosphate (PLP) is an essential cofactor for ODC activity. In mammalian cells, ODC tightly regulates intracellular polyamine levels to maintain polyamine homeostasis. ODC activity is regulated at the levels of transcription, translation, and protein degradation.

The promoter of the ODC gene contains many regulatory elements, including cAMP response element, CAAT and LSF motifs, AP-1 and AP-2 sites, GC-rich Sp1 binding sites, and TATA box (176, 254). The oncogene Myc is a well defined transcription factor which binds to ODC promoter and activates its expression (161). ODC promoter contains two E boxes with CACGTG sequences conforming to the canonical CAYGTG sequence to which Myc binds. ODC activity is also regulated by protein degradation. The degradation of mammalian ODC take places in the 26S proteasome with a very short turnover rate

($T_{1/2}$ = 10-20 min). This rapid turnover is determined by its C-terminal 37 residues (251), which is absent in the ODC of *Trypanosoma cruzi*. Therefore, *Trypanosoma cruzi* ODC is much more stable.

ODC Antizyme (OAZ)

ODC degradation is mediated by OAZ which non-covalently binds to the PLP binding site on ODC monomer to form a heterodimer. This complex is directed to the 26S proteosome for an ATP-dependent but ubiquitin-independent degradation, resulting in decreased ODC and polyamine levels (71). OAZ only enhances the interaction between ODC and proteasome; it does not increase the proteasome processing rate (252). At least three forms of mammalian OAZ have been identified; all of them inhibit ODC activity but with different tissue distribution and expression levels (127).

The levels of OAZ are regulated by polyamine levels (131, 162); suriprisingly, ODC is not involved in this regulaton (57). The expression of OAZ is translationally regulated by the levels of polyamines, particularily spermidine and spermine. OAZ transcript has two overlapping open reading frames. When polyamine levels are low, OAZ translation terminates at the stop codon located at 65 codons downstream of the translation initiation site, producing a nonfunctional OAZ protein. When polyamine levels are high, a translational frameshifting occurs and causes the paused ribosome to read through the first stop codon to produce a functional OAZ (131). OAZ is the only known mammalian protein whose translation is influenced by polyamines in this manner. Polyamine levels also regulate OAZ degradation as the process of an ubiquitin-dependent OAZ degradation in the 26S proteosome is inhibited by the addition of polyamines (162).

Antizyme Inhibitor (AZI)

AZI is a protein with high structural similarity to ODC, but AZI has no decarboxylase activity (147). It has higher OAZ binding activity than ODC; therefore, AZI releases ODC from the ODC/OAZ complex by competitive binding, leading to decreased ODC degradation and increased polyamine synthesis (147). AZI is capable of disrupting the binding of ODC to all OAZ isoforms that have been identified (128). AZI turns over very rapidly ($T_{1/2}$ < 30 min); the process of AZI degradation occurs in the 26S proteasome and is ubiquitin-dependent (21). AZI is tightly associated with cell growth; it is quickly synthesized when cells are stimulated to grow (153), and knockdown of AZI results in growth inhibition (35).

Spermidine/Spermine N1-Acetyltransferase (SSAT)

SSAT mediates polyamine catabolism in response to increased polyamine levels. SSAT acetylates spermidine and spermine to N1-spermidine and N1-spermine, respectively. These acetylated polyamines are normally excreted from cells to urine. SSAT activity is normally present at a very low level in resting cells and is induced in response to increased polyamine levels. Polyamines regulate SSAT activity at multiple levels, including transcription, mRNA stability, translation, and protein degradation.

Transcriptional activation of SSAT is mediated by the polyamine responsive element (PRE) with the sequence TATGACTAA in the SSAT promoter (237). PRE allows the binding of the transcription factor NF-E2-related factor 2 (Nrf-2) which partners with polyamine modulated factor 1 (PMF-1) to activate SSAT expression (235).

SSAT mRNA stability is regulated by alternative splicing. SSAT pre-mRNA has an extra 100 bp exon containing multiple premature termination codons between exon 3 and 4, leading to nonsense-mediated mRNA decay (81) or a truncated unfunctional SSAT (90). The function of this aberrant mRNA variant under normal physiological condition is uncertain, but it has been shown to accumulate in response to the simulation by X-rays (142), viruses (152), and hypoxia (90). Polyamine mediated SSAT translation is shown by the observation that a substantial proportion of SSAT mRNA is moved to the polyribosomes when polyamine is added (164).

The degradation of SSAT takes place in the 26S proteasome after polyubiquitination. SSAT normally has a rapid turnover rate with a half-life of 20 min. This rapid degradation is mediated by the C-termial MATEE motif (38). However, the half-life of SSAT can be as long as 12 hr in the presence of additional polyamines. This is due to the interuption of SSAT polyubiquitination mediated by polyamines (37).

Polyamine oxidase (PAO) and Spermine Oxidase (SMO)

In addition to SSAT, PAO and SMO also participate in polyamine catabolism. PAO converts N1-acetylspermine to spermidine and N1-acetylspermidine to putrescine. SMO catalyzes sperimine to become spermidine. PAO and SMO are very similar enzymes but with different substrate preference; in fact, PAO has some SMO activity and vise versa. At least four PAO isozymes have been cloned and characterized; these isozymes are encoded by the same gene which is transcribed to different mRNA splice variants (148).

PAO/SMO is present in cytosolic compartment and peroxisome in all vertebrate cells. PAO/SMO activity is dependent on the presence of the cofactor

flavin-adenin-dinucleotide (FAD). The catabolic reaction of PAO/SMO produces H_2O_2, aminodialdehyde, and ammonia. H_2O_2 is a potent oxidant with strong cytotoxicity, and activation of PAO has been shown to induce macrophages to undergo apoptosis (32).

N1,N4-bis(2,3-butadienyl)-1,4-butanediamine (MDL 72527) is an irreversible inhibitor of PAO. It inactivates PAO at a micromolar concentration in a time dependent manner *in vitro* and *in vivo*. MDL 72527 efficiently inhibits PAO and partially inhibit SMO without affecting other oxidases in cells and other enzymes in polyamine metabolism. A concentration of 200 μM of MDL-72527 has been shown to inhibit oxidation of PAO substrate N1-acetylspermine by 84% and SMO substrate spermine by about 50% (22).

Polyamine Transport

Mammalian polyamine transport system has long been a research subject of great interest but limited progress, despite having the knowledge of polyamine transporters in prokaryotic cells and yeast. In *E. coli*, the PotF/G/H/I ATP-binding cassette is responsible for putrescine uptake, PotE mediates both the uptake and excretion of putrescine, and the PotA/B/C/D ATP-binding cassette preferentially transports spermidine into the cell (82). In *S. cerevisiae*, uptake of polyamines have been shown to be mediated by a number of amino acid transporters, including DUR3 (213), SAM3 (213), AGP2 (4), and Gap1p (214). Yeast mutants deficient in any of these proteins showed decreased polyamine uptake.

The diamine exporter (DAX) is the only polyamine transporter found in mammalian cells so far (242); however, it only exports acetylated polyamines (242). There is no

evidence to suggest that it also works on other polyamines or acts as a polyamine importer.

In addition to the modulation of ODC degradation, OAZ and AZI were surprisingly found to regulate polyamine transport. OAZ decreases polyamine import (143), whereas AZI overexpression increases polyamine import (88). The mechanisms of OAZ- and AZI-mediated polyamine transport are still unknown.

α-difluoromethylornithine (DFMO)

The compound DFMO was first demonstrated to potently inhibit ODC activity and suppress tumor cell growth in the 1970s (126). DFMO inhibits ODC activity by binding to its active site at Lys 69 and Lys 360. DFMO is cleaved by ODC, but the digested products stay bound to the active site and irreversibly render the enzyme inactive (173). DFMO is the best known and most effective inhibitor of polyamine biosynthesis, and is the first anticancer drug targeting ODC. *In vitro* treatment of cells with DFMO has been shown to effectively deplete putrescine and spermidine, but spermine level is much less affected (60). DFMO inhibits cell growth by arresting cells at the G1 phase of the cell cycle (179). Although blocking polyamine synthesis has been shown to inhibit tumor growth *in vitro* and in animal models, clinical trials on anticancer activity of DFMO have not been successful. This may be due to compensatory increases in polyamine uptake (1), incomplete deprivation of spermine, or retroconversion of spermine to spermidine and putrescine (60). However, DFMO is still considered a potent agent to prevent cancer development as there have been some successes in animal and human clinical trials for tumor chemoprevention (139).

In 1980, DFMO therapy on rats with trypanosomiasis surprisingly showed significant success (10). Subsequently, successful human clinical trials made it an effective treatment regime for this disease (141) and a US FDA approved drug for sleeping sickness in 1990 (151). The selective toxicity of DFMO to *Trypanosoma* is due to the huge difference in the half-life of *Trypanosoma* (more than 10 hr) and mammalian ODC (10-20 min). In addition, *Trypanosoma* does not have a mechanism such as uptake of exogenous polyamines to compensate the loss of polyamines due to DFMO treatment (11). DFMO has also been shown to have activity against *Plasmodium falciparum* (146), *Giardia lamblia* (63), *Eimeria tenella* (69), and *Trichomonas vaginalis* (244). DFMO has been used to treat PCP in humans, but only 57% of PCP patients (40 of 70) responded to the treatment (192). This partial success suggests that polyamine metabolism is a viable target against PCP, but targeting polyamine synthesis alone may not be sufficient.

Polyamine and Apoptosis

An increasing body of evidence indicates that polyamines can induce apoptosis (also called the programmed cell death) (171, 187, 189). It is a type of cell death process involving cell shrinkage, chromatin condensation in the periphery of the nucleus, cell membrane blebbing, and cleavage of DNA into multiple fragments of approximately 180 bp. The apoptotic cells eventually break up into many membrane-bound apoptotic bodies, which are then phagocytosed by neighboring phagocytes. The activation of apoptosis can be classified into two different pathways: receptor- (extrinsic) and mitochondria-mediated (intrinsic). Receptor-mediated apoptosis is initiated by the binding of Fas-L or TNF-α to their receptors and subsequently activates caspase-8, caspase-10, and caspase-3 by a

series of protein cleavages. DNA damage or ceramide induce mitochondria-mediated apoptosis by releasing cytochrome c which binds to Afap-1 in cytosol and activates the caspase-9 cascade.

Polyamine-mediated apoptosis is induced through the intrinsic apoptosis pathway due to mitochondrial damage (32, 105). Activation of PAO-mediated polyamine catabolism in response to excessive polyamine levels has been shown to be responsible for this apoptosis, since inhibition of PAO activity by MDL-72527 prevents cells from apoptosis (32). H_2O_2 generated during polyamine catabolism is the key molecule responsible for polyamine mediated apoptois as depletion of H_2O_2 by catalase prevents cells from death (32). H_2O_2 has been shown to cause DNA damage in this apoptosis (243).

Polyamines Mediate AM Apoptosis during PCP

As described previousely, one of the mechanisms which cause AM number decrease during PCP is the increased apoptosis rate. This apoptosis has been proven to be caused by elevated polyamine levels (105). The levels of spermidine, N1-acetylspermidine, and N1-acetylspermine were greatly increased by by 7-, 5-, and 7-fold in AM and 13-, 10-, and 10-fold in BALF, respectively in rats during PCP. These polyamines have been confirmed to cause macrophage apoptosis in a depletion-and-add back experiment. BALF obtained from *Pneumocystis*-infected animals has the ability induce normal AMs to undergo apoptosis. This ability is diminished when the polyamines in the BALF are depleted and regained when polyamines are added back. This apoptosis has also been found to be associated with the activations of caspase-3 and caspase-9, release of

cytochrome c from mitochondria, and induction of ROS productions. These results suggest that polyamine-mediated AM apoptosis during PCP is through the intrinsic pathway and is very likely caused by increased polyamine catabolism (105).

OBJECTIVE

Rationale

Pneumocystis infection usually occurs in individuals with critically low CD4+ T cell numbers. Decreased CD4+ T cell-mediated immunity leads to impaired innate and adaptive immune responses to allow *Pneumocystis* infection.

AM is the major cell type responsible for innate responses in the lung. A significant body of evidence has demonstrated the crucial role of AMs in the defence of *Pneumocystis* infection (96, 103, 117). Unfortunately, the overall function of AM is defective during PCP. This is caused by at least two mechanisms: decreasd phagocytosis (96) and decreased AM number (102). Decreased AM phagocytic activity of *Pneumocystis* is at least partly caused by downregulation in the expressions of the transcription factor GATA-2 (206) and membrane receptor MR (96). Gene transfer of GATA-2 or MR enhances the ability of AMs to phagocytose *Pneumocystis* (51, 106, 249). Decreased AM number during PCP is caused by increased apoptosis (103). This apoptosis has been confirmed to be caused by greatly increased intracellular polyamine levels as described above (105).

The purpose of this study is to determine the mechanism of polyamine induced apoptosis in AMs during PCP and to search for compounds which can inhibit this apoptosis.

Hypothesis

This study is based on the hypothesis that the increase in intracellular polyamine levels in alveolar macrophages is due to both increased production and uptake of exogenous polyamines that are produced by *Pneumocystis* organisms and inflammatory cells.

Specific Aims

1. To investigate the mechanism that causes the increased polyamine levels in AMs during PCP.
2. To determine the substance which induces AM apoptosis during PCP.
3. To search for compounds which target polyamine-mediated apoptosis as a therapeutic approach against PCP.

MATERIALS AND METHODS

Rat PCP Model

Pneumocystis carinii infection in rats was established as described previously (12). Briefly, female Sprague-Dawley rats (Harlan, Indianapolis, IN) of 120-140 g were divided into three groups designated Normal, Dex, and Dex-Pc. Normal rats were immunocompetent and uninfected. Dex rats were treated continuously with 1.8 mg/liter dexamethasone in drinking water to reduce the number of CD4+ T lymphocytes, mimicking the immunosuppression status in AIDS patients. Dex-Pc rats were immunosuppressed with dexamethasone and transtracheally inoculated with 7.5×10^6 trophic form of *Pneumocystis* one week after initiation of immunosuppression. To prevent other opportunistic infections, 10,000 units of penicillin (Butler, Dublin, OH) were given intramuscularly (i.m.) each week to each Dex and Dex-Pc rat. This antibiotic had no adverse effects on the growth of *Pneumocystis* organisms in infected rats. It took approximately eight weeks for Dex-Pc rats to develop severe *Pneumocystis* pneumonia after inoculation. When Dex-Pc rats were agonal, they were sacrificed for experiments. Age-matched Normal rats were used as controls, while age-matched Dex rats were used to control for effect of the steroid treatment. Giemsa staining of lung impression smears was performed to determine the existence of *Pneumocystis* and other microorganisms. Dex-Pc lungs were excluded if they contained other microorganisms. All animal studies were approved and supervised by the Indiana University Animal Care and Use Committee under Institutional Animal Care and Use Committee (IACUC) guidelines.

Isolation of AMs

To perform bronchoalveolar lavage, rats were first anesthetized by i.m. injection of 0.1 ml ketamine mixture (80 mg/ml ketamine hydrochloride, 0.38 mg/ml atropine, and 1.76 mg/ml acepromazine) and then sacrificed. The thoracic cavity and trachea were exposed by dissection. BALF was obtained by instilling 5 ml of sterile phosphate buffered saline (PBS) into rat lungs via a 14-gauge angiocath (BD Biosciences, Bedford, MA) and then recovering the fluid. In experiments using BALF as supplement in cell cultures, Dulbecco's Modified Eagle's Medium (DMEM) instead of PBS was used for lavage. To isolate AMs, multiple lavages were performed until a total of 50 ml BALF was obtained. The cells in this 50-ml BALF were pelleted by centrifugation at 300 × *g* for 10 min and then resuspended in 5 ml of DMEM. AMs were isolated by adherence on plastic tissue culture dishes at 37°C with 5% CO_2 for 1 hr followed by washing with warm PBS three times to remove unattached cells. The purity of AMs was greater than 97% as determined by anti-RMA staining described previously (60, 63).

Real-Time RT-PCR

Total RNA was isolated using the TRIZOL reagent (Invitrogen, Carlsbad, CA) according to manufacturer's instructions. Reverse transcription was done using the iScript cDNA synthesis kit (Bio-Rad, Hercules, CA) with a thermal condition of 25°C for 2 min, 42°C for 30 min, and 85°C for 5 min. RNA (0.2 μg) from each sample was reverse transcribed to cDNA, and 2 μl of each cDNA product was used as the template for real-time PCR. Real-time PCR analyses for expression of rat ODC, SSAT, SRM, OAZ,

and AZI genes were performed using the Assays-on-Demand gene expression kits (Applied Biosystems, Foster City, CA); each of which contained two primers and a FAM-labeled probe. The mRNA levels of the ribosomal protein S8 (RPS8) gene was determined in an identical manner to serve as the internal control since its expression is not affected by immunosuppression or infection (247). The primers and probe used for the rat RPS8 real-time RT-PCR were described previously (247). Real-time PCR reactions were performed with TaqMan Universal PCR Master Mix (Applied Biosystems) on a Smartcycler (Cepheid, Sunnyvale, CA) using the following temperature cycling conditions: 50°C for 2 min, 95°C for 10 min, and 40 cycles of 92°C for 15 sec and 60°C for 1 min.

Western Blotting

AMs adhered in one well of a 6-well plate (approximately 2×10^6 cells) were scraped in 100 µl cold (4°C) cell lysis buffer (150 mM NaCl, 1.0% Triton X-100, 1% deoxycholate, 5 mM EDTA, 10 mM Tris, pH 7.2) containing 1% protease inhibitor cocktail (Sigma #P8340). Protein samples for Western blot analysis were prepared by adding NuPAGE LDS Sample Buffer (Invitrogen) and NuPAGE Sample Reducing Agent (Invitrogen) to the cell lysates to a final concentration of 1 × of each reagent and then boiling for 5 min. Proteins in each sample were electrophoresed in a 10% polyacrylamide gel and then transferred onto a polyvinylidene difluoride (PVDF) membrane using the NuPAGE System (Invitrogen). Membranes were blocked by soaking in a buffer containing 3% bovine serum albumin (BSA), 0.9% NaCl, 100 mM Tris-HCl (pH 7.6) at 25°C for 1 h and then reacted with the primary antibody anti-ODC (Lab Vision, Fremont,

CA), anti-SSAT (Novus Biologicals, Littleton, CO), anti-OAZ (87, 88), anti-AZI (147), anti-cleaved or activated caspase 3 (Cell Signaling, Danvers, MA), or anti-glyceraldehyde-3-phosphate dehydrogenase (GAPDH) (Research Diagnostics, Flanders, NJ) in blocking buffer for 2 hr. After washing with TBST (100 mM Tris-HCl, 0.9% NaCl, 0.1% Tween 20, pH 7.6) six times, the blots were reacted with a secondary antibody anti-mouse IgG or anti-rabbit IgG conjugated with horseradish peroxidase (HRP) for 1 hr at 25°C followed again by six washes with TBST. The reaction signals on the blots were developed by chemiluminescence with the ECL Plus reagent kit (Amersham Biosciences, Piscataway, NJ) and revealed by exposing the blots to an X-ray film. Densitometry analysis of results on X-ray films was performed by using the ImageJ software (http://rsb.info.nih.gov/ij/).

Fluorescence Labeling of Spermidine

Labeling of spermidine with fluorescein was performed as previously described (1) with modifications. Due to poor stability in solution, the fluorophore 5-(and-6)-carboxyl fluorescein succinimidyl ester (FAM) (Invitrogen) was freshly prepared in dimethylsulfoxide (DMSO) at a final concentration of 100 mM immediately before use. Spermidine was dissolved in 200 mM $NaHCO_3$ (pH 8.3) to a final concentration of 2 mM. The labeling reaction was performed by mixing 20 µl of FAM with 1 ml of spermidine in a 2-ml eppendorf tube. The tube was fastened on a vortexer and shaken for 1 hr at room temperature. The labeled products were separated by electrophoresis in a 1% agarose gel in 40 mM 2-(N-morpholino) ethanesulfonic acid monohydrate (MEM) buffer (pH 6.0) at 100 V for 1 hr and then visualized by UV transillumination. The FAM-labeled spermidine

(FAM-SPD) moved toward the anode and exhibited an extra band as compared to the sample containing FAM only. The portion of the gel containing FAM-SPD or FAM was excised, chopped to small cubes, and placed at -80°C until completely frozen. FAM-SPD was recovered by centrifugation at 10,000 × *g* for 2 h at 4°C. Additional centrifugations were performed if the gel was not completely thawed. The concentration of recovered FAM-SPD was determined by spectrophotometry at 494 nm using known concentrations of FAM as standards. The yield of FAM-SPD was ≥ 30 μM. Purified FAM-SPD was stored in small aliquots at -80°C until use.

Polyamine Uptake Assay

For *in vivo* polyamine uptake assay, each Normal, Dex, and Dex-Pc rat was anesthetized with 100 μl ketamine cocktail i.m. and then transtracheally instilled with 200 μl of 5 μM FAM-SPD or FAM. AMs were then isolated as described above 1 hr after the FAM-SPD or FAM instillation. The cells were mounted on slides in a mounting medium containing 4',6-diamidino-2-phenylindole (DAPI) to stain the nuclei. The macrophages which took up FAM-SPD were detected and enumerated by fluorescence microscopy. To examine polyamine uptake in *Pneumocystis*-infected lungs, frozen lung sections of FAM-SPD instilled rats were used. The lungs were first lavaged with 2 ml of PBS 3 times to remove free FAM-SPD or FAM, then instilled with 2 ml of the OCT compound (Sakura, Tokyo, Japan) via a 14-gauge angiocatheter. Each lung was then placed in a base mold filled with OCT and frozen at -80°C. The frozen lungs were sectioned with a cryostat microtome, and the sections were stored at -80°C until use. Frozen lung sections were air dried for 15 sec and fixed in acetone for 2 min before staining. After an

incubation in 5% BSA for 1 hr, the lung sections were reacted with Phycoerythrin (PE)-conjugated anti-CD68 antibody in 5% BSA in PBS for 1 hr to stain macrophages followed by three washes with PBS. The nuclei were counterstained with DAPI, and the stained slides were examined by fluorescence microscopy. The polyamine uptake assay was also performed in isolated AMs after AZI siRNA knockdown. This *ex vivo* polyamine uptake assay was performed by incubating AMs with 2.5 μM FAM-SPD in serum-free DMEM for 1 hr followed by fluorescence microscopy described above.

Immunohistochemical (IHC) Staining

Rat lungs were fixed in 4% paraformaldehyde overnight and then embedded in paraffin. Tissue sections on slides were processed for IHC staining by boiling the deparaffinized sections in the High pH Target Retrieval Solution (DAKO, Carpinteria, CA) for 20 min to expose hidden antigens. After three PBS washes, sections were immersed in 3% hydrogen peroxide for 5 min to deplete the endogenous peroxidase activity. Immunostaining was performed using the UltraVision LP System with HRP Polymer (Lab Vision, Fremont, CA). Briefly, sections were incubated in 1% BSA in PBS for 30 min followed by antibody staining at room temperature for 2 hr. Monoclonal antibodies against rat ODC (MP16-2), CD68 (KP1), CD79a (HM47/A9), and CD3ζ (6B10) were purchased from Lab Vision, while polyclonal anti-spermidine antibody was acquired from Abcam (Cambridge, MA). The anti-spermidine antibody also cross reacts with spermine according to the manufacturer. Primary Antibody Enhancer and HRP polymer were used according to manufacturer's instructions. Final chromogenic reaction was performed with the metal enhanced DAB substrate (Pierce, Rockford, IL).

Flow Cytometry

Isolation of single cells from *Pneumocystis*-infected rat lungs was performed as described previously (234). Each anesthetized rat was perfused with 30 ml cold Dulbecco's PBS (D-PBS) via right ventricle. A total of 5 ml Dispase II (neutral protease) (5 mg/ml) (Sigma) was transtracheally injected into the lungs, and the trachea was ligated with suture silk to avoid leakage. Lungs containing Dispase II were incubated in D-PBS for 45 min at 37°C. The lungs were then cut into small pieces and incubated in 5 ml D-PBS containing 1 mg/ml of collagenase/Dispase (Roche, Indianapolis, IN) and 0.08 mg/ml of DNase I Type II (Sigma) for 10 min at 37°C with shaking. Digested lungs were forced through an 18 g needle ten times and then mixed with 2 ml of fetal bovine serum. Single cells were isolated by filtering through a 70-μm nylon mesh and collected by centrifugation at 300 × *g* for 10 min. The pelleted cells were treated with 2 ml RBC lysis buffer (Sigma) to remove red blood cells, followed by washing with 10 ml PBS two times and then enumerated with a hematocytometer. Approximately one million cells were used for each flow cytometric analysis. FITC-conjugated anti-ODC antibody was made by using the FITC Microscale Protein Labeling Kit (AnaSpec, San Jose, CA). PE-conjugated antibodies against CD4, CD8, and CD45RA were purchased from Cedarlane (Burlington, NC). The PE-conjugated anti-CD68 antibody was acquired from AbD Serotec (Raleigh, NC). FITC- and PE-conjugated mouse IgG_1 antibodies were used as isotype controls. The stained cells were analyzed with a FACScan flow cytometer (BD Biosciences, San Jose, CA), and the data were interpreted by the BD CellQuest Software.

AZI Knockdown with siRNA

The rat AZI siRNA duplex and scrambled siRNA were synthesized by Integrated DNA Technologies (Coralville, IA). The sequence of the AZI siRNA was AAGAUCGUGAAGAAGCACAGU which has been shown to be effective against AZI expression (61). To perform siRNA knockdown, approximately 2×10^6 AMs were placed in a well of a 6-well plate containing 2 ml serum-free DMEM. The cells were transfected with the siRNAs by adding 2 μl of 1 μg/μl of siRNA molecules and 5 μl of TransMessenger (Qiagen, Valencia, CA) to the well. After 6 hr of incubation at 37°C with 5% CO_2, the culture medium was supplemented with a final concentration of 10% FBS, 1% antibiotic mixture (Sigma #P4333), and 2 ml of DMEM-based BALF to mimic the original lung environment. The cells were harvested after three days of incubation for real-time RT-PCR, Western blotting, and polyamine uptake assays described above.

Apoptosis Assay

Macrophage apoptosis was determined using the DeadEnd Fluorimetric Fluorescent terminal deoxynucleotidyl transferase dUTP nick end labeling (TUNEL) System (Promega, Madison, WI). Briefly, deparaffinized and rehydrated rat lung sections on slides were digested with 20 μg/ml of proteinase K at room temperature for 10 min. After washing with PBS, the sections were incubated with terminal deoxynucleotidyl transferase and fluorescein-12-dUTP at 37°C for 1 hr to label DNA fragments at their 3' ends. Unincorporated fluorescein-12-dUTPs were removed by washing the slides two

times with 2 × saline sodium citrate buffer. Slides were mounted with ProLong Gold antifade reagent containing DAPI (Invitrogen) which stains DNA.

Cytosolic Cytochrome c Assay

Determination of cytosolic cytochrome c levels was performed as described previously (105). Briefly, 2×10^6 AMs were lysed, and the protein concentrations in the cell lysate were determined by the Bradford protein assay method (Bio-Rad). A total of 5 μg protein in 100 μl blocking buffer was used to determine the levels of cytochrome c by the FunctionELISA cytochrome c assay kit (Active Motif, Carlsbad, CA). This kit uses the Sandwich ELISA technique with the first antibody to capture and the biotin-conjugated second antibody coupled with HRP-conjugated streptavidin to quantify cytochrome c.

PAO and SMO Activity Assay

PAO activity was assayed by the method of Suzuki *et al.* (202), which measures the levels of H_2O_2 formed. H_2O_2 converts homovanillic acid to a fluorescent compound in the presence of HRP. AMs (approximately 2×10^6 cells) from each rat were suspended in 1 ml of 83 mM sodium borate (pH 9.0) and broken up by passing through a 1 ml syringe with 25 gauge needle 20 times. Five hundred microliters of cell lysate was preincubated with 5U of HRP for 20 min at 37°C to remove endogenous substrates of hydrogen peroxide-producing enzymes. One hundred micrograms of homovanillic acid and N1-acetylspermine (final concentration 250 μM) were then added, followed by an

incubation at 37°C for 30 min. The PAO reaction was stopped by adding 1 ml of 0.1 M NaOH solution. The intensity of fluorescence generated in the reaction was measured by fluorometry with an excitation wavelength of 323 nm and emission wavelength of 426 nm. Protein concentration was determined with Bradford protein assay dye (Bio-Rad), and PAO activity was shown in the amount H_2O_2 produced per min per mg of protein. SMO activity was measured by the same method except that the substrate was replaced by spermine.

Cytotoxicity of Polyamine Transport Ligands

The anthracene-polyamine conjugates Ant-(butanediamine) (232), Ant-(4,4) (231), Ant-(4,4,4) (230), 44-Ant-44 (86), and 44-Bn-44 (86) were previously synthesized and characterized in terms of their structures, K_i values versus radiolabeled spermidine, and polyamine transport targeting abilities in CHO cell lines (Fig. 26). Toxicity of polyamine transport inhibitors to AMs was determined by Trypan blue exclusion assay. AMs were isolated as described previously (115). A total of one million AMs from normal rats were placed in one well of a 12-well plate and incubated with a certain compound at various concentrations. After a 3 hr incubation, cells were stained with 0.4% Trypan Blue solution (Invitrogen, Carlsbad, CA), and the numbers of viable cells (unstained cells) were enumerated.

Treatment of PCP rats with Polyamine Transport Ligands

Dex-Pc rats were given 50 µl of 1 mM 44-Ant-44 or 44-Bn-44 intranasally every two days starting at the 28th day after infection. All rats were sacrificed after 84 days of infection.

Pulmonary Pathology

Rats were anesthetized by i.m. injection of 100 µl ketamine mixture (80 mg/ml ketamine hydrochloride, 0.38 mg/ml atropine, and 1.76 mg/ml acepromazine) and then sacrificed. The thoracic cavity was exposed by dissection. The whole lung was excised and then fixed with 4% paraformaldehyde in PBS (137 mM NaCl, 2.7 mM KCl, 4.3 mM Na_2HPO_4, 1.47 mM KH_2PO_4, pH 7.4) overnight. Sections of paraffin-embedded lung were stained with hematoxylin & eosin (H&E) and then examined by light microscopy. The degree of pulmonary inflammation was graded on a scale of 0 to 5 as previously described (183). Briefly, grade 0 had no lesions; grade 1 had minimal lymphocytic inflammation restricted to perivascular and peribronchiolar regions; grade 2 had moderate perivascular and peribronchiolar inflammation with a slight increase in the numbers of AMs, lymphocytes, and eosinophils; grade 3 had profound perivascular and peribronchiolar inflammation with moderately increased numbers of alveolar macrophages, lymphocytes, eosinophils, and multinucleated giant cells; grade 4 had severe perivascular and peribronchiolar inflammation with markedly increased numbers of alveolar macrophages, eosinophils, lymphocytes and multinucleated giant cells; grade 5 had severe perivascular and peribronchiolar inflammation with effacement of alveolar

parenchyma and small airways by sheets of inflammatory cells. This grading was performed by a pathologist on blinded samples.

Pneumocystis Burden

The numbers of Pneumocystis organisms in lung sections were enumerated after being stained with GMS silver (Sigma). Briefly, deparaffinized and rehydrated lung tissue sections were placed in 1% periodic acid solution for 5 min and then washed with water. Silver staining was performed by incubating the lung sections with freshly prepared working silver solution (110 mg silver methenamine in 0.4% sodium borax) at 62°C for 20 min. The sections were then reacted with 0.2% gold chloride for 30 sec. Excess silver was removed by incubating the slides with 2% sodium thiosulfate for 2 min. Sections were counterstained with 0.2% Light Green and then examined by light microscopy. Organism burden was graded on a scale of 0 to 4 as previously described (183). Briefly, grade 0 indicated no cysts; grade 1 had scattered cysts; grade 2 had cysts in most alveoli surrounding tertiary bronchioles; grade 3 had cysts throughout alveoli in many regions; grade 4 had cysts and foamy exudate throughout alveoli in most regions. This grading was performed by a pathologist on blinded samples.

Statistical Analysis

Data were presented as means ± SD with indicated number of experiments. Two-tailed student's t-test was used for statistical analysis, and the difference between the two groups analyzed was considered statistically significant if the p value was < 0.05.

RESULTS

Polyamine Synthesis in AMs during PCP

To examine whether the increased polyamine levels in AMs during PCP are due to increased polyamine synthesis, the expression levels of ODC, SSAT, and SRM were determined by real-time RT-PCR and Western blotting. The results showed that the mRNA levels of ODC, SSAT, and SRM in AMs from immunosuppressed (Dex) rats were 0.93, 1.54, and 1.21 fold, respectively of those of Normal rats (Fig. 4). Since these differences were not statistically significant, the results indicated that long-term treatment of rats with dexamethasone did not significantly affect polyamine synthesis mediated by ODC, SSAT, or SRM. In AMs from Dex-Pc rats, ODC, SSAT, and SRM mRNA levels were 1.01, 0.94, and 1.01 fold that of Dex rats (data not shown), indicating that *Pneumocystis* infection also did not significantly affect the transcription of these genes. Western blotting analysis revealed that the level ODC protein in AMs was not changed by immunosuppression but was increased approximately 8-fold during *Pneumocystis* infection (Fig. 5). In contrast, the SSAT protein level was not altered during *Pneumocystis* infection (Fig. 5). The protein level of SRM was not determined because an anti-rat SRM antibody was not commercially available. The change in ODC protein but not mRNA levels indicated that ODC expression was regulated by a posttranscriptional mechanism in AMs during PCP.

Polyamine Uptake by AMs during PCP

Elevated intracellular polyamine levels could also be due to increased polyamine uptake; therefore, polyamine uptake assays were performed. Purified FAM-labeled spermidine (FAM-SPD) (Fig. 6) was transtracheally instilled into the lungs of Normal, Dex, and Dex-Pc rats. Rats were sacrificed and lavaged to obtain AMs one hour after the transtracheal instillation. Fluorescence microscopy showed that less than 0.1% of AMs from Normal and Dex rats but greater than 2% of those from Dex-Pc rats contained FAM-SPD (Fig. 7), suggesting that the number of AMs that can take up exogenous polyamines was increased by approximately 20 fold during PCP (Fig. 7). To confirm that these cells took up FAM-SPD not FAM non-specifically, a separate group of Dex-Pc rats were transtracheally instilled with FAM. This experiment revealed that less than 0.1% AMs in this group of rats internalized FAM (Fig. 7), confirming the specificity of polyamine uptake. To identify the cells which took up polyamines, frozen lung sections from FAM-SPD instilled Dex-Pc rats were stained for the macrophage marker CD68, and all the cells that contained FAM-SPD were positive for CD68 (Fig. 8), indicating that they were macrophages.

ODC Expression in Rat Lungs during PCP

To determine the sources of polyamines in the lung during PCP, IHC staining for ODC was performed on lung sections from Normal, Dex, and Dex-Pc rats. H&E and ODC staining revealed no differences in the microscopic features of the lungs from Normal and Dex rats, indicating that immunosuppression of rats with dexamethasone had

no effect on ODC expression. However, ODC expression in the lung was greatly affected by *Pneumocystis* infection. The ODC protein was not detectable in most pulmonary cells, but was highly expressed in the mononuclear cells located around blood vessels and bronchioles (Fig. 9), suggesting that these inflammatory cells were sources of polyamines during PCP. Interestingly, the intracellular location of ODC was changed during PCP. In uninfected rats, ODC was found distributed evenly in the cytoplasm of inflammatory cells from uninfected rats, but was located in pericytoplasmic areas in those from infected rats (Fig. 9). To identify these cells, serial lung sections from Dex-Pc rats were stained with cell-specific markers CD68 (monocyte), CD79a (B lymphocyte), and CD3ζ (T lymphocyte). Results showed that these ODC-positive cells may be monocytes and B or T lymphocytes (Fig. 10). Polyamine production determined by anti-spermidine staining also showed that the cells in this area contain high levels of polyamines (Fig. 10).

Flow cytometry analysis of ODC-positive cells in *Pneumocystis*-infected lungs

To quantify and further identify ODC-positive cells, total lung cells isolated from Dex-Pc rats were analyzed by flow cytometry. Anti-ODC antibody was labeled with FITC, and antibodies against CD4, CD8, CD45RA, and CD68 were labeled with PE. In this assay, 24.44% of total lung cells from Dex-Pc rats were ODC-positive (Table 1). Dual staining of the cells with ODC and CD4, CD8, CD45RA, or CD68 antibodies revealed that 1.83% of the cells were ODC+CD4+, 8.27% were ODC+CD8+, 9.79% were ODC+CD45RA+ (B lymphocytes), and 7.80% were ODC+CD68+ (monocytes/macrophages).

OAZ and AZI Expression in AMs during PCP

Since OAZ and AZI have been shown to regulate both polyamine production and transport (59, 96), their expressions in AMs from Normal, Dex, and Dex-Pc rats were determined. Real-time RT-PCR results revealed that the mRNA expression levels of OAZ in AMs from Dex and Dex-Pc rats were 0.93 and 0.96 fold, respectively of those of Normal rats (Fig. 11); these differences were not statistically significant. Western blotting results also showed that OAZ protein levels in AMs were not affected by immunosuppression or *Pneumocystis* infection (Fig. 12). In contrast, AZI mRNA levels in AMs from Dex-Pc rats were 3.16 fold higher than those from Dex rats (Fig. 11), and AZI protein levels in AMs were increased by 6 fold during PCP as determined by Western blotting (Fig. 12).

Polyamine Synthesis and Uptake after AZI Knockdown

To correlate AZI overexpression with AM apoptosis during PCP, AMs isolated from Dex-Pc rats were analyzed for AZI expression, polyamine synthesis, polyamine uptake, and apoptosis after AZI siRNA knockdown. Results from real-time PCR showed that AZI siRNA successfully decreased AZI mRNA levels by approximately 70% in AMs from Dex-Pc rats (Fig. 13). This AZI knockdown was also found to cause a 60% decrease in ODC protein level in these AMs (Fig. 14). In the *ex vivo* spermidine uptake assay, a 50% reduction in the number of cells taking up polyamines was observed in the group of cells transfected with AZI siRNA as compared to control transfectants (Fig. 15).

Macrophage Apoptosis after AZI Knockdown

BALF from *Pneumocystis*-infected rats have been shown to induce macrophages to undergo apoptosis due to elevated levels of polyamines (105). To determine whether AZI plays a role in this BALF-induced apoptosis, 2×10^6 normal rat AMs were transfected with AZI siRNA and then incubated with BALF from Dex-Pc rats 6 hr after siRNA transfection. Three days after the transfection and BALF treatment, cells were analyzed for apoptosis by three different methods. Results from TUNEL assay showed that the number of apoptotic cells was decreased by 53% (Fig. 16). The levels of cytosolic cyotochrome c showed a 58% reduction (Fig. 17), and those of activated caspase-3 determined by Western blotting were decreased by 75% in macrophages transfected with AZI siRNA as compared to controls that were transfected with scrambled siRNA (Fig. 18).

Substances That Induce AZI Overexpression

Since AZI was found overexpressed in AMs from Dex-Pc rats, experiments were performed to determine whether certain substances capable of inducing the expression of AZI are present in BALF from Dex-Pc rats. AMs from normal rats were first treated with the Dex-Pc BALF and then measured for AZI mRNA by RT-PCR. This treatment resulted in a 1.5 fold increase in AZI mRNA levels in AMs compared to the same cells treated with Dex BALF (Fig. 19), suggesting that AZI expression in AMs can be induced by a certain substance in *Pneumocystis*-infected lungs. To identify this substance, AMs from normal rats were treated with *Pneumocystis* organisms and the cytokine TNF-α which is

present in high levels in *Pneumocystis*-infected lungs. Results showed that *Pneumocystis* organisms but not TNF-α increased AZI mRNA levels in a dose-dependent manner (Fig. 20). The same result was observed when normal rat AMs were treated with zymosan A (Fig. 20). These results suggest that a component of the *Pneumocystis* cell wall is responsible for the increase in AZI expression during PCP.

Polyamine Catabolism and AM Apoptosis

To investigate whether polyamine catabolism plays a role in AM apoptosis during PCP, the expression and activity levels of PAO and SMO in AMs from *Pneumocystis*-infected rats were determined. Results of real-time RT-PCR showed that PAO mRNA levels in AMs from Dex-Pc rats were 2.82 fold that of those from Dex rats, but SMO mRNA levels were not significantly changed (Fig. 21). PAO protein levels were found increased approximately 4 fold in AMs during PCP (Fig. 22), and PAO activity in AMs from *Pneumocystis*-infected rats showed a 2.24 fold increase as compared to the Dex control (Fig. 23). These results suggest that polyamine oxidation plays a role in AMs apoptosis in *Pneumocystis*-infected lungs.

Acetylated Polyamines Induce PAO expression

As described previously, the activity and levels of both mRNA and protein of PAO are increased in AM during PCP (115). To determine whether this increase is caused by the markedly increased levels of N1-acetylspermidine and N1-acetylspermine which are the substrates of PAO (105), mouse macrophage cell line RAW 264.7 cells were

incubated with varying concentrations (20 - 160 μM) of spermidine, spermine, N1-acetylspermidine, and N1-acetylspermine for 24 hrs and then assessed for PAO mRNA and protein levels. Results from real-time RT-PCR revealed that N1-acetylspermidine and N1-acetylspermine induced PAO mRNA expression in a dose-dependent manner and caused a 4.84 ± 0.62 and 22.12 ± 0.75 fold increase, respectively (Fig. 24), in PAO mRNA levels at a concentration of 160 μM. PAO mRNA levels were also increased by spermidine and spermine, although at much lower levels. The highest level of PAO mRNA induced by spermidine was 1.44 ± 0.17 fold at 160 μM, and that induced by spermine was 1.83 ± 0.3 fold at 80 μM. With Western blotting, PAO protein levels in AMs were also found to be elevated by treatment of the cells with spermidine, spermine, N1-acetylspermidine, and N1-acetylspermine at 160, 80, 40, and 40 μM, respectively (Fig. 25). These results confirm the hypothesis that PAO expression is induced by its substrates N1-acetylspermidine and N1-acetylspermine. Since PAO also utilizes spermine as its substrate and converts it to spermidine (188), it is not surprising to see a moderate PAO induction by spermine. Spermidine is not the natural substrate of PAO, but it can be converted to N1-acetylspermidine by SSAT (235). This may be why PAO expression was also induced by spermidine.

Cytotoxicity of Polyamine Transport Inhibitors

Polyamine uptake is increased in AMs during PCP and this increase is very likely to contribute to disease progress during PCP. To investigate whether inhibiton of polyamine transport can be a therapeutic target against PCP, five potential polyamine transport inhibitors, compounds Ant-(butanediamine), Ant-(4,4), Ant-(4,4,4), 44-Ant-44, and

44-Bn-44 (Fig. 26), were tested *in vivo*. Since these compounds had not been used *in vivo*, their toxicity to AMs from normal rats was first determined. Trypan blue exclusion assays showed that less than 16% of the cells were viable after 3 h incubation with 0.4 mM of Ant-(butanediamine) or Ant-(4,4), indicating that these two compounds were toxic to AMs. Compound Ant-(4,4,4) was less toxic as 88% of the cells remained viable after 3 hr of treatment with the lowest concentration (0.4 mM) and 42% with the highest concentration (2 mM). There was no significant change in viability after the cells were treated for 3 h with compound 44-Ant-44 or 44-Bn-44 at concentrations up to 2 mM, indicating that these two compounds were not toxic to AMs (Fig. 27).

Effects of 44-Ant-44 and 44-Bn-44 on Survival of Rats with PCP

Since compounds 44-Ant-44 and 44-Bn-44 showed no cytotoxicity *in vitro*, their therapeutic effects on PCP were examined. Eight rats that had been infected with *Pneumocystis carinii* (Dex-Pc rats) for 28 days were treated intranasally with 50 μl of 1 mM of 44-Ant-44 or 44-Bn-44 every two days. Immunosuppressed and uninfected (Dex rats, n=4) and untreated Dex-Pc (n=9) rats were included in this study as controls. All Dex rats survived the entire 84 days of the study, while untreated Dex-Pc rats died at different times. On average, 44-Ant-44-treated Dex-Pc rats lived eight days longer and 44-Bn-44 treated Dex-Pc rats lived two days longer than untreated Dex-Pc rats (Fig. 28).

Effects of 44-Ant-44 and 44-Bn-44 on Lung Pathology and Organism Burden

Light microscopy of H&E stained lung sections from Dex-Pc rats treated for 21 days with the compounds revealed that 44-Ant-44 treatment increased open alveolar space, reduced alveolar septa thickness, reduced inflammation, and decreased foamy exudates in alveoli as compared to those from untreated Dex-Pc rats. Lung sections from 44-Bn-44 treated Dex-Pc rats showed a slight decrease in inflammatory cell infiltration but no apparent changes in alveolar structure and foamy exudates. The overall inflammatory scores for untreated, 44-Ant-44-treated, and 44-Bn-44-treated Dex-Pc rats were determined to be 3.63 ± 0.48, 2.3 ± 0.27, and 3.17 ± 0.29, respectively on a scale of 0 to 5 (Fig. 29). These results indicated that 44-Ant-44 substantially reduced the pulmonary damage caused by *Pneumocystis* infection ($p = 0.001$), but 44-Bn-44 had little effect ($p = 0.206$). The overall organism burden on a scale of 0 to 4 of 44-Ant-44-treated Dex-pc rats was determined to be 0.8 ± 0.27, whereas those of untreated and 44-Bn-44 treated Dex-Pc rats were 3 ± 0 and 2.17 ± 0.29, respectively (Fig. 30). These results indicated that both 44-Ant-44 ($p = 0.000001$) and 44-Bn-44 ($p = 0.002$) decreased the organism burden in *Pneumocystis*-infected lungs, but 44-Ant-44 worked much better than 44-Bn-44.

Effects of 44-Ant-44 and 44-Bn-44 on Apoptosis of AM

Results of TUNEL assays on lung sections from untreated, 44-Ant-44-treated, and 44-Bn-44-treated Dex-Pc rats revealed that 21 days of treatment with 44-Ant-44 reduced

the number of apoptotic alveolar macrophages by 80% in the lungs (Fig. 31). In contrast, 44-Bn-44 did not significantly reduce the apoptosis rate of AMs.

Table 1. Flow cytometry analysis of lung cells from *Pneumocystis*-infected rats.

	FITC(-)PE(-)	FITC(-)PE(+)	FITC(+)PE(-)	FITC(+)PE(+)
Isotype Control	95.75 ± 0.81	0.04 ± 0.07	2.54 ± 0.10	1.66 ± 0.84
ODC-FITC	73.95 ± 5.43	0.00 ± 0.00	24.44 ± 6.78	1.61 ± 1.34
ODC-FITC+CD4-PE	77.04 ± 4.37	0.07 ± 0.06	21.06 ± 5.40	1.83 ± 1.09
ODC-FITC+CD8-PE	82.07 ± 2.59	0.02 ± 0.01	9.63 ± 1.60	*8.27 ± 0.99
ODC-FITC+CD45RA-PE	82.73 ± 1.12	0.77 ± 0.58	6.71 ± 1.37	*9.79 ± 1.91
ODC-FITC+CD68-PE	76.73 ± 3.19	0.00 ± 0.01	15.20 ± 8.01	*7.80 ± 4.42

Results represent means ± SD from 4 experiments.

* $p < 0.05$ compared to the FITC(+)PE(+) quadrant of the ODC-FITC group.

Polyamine Structures

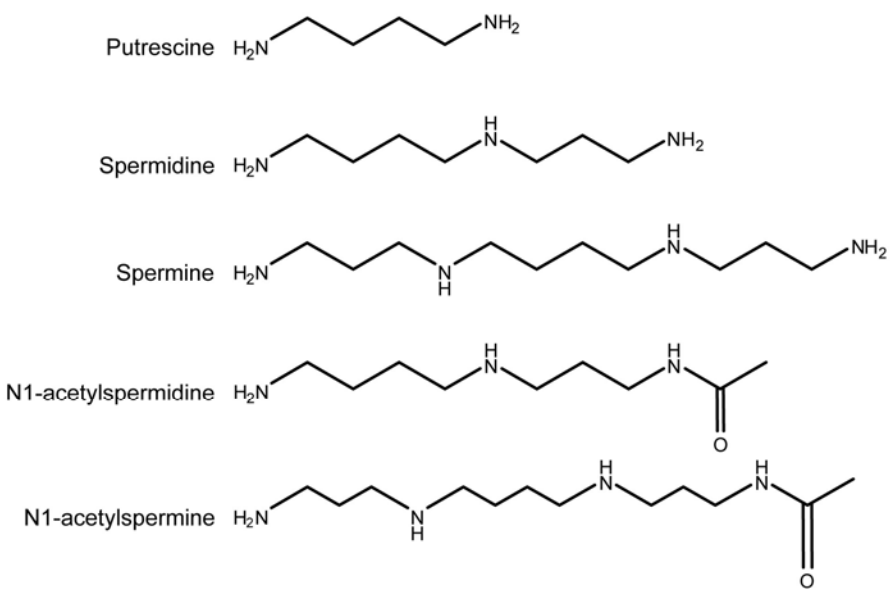

Fig. 1. Polyamine structures.

Polyamine Metabolism Pathway

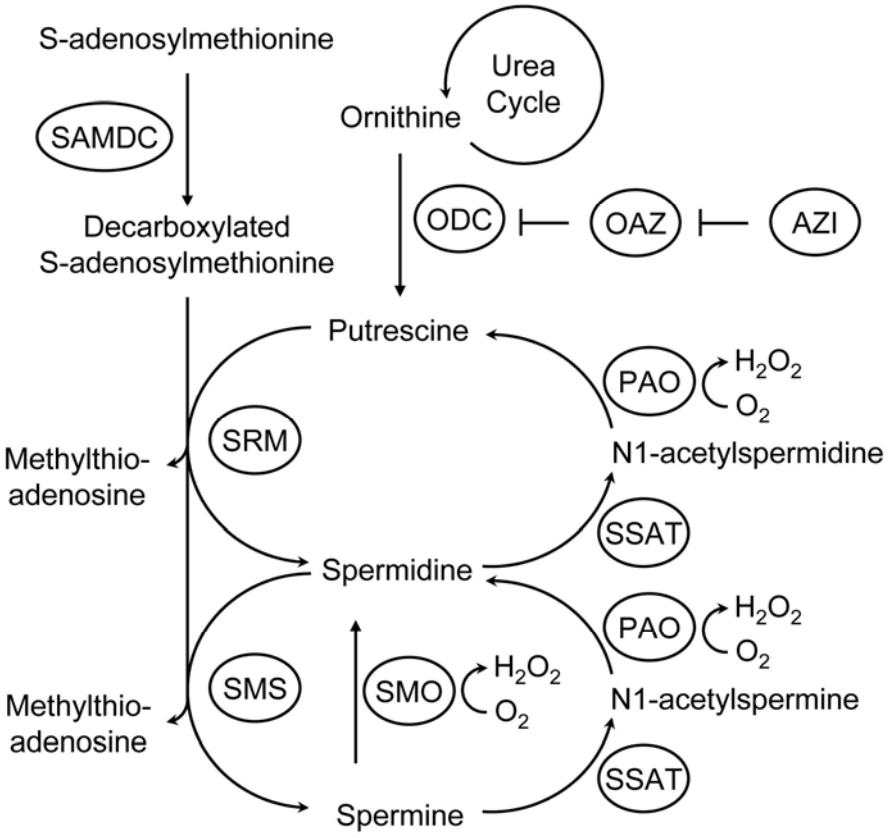

Fig. 2. Polyamine metabolism pathway. ODC, ornithine decarboxylase; OAZ, ODC antizyme; AZI, ODC antizyme inhibitor; PAO, polyamine oxidase; SMO, spermine oxidase, SSAT, spermidine/spermine N1-acetyltransferase; SRM, spermidine synthase; SMS, spermine synthase; SAMDC, S-adenosylmethionine decarboxylase.

AM Apoptosis during PCP

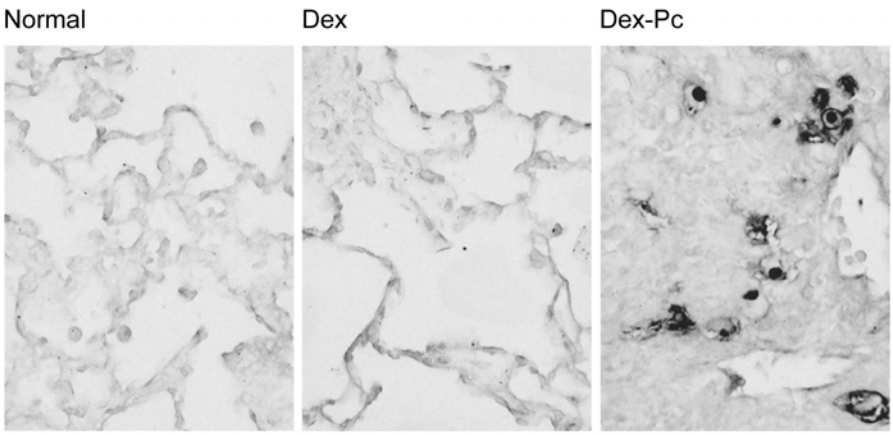

Fig. 3. AM apoptosis during PCP. Lung sections from Normal, Dex, and Dex-Pc rats were analyzed by TUNEL assay which stains the apoptotic cell nuclei. TUNEL(+) cells were identified as AMs by their morphology and location.

mRNA Expressions of Polyamine Synthesis Enzymes in AMs

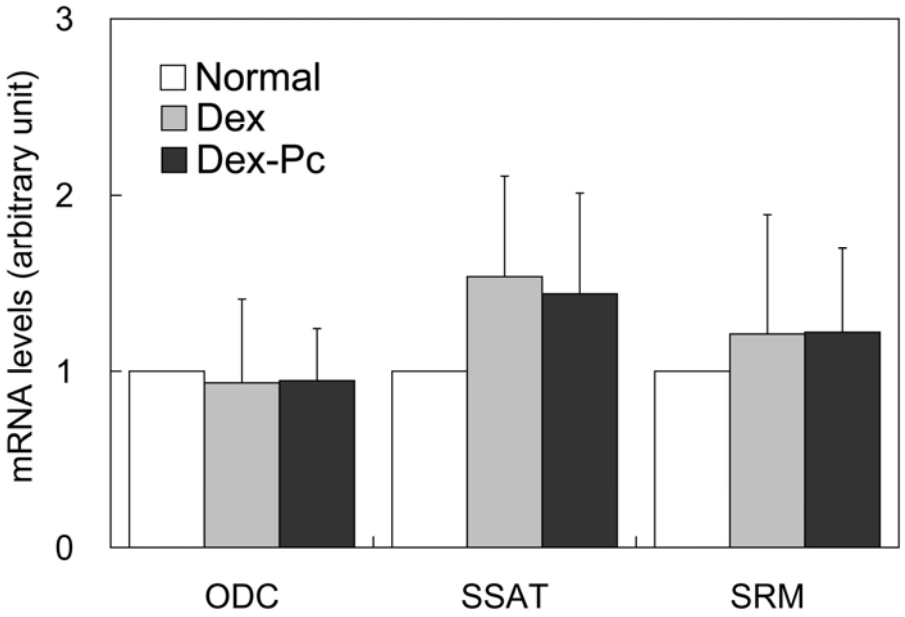

Fig. 4. mRNA Expressions of Polyamine Synthesis Enzymes in AMs. mRNA levels of ODC, SSAT, and SRM in AMs were determined by real-time RT-PCR. Results represent mean ± S.D. from four experiments. No significant changes were found during PCP.

Protein Expressions of Polyamine Synthesis Enzymes in AMs

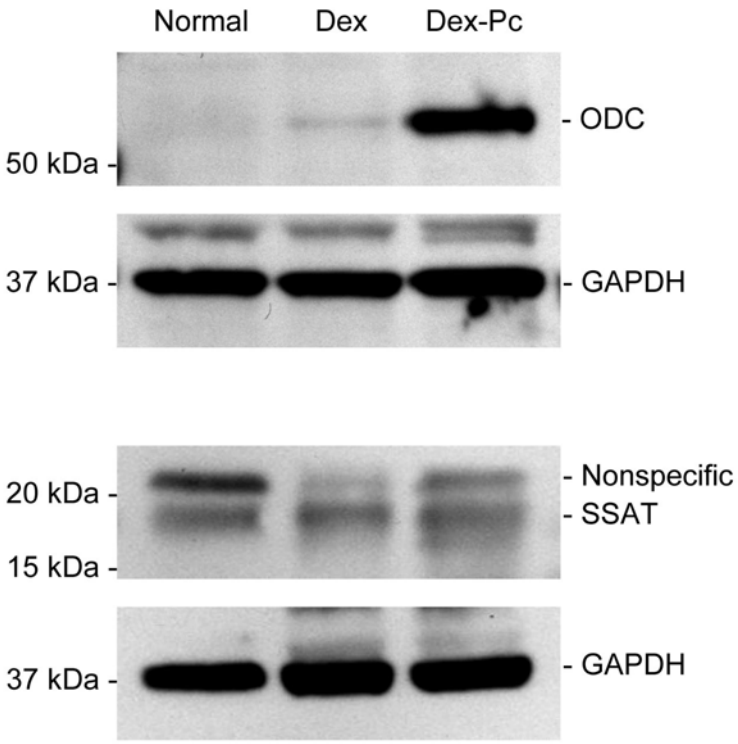

Fig. 5. Protein expressions of polyamine synthesis enzymes in AMs. Protein levels of ODC and SSAT in AMs were analyzed by Western blotting. Results shown are representative of three independent experiments.

Purity of FAM-Labeled Spermidine

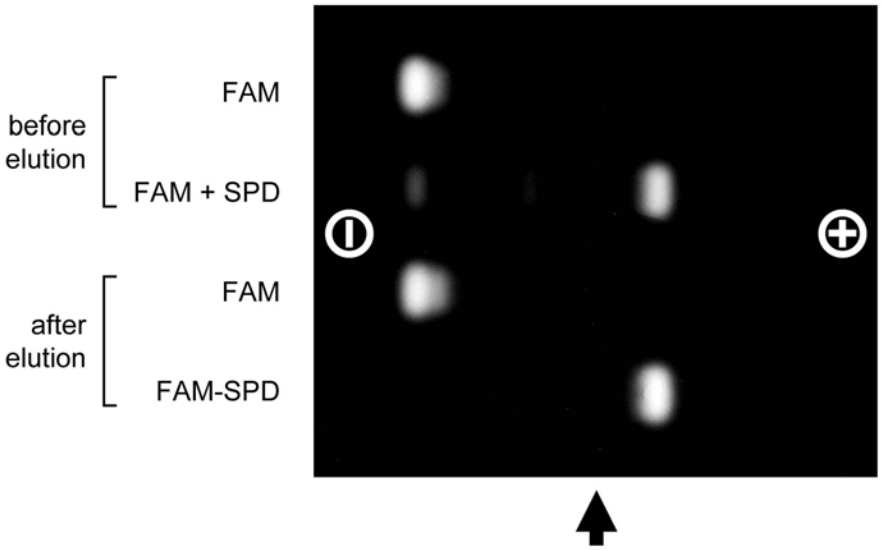

Fig. 6. Purity of FAM-labeled spermidine. A totoal of 10 μl of 40 μM FAM and FAM-labeled spermidine (FAM-SPD) before and after purification by gel elution were electrophoresed in 1% agarose gel in 40 mM MES buffer and visualized by UV transillumination. FAM moved toward cathode, whereas FAM-SPD moved toward anode. Arrow indicates the position of loading wells.

Polyamine Uptake Assay

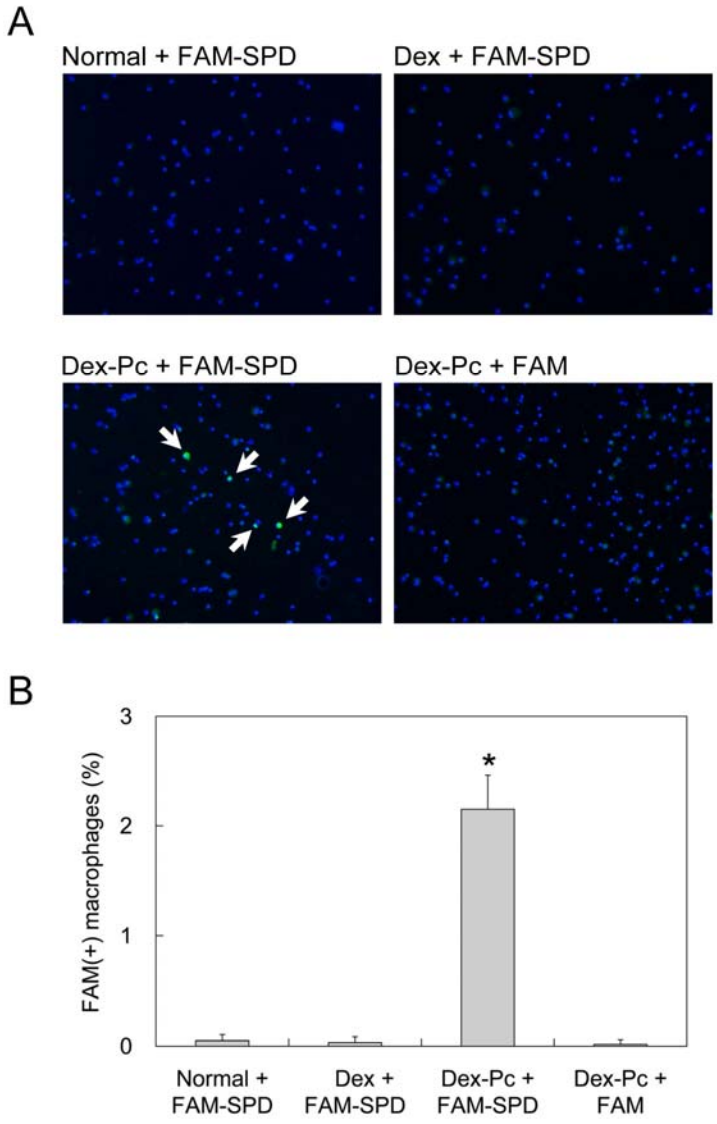

Fig. 7. Polyamine uptake assay. (A) 200 µl of 5 µM FAM-SPD or FAM was transtracheally instilled into Normal, Dex, and Dex-Pc rats. AMs were isolated one hour after the instillation and examined by fluorescence microscopy. Arrows indicate the cells with internalized FAM-SPD. (B) A total of 1000 randomly selected cells of each sample shown in Panel A were counted, and the percentages of cells with internalized FAM or FAM-SPD were determined and diagrammed. Results represent mean ± S.D. from four experiments. Asterisk (*) indicates $p < 0.05$ as compared to Dex control.

Polyamine Uptake is Increased in AMs

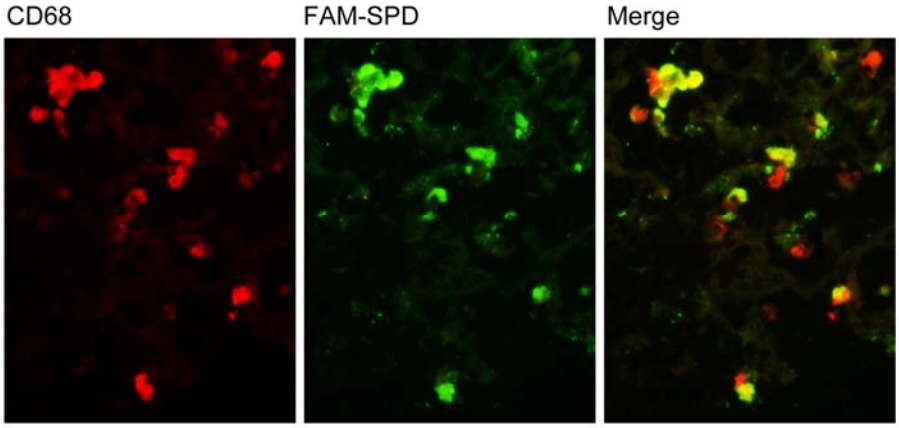

Fig. 8. Polyamine uptake is increased in AMs. Dex-Pc rats were transtracheally instilled with FAM-SPD. One hour after the instillation, rats were sacrificed, and frozen lung sections were made then stained for the macrophage marker CD68. Merged images showed that the cells that took up FAM-SPD were exclusively alveolar macrophages since every cell that took up polyamine was CD68 positive, and no CD68-negative cells took up polyamines.

ODC Expression in the Lung

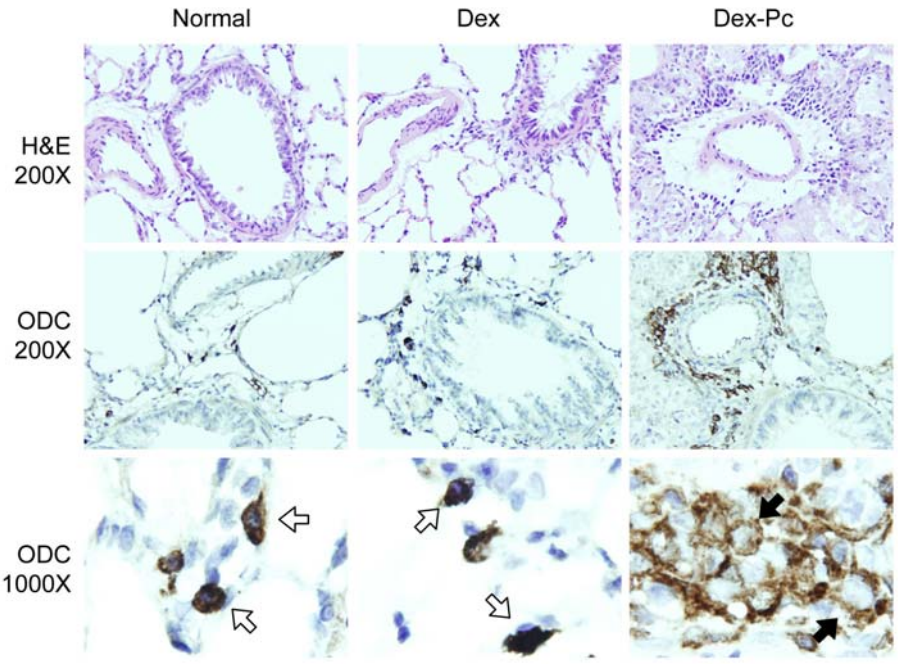

Fig. 9. ODC expression in the lung. H&E staining (top) and IHC staining for ODC were performed on lung sections form Normal, Dex, and Dex-Pc rats. Cells reacted with anti-ODC antibody were examined at the magnifications of 200 × (middle) and 1000 × (bottom). Open and solid arrows indicate the cells with homogenous and pericytoplasmic ODC expression patterns, respectively. Results shown are representative of three sets of animals.

Colocalization of ODC(+) and Inflammatory Cells

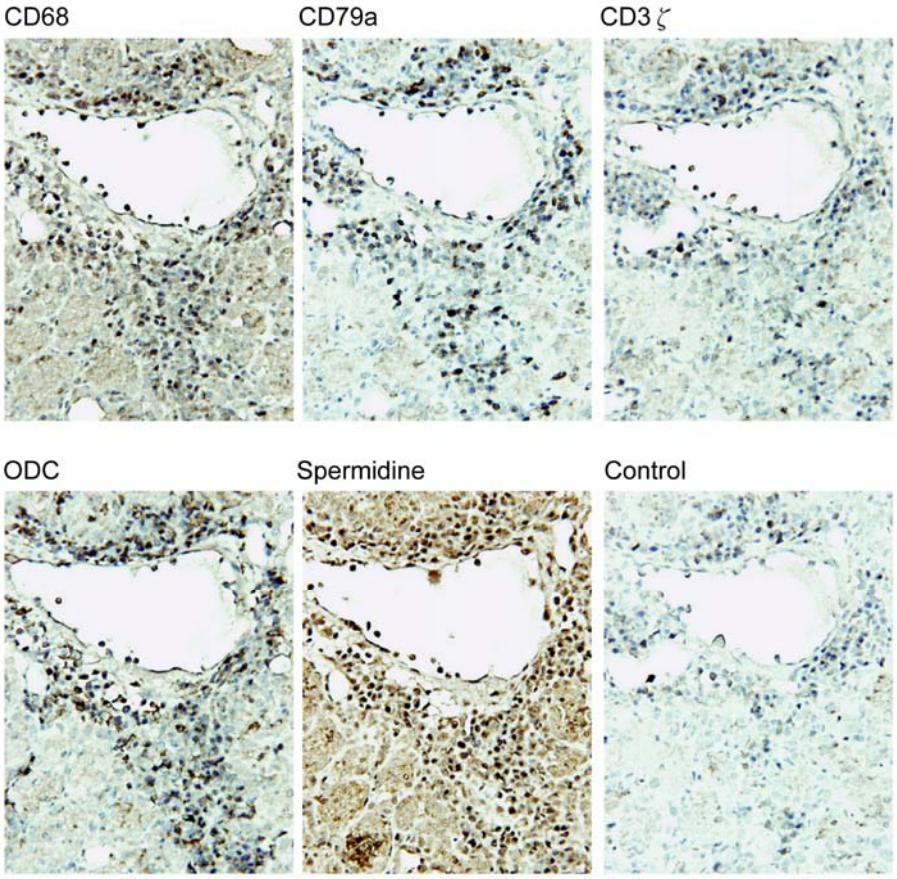

Fig. 10. Colocalization of ODC(+) and inflammatory cells. IHC staining for CD68 (monocyte), CD79a (B cell), CD3ζ (T cell), ODC, and spermidine was performed on serial sections from Dex-Pc lungs. The control was processed in an identical manner except that no primary antibody was used. Magnification = 200 ×.

OAZ and AZI mRNA Expressions in AMs

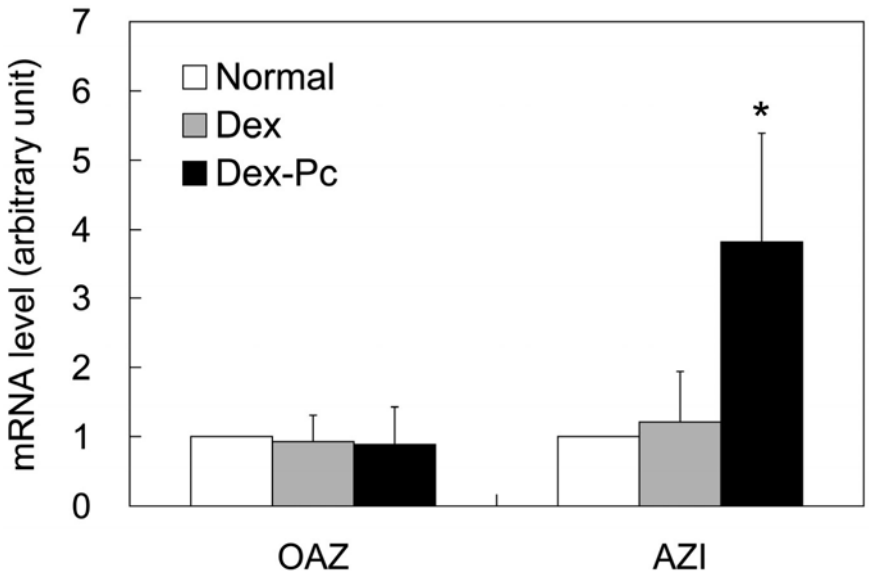

Fig. 11. OAZ and AZI mRNA expressions in AMs. mRNA levels of OAZ and AZI in AMs from Normal, Dex, and Dex-Pc rats were determined by real time RT-PCR. Results represent means ± SD from 5 experiments. Asterisk (*) indicates $p < 0.05$ as compared to Dex control.

OAZ and AZI Protein Expressions in AMs

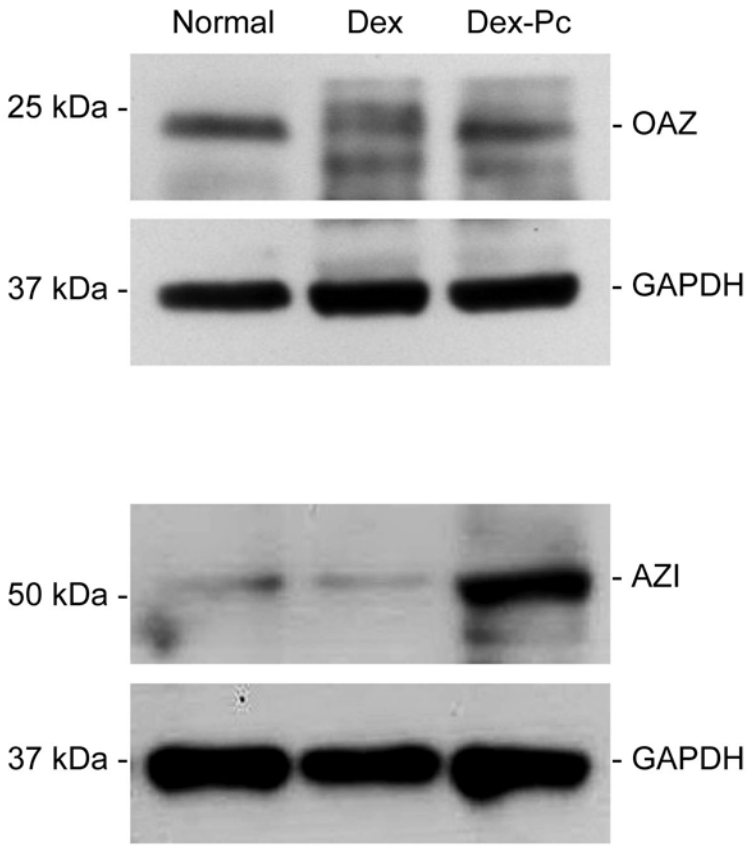

Fig. 12. OAZ and AZI protein expressions in AMs. Protein levels of OAZ and AZI in AMs from Normal, Dex, and Dex-Pc rats were determined by Western blotting (n = 3).

siRNA Knockdown of AZI

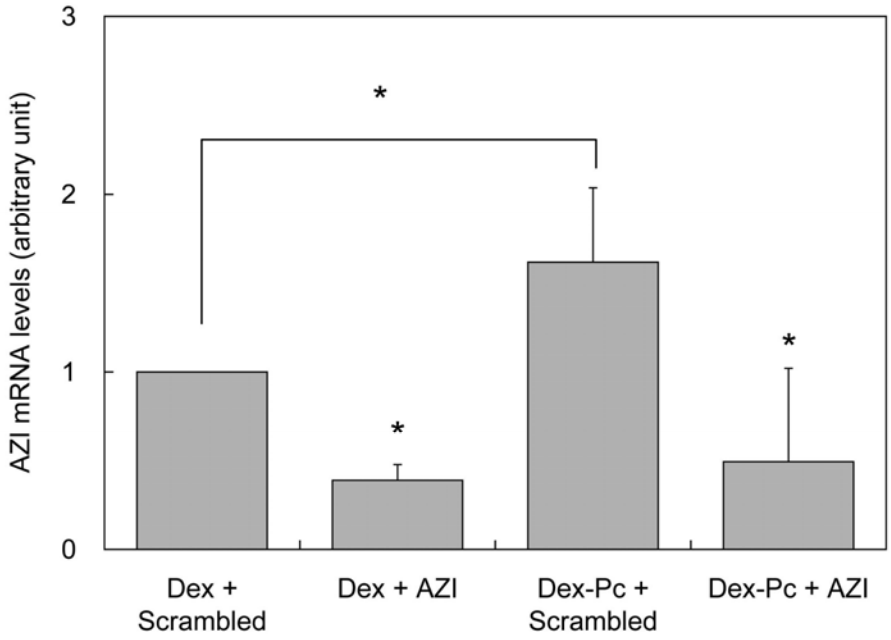

Fig. 13. siRNA knockdown of AZI. Real time RT-PCR analysis of AZI mRNA levels after siRNA knockdown. AMs from Dex and Dex-Pc rats were transfected with AZI siRNA or scrambled siRNA and then measured for AZI mRNA levels. Results represent means ± SD from 4 experiments. Asterisk (*) indicates $p < 0.05$ as compared to scrambled control unless illustrated elsewhere.

Polyamine Synthesis after siRNA Knockdown of AZI

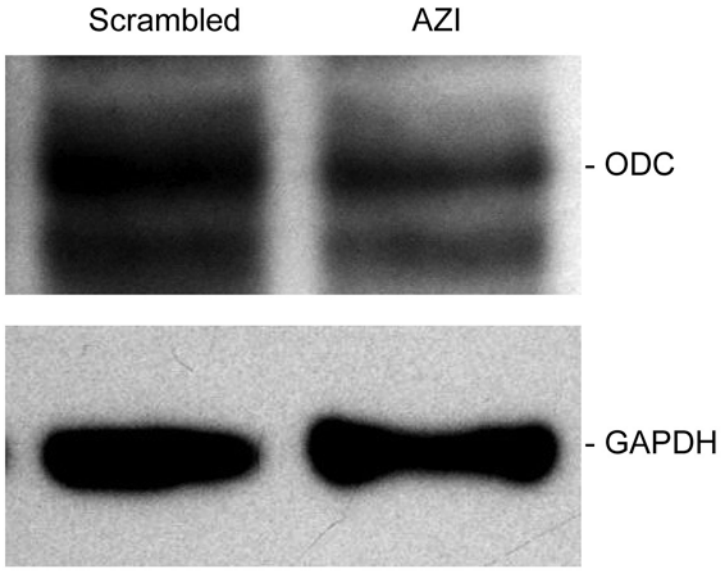

Fig. 14. Polyamine synthesis after siRNA knockdown of AZI. The ODC protein level in AMs from Dex-Pc rats was determined by Western blotting after transfection with AZI siRNA or scrambled siRNA.

Polyamine Uptake after siRNA Knockdown of AZI

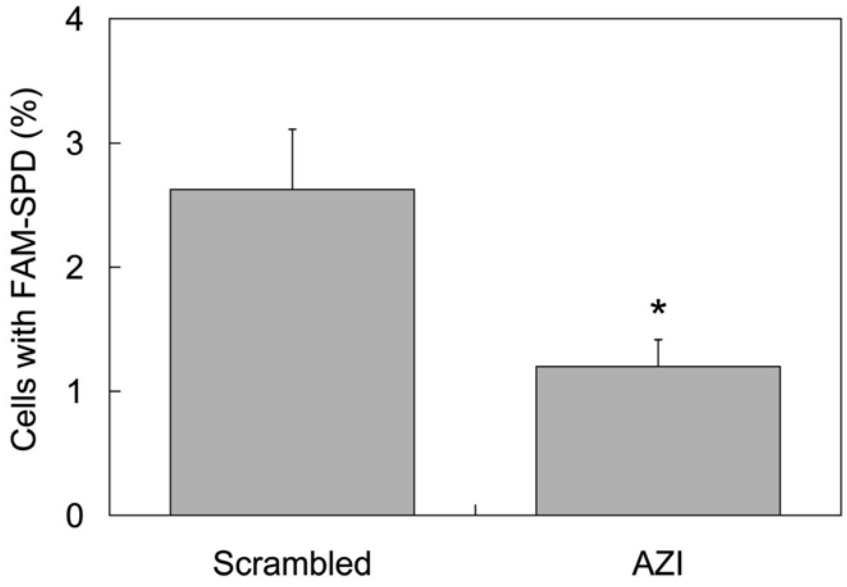

Fig. 15. Polyamine uptake after siRNA knockdown of AZI. AMs from Dex-Pc rats were assayed for FAM-SPD uptake after transfection with AZI siRNA or scrambled siRNA. A total of 1000 cells of each sample were counted, and the percentages of cells with internalized FAM-SPD were determined and diagrammed. Results represent means ± SD from 4 experiments. Asterisk (*) indicates $p < 0.05$ as compared to scrambled control.

Macrophage Apoptosis after siRNA Knockdown of AZI

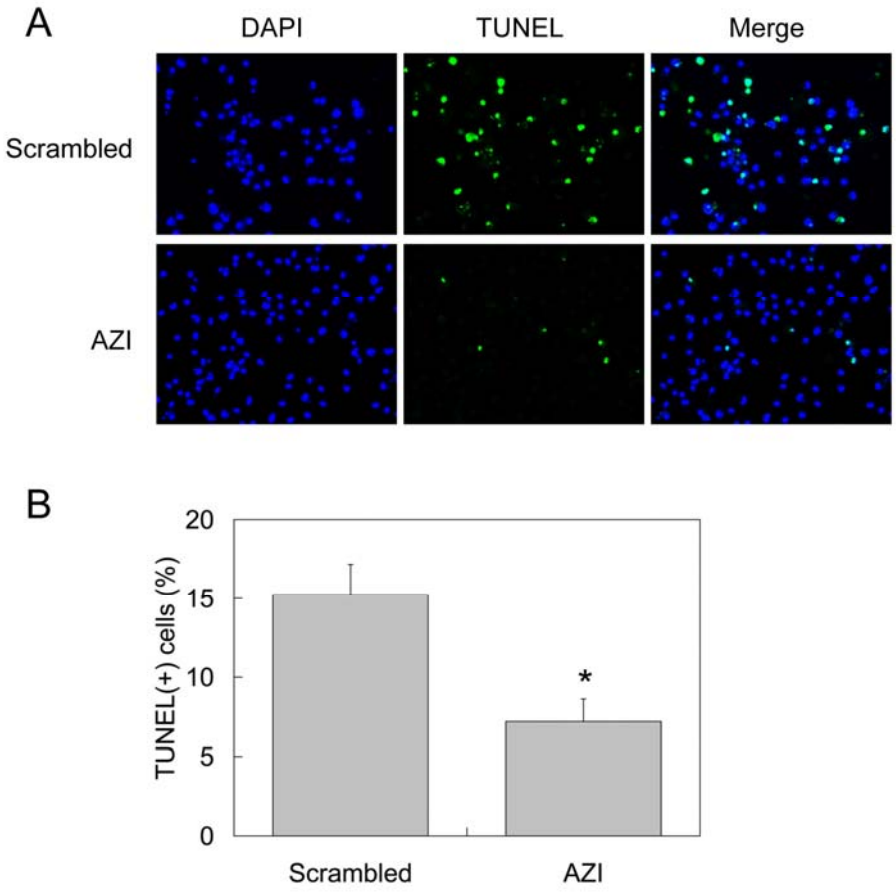

Fig. 16. Macrophage apoptosis after siRNA knockdown of AZI. (A) Normal rat AMs were transfected with AZI siRNA or scrambled siRNA and then treated with BALF from Dex-Pc rats. Three days after transfection, TUNEL assay was performed, and cells were examined by fluorescence microscopy. (B) A total of 1000 randomly selected cells of each sample shown in Panel A were counted, and the percentages of apoptotic cells were diagrammed. Results represent mean ± S.D. from three experiments. Asterisk (*) indicates $p < 0.05$ as compared to scrambled control.

Cytochrome c Release after siRNA Knockdown of AZI

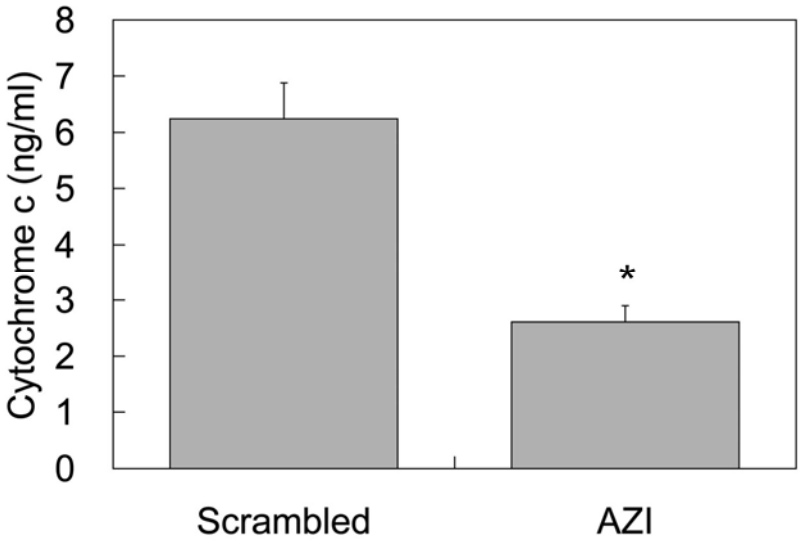

Fig. 17. Cytochrome c release after siRNA knockdown of AZI. Normal rat AMs were transfected with AZI siRNA or scrambled siRNA and then treated with BALF from Dex-Pc rats. Three days after transfection, cytosolic cytochrome c levels were measured. Results represent mean ± S.D. from three experiments. Asterisk (*) indicates $p < 0.05$ as compared to scrambled control.

Caspase-3 Activation after siRNA Knockdown of AZI

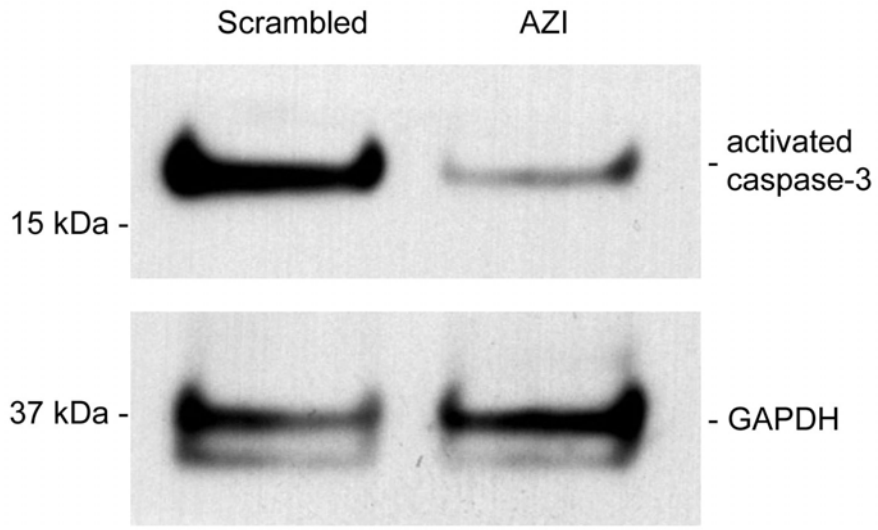

Fig. 18. Caspase-3 activation after siRNA knockdown of AZI. Normal rat AMs were transfected with AZI siRNA or scrambled siRNA and then treated with BALF from Dex-Pc rats. Three days after transfection, the level of activated caspase-3 in AMs was determined Western blotting.

Dex-Pc BALF Induces AZI Overexpression

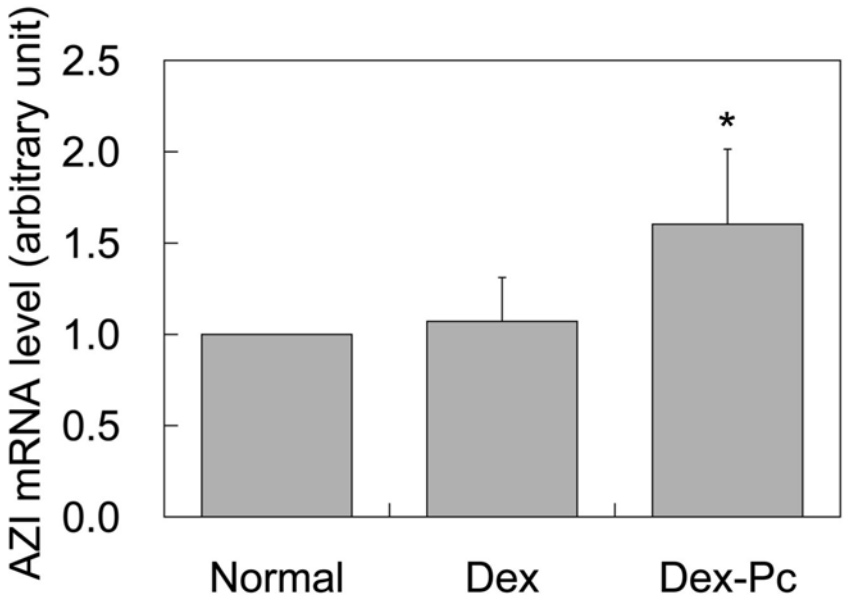

Fig. 19. Dex-Pc BALF induces AZI overexpression (*A*) Normal rat alveolar macrophages were incubated with Normal, Dex and Dex-Pc BALF for 24 hours and then examined by real-time RT-PCR for AZI expression. Results represent mean ± S.D. from five experiments. Asterisk (*) indicates $p < 0.05$ as compared to the Dex control.

***Pneumocystis* and Zymosan Induce AZI Overexpression**

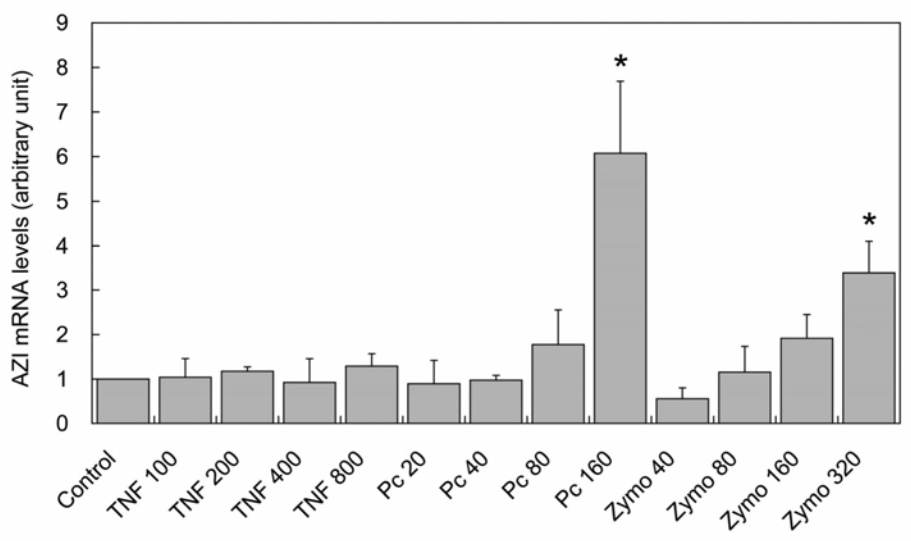

Fig. 20. *Pneumocystis* and zymosan induce AZI overexpression. Normal rat AMs were incubated with TNF-α (TNF, 100 - 800 pg/μl), *Pneumocystis carinii* organisms (Pc, 20 - 160 nuclei/μl), or zymosan A (Zymo, 40 - 320 ng/μl) for 18 hours and then examined by real-time RT-PCR for AZI expression. Results represent mean ± S.D. from three analyses. Asterisk (*) indicates $p < 0.05$ as compared to mock control.

PAO and SMO mRNA Expressions in AMs

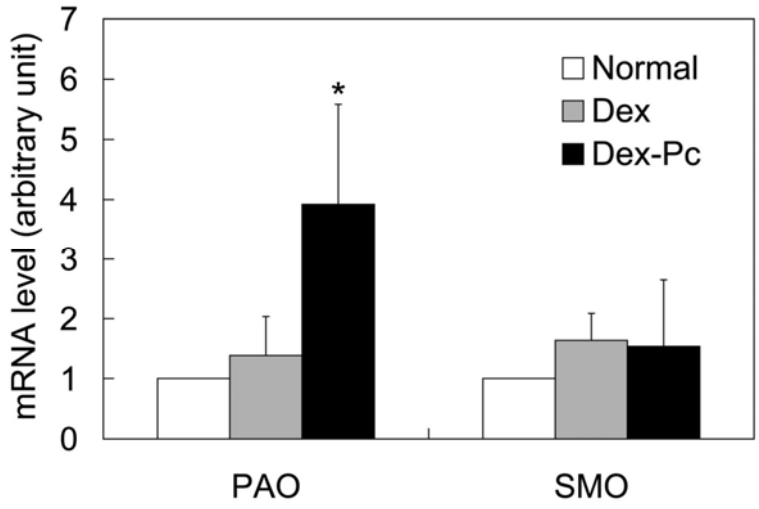

Fig. 21. PAO and SMO mRNA expressions in AMs. mRNA levels of PAO and SMO in AMs from Normal, Dex, and Dex-Pc rats were determined by real time RT-PCR. Results represent means ± SD from 5 experiments. Asterisk (*) indicates $p < 0.05$ as compared to Dex control.

PAO Protein Expression in AMs

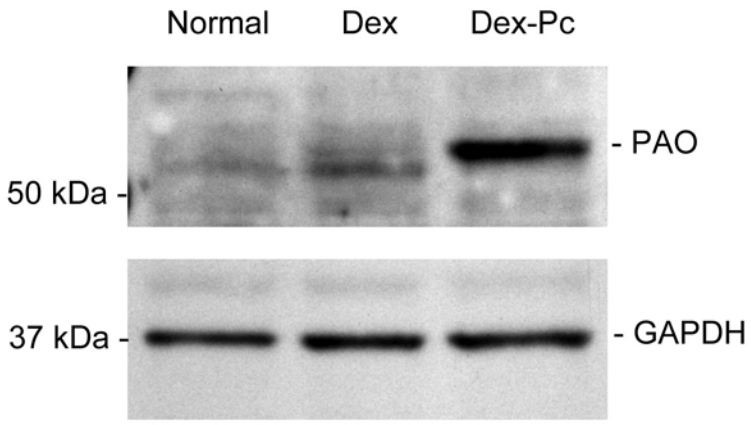

Fig. 22. PAO protein expression in AMs. Protein levels of PAO in AMs from Normal, Dex, and Dex-Pc rats were determined by Western blotting.

PAO and SMO Activities in AMs

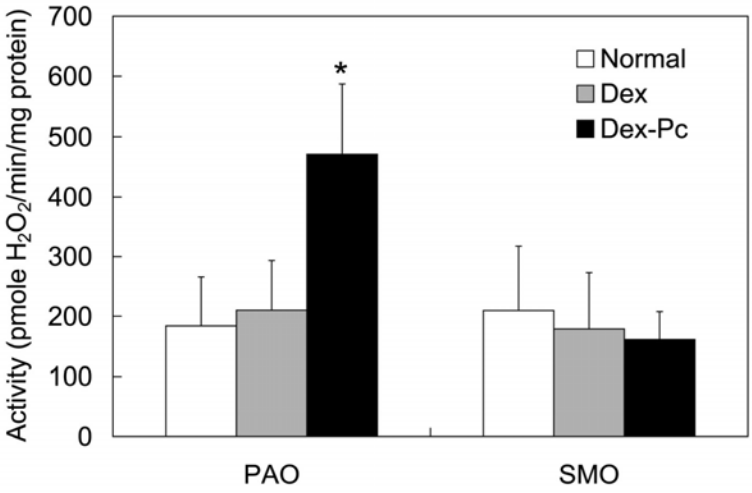

Fig. 23. PAO and SMO activities in AMs. The enzyme activities of PAO and SMO in AMs from Normal, Dex, and Dex-Pc rats were determined. Results represent mean ± S.D. from 5 experiments. Asterisk (*) indicates $p < 0.05$ as compared to Dex control.

Polyamines Induce PAO mRNA Expression

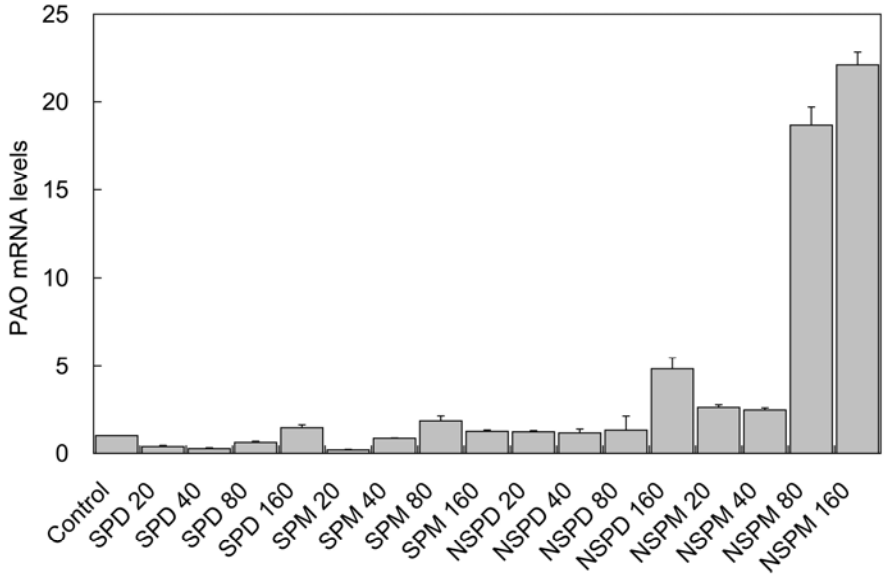

Fig. 24. Polyamines induce PAO mRNA expression. RAW 264.7 cells were incubated with spermidine (SPD), spermine (SPM), N1-acetylspermidine (NSPD), and N1-acetylspermine (NSPM) at indicated concentrations (20-160 μM) for 24 hr. The PAO mRNA levels of polyamine-treated cells were analyzed by real time RT-PCR. Results represent mean ± S.D. from five analyses.

Polyamines Induce PAO Protein Expression

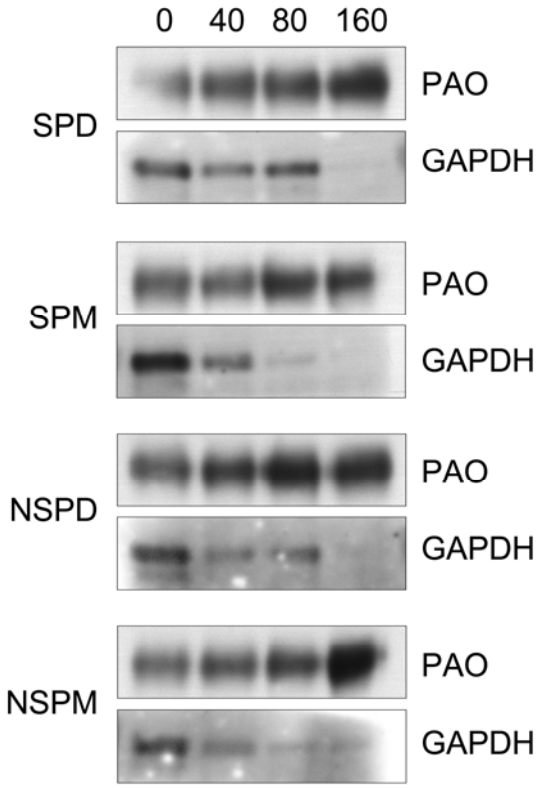

Fig. 25. Polyamines induce PAO protein expression. RAW 264.7 cells were incubated with spermidine (SPD), spermine (SPM), N1-acetylspermidine (NSPD), and N1-acetylspermine (NSPM) at indicated concentrations (0-160 μM) for 24 hr. The PAO protein levels of polyamine-treated cells were analyzed by Western blotting.

Structures of Polyamine Transport Inhibitors

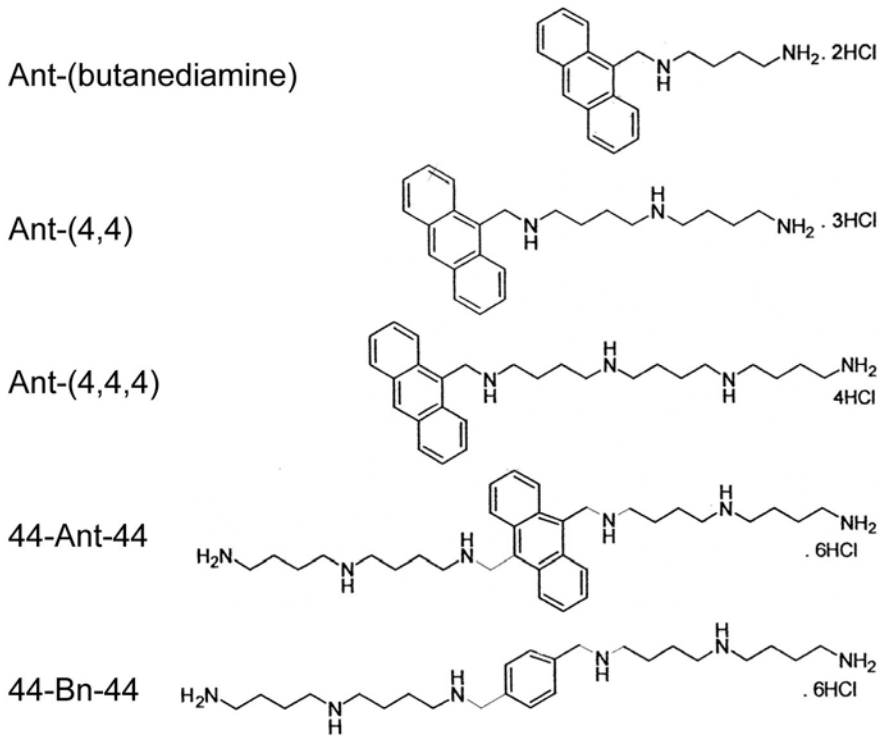

Fig. 26. Structures of polyamine transport inhibitors.

Cytotoxicity of Polyamine Transport Inhibitors

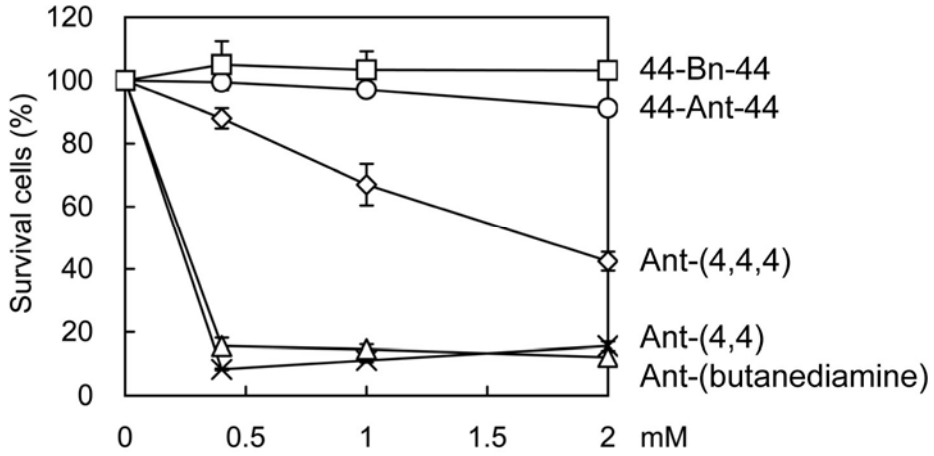

Fig. 27. Cytotoxicity of polyamine transport inhibitors. AMs from normal rats were incubated with polyamine transport inhibitors at indicated concentrations for 3 hr and then examined for viability by the Trypan blue exclusion method.

Rat Survival after 44-Ant-44 and 44-Bn-44 Treatments

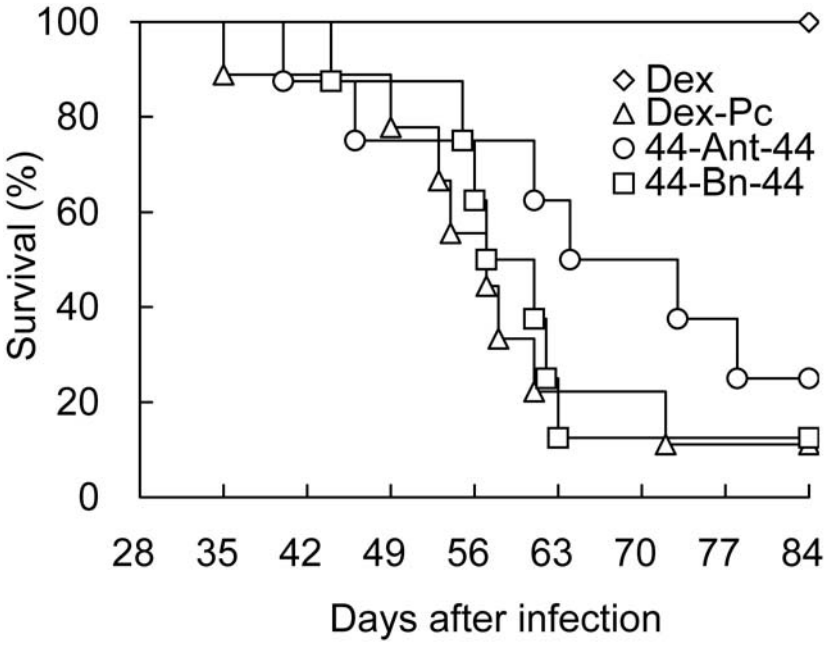

Fig. 28. Rat survival after 44-Ant-44 and 44-Bn-44 treatments. Eight rats each with PcP (Dex-Pc rats) were treated with 44-Ant-44 or 44-Bn-44 by intranasal instillation of 50 µl of 1 mM of the compound every two days starting at the 28th day after infection. Untreated Dex-Pc (n = 9) and uninfected Dex (n = 4) rats were used as controls. The numbers of treated and untreated rats survived were recorded daily for 84 days from the day of infection.

Pulmonary Pathology after 44-Ant-44 and 44-Bn-44 Treatments

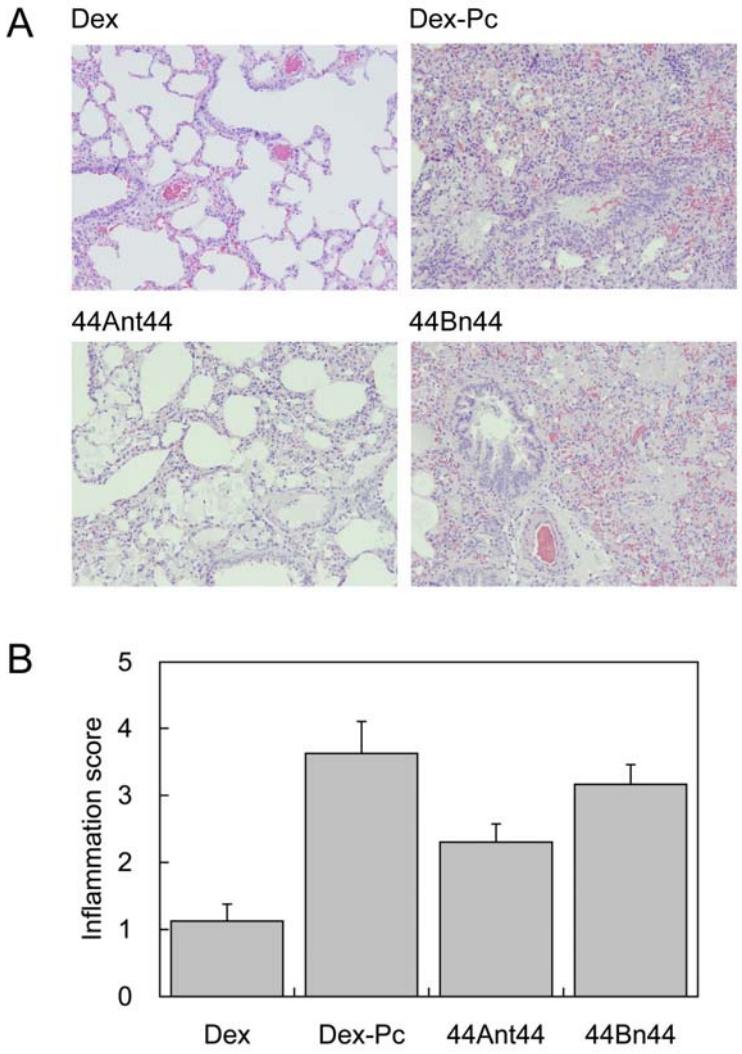

Fig. 29. Pulmonary pathology after 44-Ant-44 and 44-Bn-44 treatments. The effects of 44-Ant-44 and 44-Bn-44 on PcP-mediated pulmonary damage were examined after three weeks of treatment. (A) Microscopic observation of H&E stained lung sections (magnification = 100 ×). (B) Severity of inflammation. The degree of inflammation was graded with a scale of 0 to 5. Results shown are representative images or means ± SD of three 44-Bn-44-treated, five 44-Ant-44-treated, and four untreated Dex and Dex-Pc rats. Asterisk (*) indicates $p < 0.05$ as compared to Dex-Pc group.

***Pneumocystis* Burden after 44-Ant-44 and 44-Bn-44 Treatments**

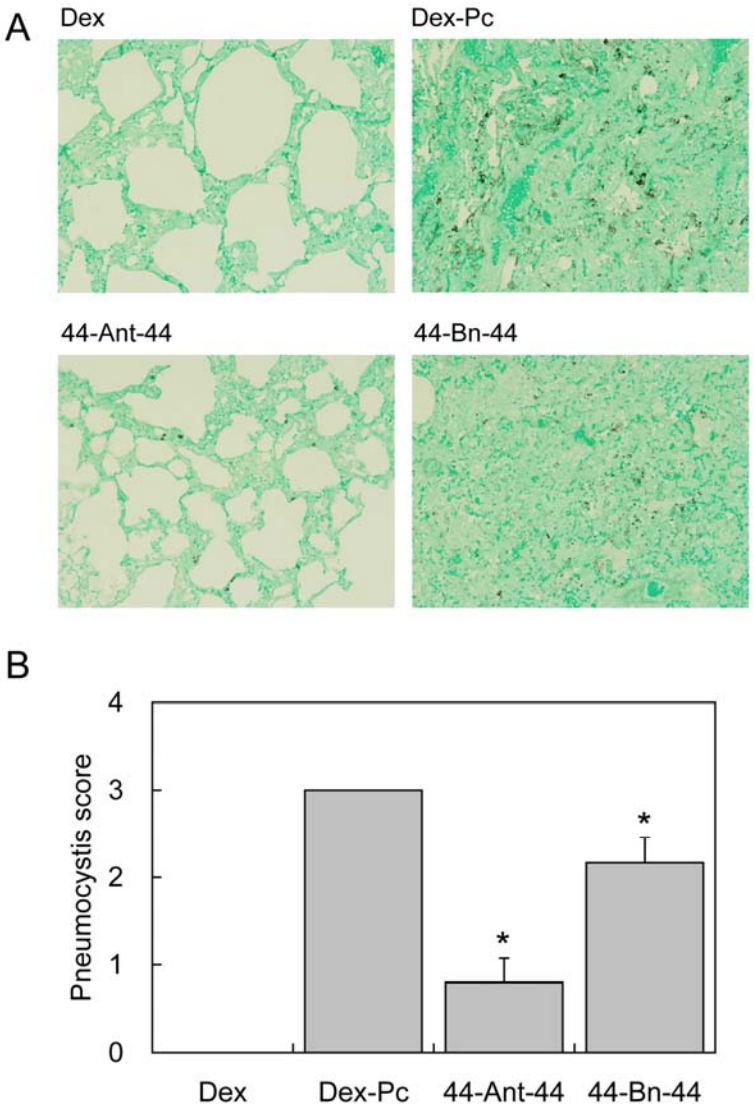

Fig. 30. *Pneumocystis* burden after 44-Ant-44 and 44-Bn-44 treatments. The effects of 44-Ant-44 and 44-Bn-44 on *Pneumocystis* burden were examined by silver staining on lungs after three weeks of treatment. (A) Microscopic observation of silver-stained lung sections (magnification = 100 ×). (B) Organism burden was scored 0 to 4. Results shown are representative images or means ± SD of three 44-Bn-44-treated, five 44-Ant-44-treated, and four untreated Dex and Dex-Pc rats. Asterisk (*) indicates $p < 0.05$ as compared to Dex-Pc group.

AM Apoptosis after 44-Ant-44 and 44-Bn-44 Treatments

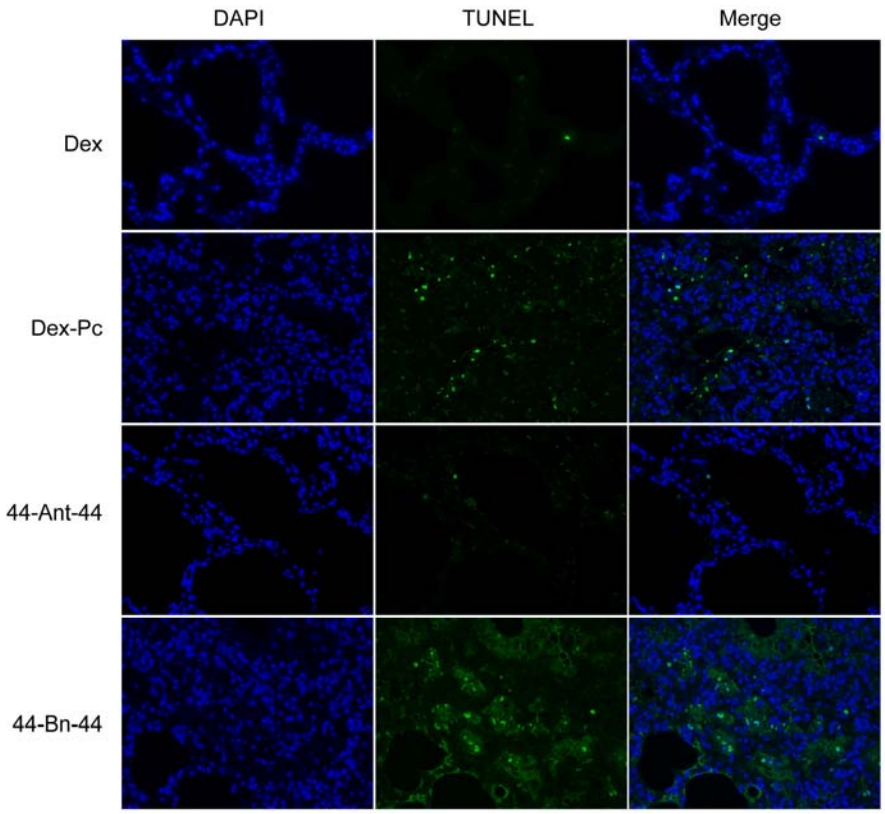

Fig. 31. AM Apoptosis after 44-Ant-44 and 44-Bn-44 treatments. The effects of 44-Ant-44 and 44-Bn-44 on pulmonary apoptosis was examined by TUNEL assay performed on lung sections after three weeks of treatment. Green dots represent the nuclei of apoptotic cells. Cell nuclei were stained blue with DAPI. Magnification = 100 ×. Results shown are representative images of three 44-Bn-44-treated, five 44-Ant-44-treated, and four untreated Dex and Dex-Pc rats.

DISCUSSION

Polyamines are essential molecules for all cells. However, elevated levels of intracellular polyamines are associated with diseases, such as cancers (38) and with susceptibility to infections by microorganisms such as *H. pylori* (32) and *Pneumocystis* (105). The levels of spermidine, N1-acetylspermidine, and N1-acetylspermine in both the alveoli and AMs are elevated, leading to increased rate of AM apoptosis during PCP (105). In this study, possible mechanisms for the great increase in polyamine levels were investigated. The transcription of the ODC gene, which encodes the key enzyme in polyamine synthesis in AMs was found not affected by *Pneumocystis* infection. However, the ODC protein level in AMs was greatly (8 fold) increased during PCP (Fig. 5), indicating that the balance between ODC synthesis and degradation is altered during *Pneumocystis* infection. As described above, the ODC protein level is controlled by both OAZ and AZI. OAZ binds to ODC and transports it to the 26s proteasome for degradation, whereas AZI competes with ODC for binding to OAZ. When AZI binds to OAZ, less ODC is degraded and thus a steady-state level of polyamines in the cells is maintained. Since OAZ mRNA and protein levels were not changed (Fig. 11) but both the mRNA (3 fold) and protein (6 fold) levels of AZI were greatly increased (Fig. 12), it is likely that the ODC turnover rate in AMs during PCP is decreased due to AZI overexpression. The result that AZI knockdown by siRNA decreased the ODC protein level by 60% (Fig. 14) confirmed this possibility, although the intracellular polyamine levels afte AZI knockdown were not measured. Higher polyamine synthesis during PCP was demonstrated by an IHC experiment in which ODC-positive cells, mainly

inflammatory cells, were shown to react with the anti-spermidine antibody (Fig. 10 & Table 1), indicating polyamine synthesis in these cells.

This study used rats instead of mice as PCP model mainly to take advantage of much higher alveolar macrophage yields. Since the rats were immunosuppressed with dexamethasone, there is always a concern whether dexamethasone also affects ODC expression or activity. To control for this effect, both normal and dexamethasone-treated rats were used as controls. In all the experiments performed in this study, results derived from dexamethasone-treated rats were very similar to those from normal rats. Therefore, dexamethasone did not appear to have a significant effect on polyamine synthesis or uptake examined in this study. Previous studies by another group showed that treatment of normal rats with dexamethasone actually decreased ODC activity in their lungs (13). Therefore, the increased ODC activity observed in alveolar macrophages during PCP was not due to dexamethasone treatment but due to *Pneumocystis* infection.

An interesting finding in this study is that ODC distribution in inflammatory cells was changed from cytoplasmic to pericytoplasmic (Fig. 9). ODC translocation has been shown to be associated with cell cycle progression (186) or cell activation and transformation (72). Since inflammatory cells are activated when they are recruited to the lung, it is very likely that the change in ODC distribution is due to cell activation during PCP and that this activation leads to elevated polyamine synthesis.

In addition to increased synthesis, increased uptake of exogenous polyamines is another possible cause of elevated polyamine levels in AMs during PCP. However, polyamine transporters in mammalian cells remain largely unknown. Synthetic fluorescent polyamines have been used to explore mammalian polyamine transport systems (23, 127, 128), and a receptor-mediated endocytosis mechanism has been

suggested (23, 127). Another study showed that polyamine uptake was unaffected in endocytosis-deficient cells and that the internalized polyamines were colocalized with acidic vesicles of the late endocytic compartment and the trans Golgi (128). This finding suggests that polyamines are imported by a membrane carrier (128). The mammalian polyamine transport systems appear to have a broad substrate specificity and can transport a variety of polyamines (41). Therefore, it is possible that the spermidine uptake system (Fig. 7) is also responsible for the uptake of N1-acetylspermidine and N1-acetylspermine into AMs during PCP. Polyamine uptake assays are commonly performed using radioactive polyamines (50, 117, 147). Aziz et al. (9) and Aouida et al. (1) used fluorescein-labeled polyamines to perform these assays in cultured cells and yeasts by fluorescence microscopy. It was demonstrated that the fluorescein moiety does not affect the transport of polyamines (9). In this study, fluorescein-labeled spermidine was used to investigate polyamine uptake in *Pneumocystis*-infected rats showed for the first time that FAM-labeled spermidine can be used for polyamine uptake assay *in vivo* (Fig. 7).

Although the number of AMs which took up fluorescent spermidine (FAM-SPD) in the polyamine uptake assay was found to be 20 fold higher in *Pneumocystis*-infected than in uninfected rats, only approximately 2% of AMs in *Pneumocystis*-infected rats internalized FAM-SPD (Fig. 7). The reason for this low number of cells taking up FAM-SPD is unknown. It may be that most AMs in *Pneumocystis*-infected lungs already contain high levels of polyamines (105) and are no longer able to take up exogenous polyamines. The AMs that took up FAM-SPD in the polyamine uptake assay were probably those containing lower levels of intracellular polyamines. This possibility remains to be investigated.

Since overexpression of AZI has been shown to increase polyamine uptake (88), it is conceivable that the increased level of AZI in AMs contributes to this increased uptake of exogenous polyamines. The result that AZI expression knockdown by siRNA decreased the number of cells that can take up polyamines by 50% (Fig. 15) strongly supports this possibility. A likely source of exogenous polyamines is *Pneumocystis* organisms, as they have been shown to produce and secrete polyamines, mainly N1-acetylspermine and N1-acetylspermidine (134). Since SSAT levels were not increased in AM during PCP (Fig. 4 & 5), the elevated levels of acetylated polyamines in AMs are more likely due to uptake of such polyamines from exogenous sources. Like SSAT, the expression level of the spermidine synthase, which converts putrescine to spermidine, was also not increased in AM during PCP (Fig. 4), suggesting that spermidine synthase is not responsible for the increased spermidine level. It is possible that the increased spermidine level is due to conversion of N1-acetylspermine to spermidine.

Pneumocystis has been shown to produce and excrete high levels of N1-acetylspermine and N1-acetylspermidine due to high levels of polyamine catabolism rate in an *in vitro* study (134). Taken together with the results that SSAT expression was not increased in AMs during PCP, the high levels of these acetylated polyamines in AMs during PCP are likely due to uptake of polyamines produced by *Pneumocystis*. To investigate whether other host cells could also contribute to the acetylated polyamine pool, IHC staining for SSAT on lungs with PCP was performed; unfortunately, the results showed too much background and were not interpretable. A recent unpublished data (from Dr. Merali, Temple University) indicated that AMs from SSAT-KO mice with PCP also contain high levels of N1-acetylspermine and N1-acetylspermidine. These results

further suggest that the increased levels of acetylated polyamines in AMs during PCP are more likely due to uptake of acetylated polyamines produced by *Pneumocystis*.

In addition to *Pneumocystis* organisms, inflammatory cells are another possible source of polyamines as they were stained positive for ODC (Table 1), and spermidine levels were high in these cells (Fig. 10). These cells were mainly located around blood vessels and bronchioles (Fig. 10) and therefore are considered inflammatory cells that are recruited into the lung during PCP. Approximately 25% of the total lung cells from infected rats were ODC positive. These inflammatory cells were shown by flow cytometry to be CD4+ T cells (1.83%), CD8+ T cells (9.79%), B cells (9.79%), and CD68+ cells (7.80%) that may be monocytes or macrophages. In this study, ODC was found to be present only in inflammatory cells by IHC staining (Fig. 9) and flow cytometry (Table 1), indicating that ODC levels are higher in inflammatory cells than in other types of pulmonary cells and these inflammatory cells could possiblely contribute to the exogenenous polyamine pool. However, these polyamines must be transported through pulmonary parenchyma to alveoli. Such transport system has not been identified.

Conversion of N1-acetylspermine to spermidine and N1-acetylspermidine to putrescine by PAO is accompanied by the production of H_2O_2 which may damage mitochondria leading to induction of apoptosis. This mechanism is thought to be responsible for the loss of AMs during PCP as ROS levels are increased in AMs during PCP (105). Since the mRNA, protein expression, and enzymatic activity levels of PAO were all increased in AMs during PCP (Fig. 21, 22 & 23), it is conceivable that the ROS generated by PAO plays an important role in AM apoptosis during *Pneumocystis* infection. It is possible that PAO overexpression in AMs during PCP is induced by the increased intracellular levels of PAO substrates N1-acetylspermidine and

N1-acetylspermine (105). Although attempts were made to measure H_2O_2 levels in AMs, the readings from all groups were too low to interpretate, probably due to the fast conversion among different ROS.

An important finding in this study is that AZI expression knockdown by siRNA resulted in a 53% decrease in the number of apoptotic AMs (Fig. 16), a 58% decrease in cytosolic cytochrome c levels (Fig. 17), and a 75% decrease in the level of activated caspase-3 (Fig. 18). This result indicates that decreasing AZI protein levels also decreases the apoptosis rate of AMs. It is possible that the reduction in AZI levels causes a decreased uptake of exogenous acetylated polyamines; therefore, less acetylated polyamines are available to be converted to regular polyamines, and thus less H_2O_2 is produced to trigger apoptosis. This is the first demonstration that AZI is involved in apoptosis. A previous study showed that transfection of the gene encoding OAZ, the negative regulator of AZI, can also to induce apoptosis by activating mitochondrial depolarization and caspase cascade (83). It is not surprising that both OAZ and AZI have a pro-apoptotic activity due to the multiple roles of polyamines (38, 122).

Polyamines have also been found to be involved in the pathogenesis of *Helicobacter pylori*. *H. pylori* activates the transcriptional factor c-Myc which induces ODC expression, resulting in increased intracellular polyamine pools in macrophages (18). This polyamine accumulation greatly reduces the uptake of L-arginine which is the substrate of inducible nitric oxide synthase (iNOS) and is also the rate-limiting factor for iNOS translation (31). Therefore, increased polyamine levels consequently decrease the synthesis of iNOS in macrophages and result in loss of innate immune responses against *H. pylori* infection (10). *H. pylori* also activates SMO to convert spermidine to spermine accompanied by generation of H_2O_2 which causes macrophages to undergo apoptosis (16,

166). Therefore, induction of apoptosis by polyamines appears to be a survival mechanism for microbes to evade the clearance by immune systems.

Although both *Pneumocystis* and *H. pylori* cause macrophages to undergo apoptosis due to elevated levels of polyamines, the mechanisms in polyamine acquisition are different. Unlike *H. pylori*, *Pneumocystis* does not upregulate ODC synthesis. Instead, it upregulates AZI expression leading to increased uptake of exogenous polyamines and decreased degradation of ODC thus increasing polyamine synthesis. Therefore, the increase in polyamine levels in AMs during PCP is due to both increased uptake and polyamine synthesis. Upregulation of AZI expression has also been shown in other diseases. A comparative clinical study showed that gastric cancer tissue removed during surgery expresses higher levels of AZI than the surrounding normal tissue (83). Oncogene Ras transformed NIH3T3 cells also have increased AZI expression (88). Although AZI levels have been shown to be increased in a number of conditions, the mechanisms for AZI overexpression were largely unknown. In this study, both *Pneumocystis* organisms and zymosan A were found to induce AZI expression in a dose-dependent manner (Fig. 20). Since the major component of zymosan A is β-glucan which is also the major component of *Pneumocystis* cell wall, it is very likely that β-glucan induces AZI overexpression in AMs. The dectin-1 receptor has been shown to be the main receptor for β-glucan on AMs (23), and binding of β-glucan to dectin-1 has been shown to activate the NF-κB signaling pathway (65). Therefore, it is possible that AZI expression is regulated by NF-κB. This possibility is being investigated.

The phenomenon of increased polyamine levels in AMs during PCP is very similar to that in cancers. The major cause of increase in polyamine levels in cancer cells is increased synthesis of polyamines due to increased levels of ODC. Therefore, inhibition

of ODC activity with DFMO is a potential therapy for cancer. Unfortunately, clinical trials show that DFMO has no or little effect against cancers (114, 159, 224). One possible reason for this treatment failure is the increased uptake of exogenous polyamines, which compensates the loss of polyamine synthesis during DFMO therapy (74).

Although DFMO therapy has not been successful in cancer, it was found to be very effective against trypanosomiasis. The selective toxicity of DFMO to *Trypanosoma* is probably due to the huge difference in the half-life of *Trypanosoma* (more than 10 hr) and mammalian ODC (10 - 20 min). Since *Trypanosoma* ODC has a very long half-life, ODC molecule numbers may be low. Therefore, *Trypanosoma* ODC is more susceptible to DFMO inhibition. In addition, *Trypanosoma* do not have a mechanism of exogenous polyamine uptake to compensate for the loss of polyamines synthesis due to DFMO treatment (11).

DFMO has also been used to treat PcP. The effect of DFMO on *Pneumocystis*-infected animals is controversial. One animal study showed that *Pneumocystis*-infected rats receiving 3% DFMO in drinking water had a significant decrease in organism burden after three weeks of treatment ($p < 0.001$) (36). In contrast, another study showed that DFMO was ineffective against PCP under a similar treatment condition (229). Human clinical trials revealed that 57% of patients with PCP responded to DFMO treatment (192), suggesting that inhibition of polyamine synthesis is a viable therapeutic approach against PcP.

The actual target of DFMO in the treatment of PCP is not well defined. ODC activity was reported to be absent in *Pneumocystis* organisms in at least two independent studies (120, 167). In this case, host ODC would be the only target of DFMO. However,

a later study reported the presence of ODC activity in dialyzed *Pneumocystis* extracts (185). Another study performed by the same group demonstrated that polyamine levels in *Pneumocystis* extracts were decreased after DFMO treatment. This result supports their conclusion as to the presence of *Pneumocystis* ODC, and its potential as a target of DFMO (135).

Although DFMO has a certain degree of therapeutic activity against PCP, it is not completely effective, indicating that targeting polyamine synthesis alone is not sufficient for PcP treatment. Our previously studies have found that AM apoptosis is a cause of disease progression during PcP (103) and that this apoptosis is triggered by increased polyamine levels due to both increased synthesis and uptake of polyamines (115). These findings may explain the partial success of DFMO therapy against PCP, because DFMO only inhibits polyamine synthesis, not uptake.

In this study, we used aryl-polyamine conjugates, which target the polyamine transport (PAT) with high affinity and inhibit uptake of native polyamines. Two compounds, 44-Ant-44 and 44-Bn-44, were tested *in vivo*, and 44-Ant-44 was found to reduce organism burden (Fig. 30), decrease lung inflammation (Fig. 29), and prolonged survival of treated PcP animals by more than eight days (Fig. 28). It is possible that the effectiveness of this treatment is due to decreased rate of apoptosis of AMs (Fig. 31) as polyamine transport ligands would block polyamine uptake and thus decrease the levels of intracellular polyamines. This action leads to decreased production of H_2O_2. As the result, AMs survive to clear the organisms, thus reducing organism burden and lung inflammation leading to longer survival.

Polyamine transport inhibitors can be structurally classified into two major types: polyamine polymer and polyamine-lysine conjugate. The homodimers of putrescine (39)

and spermine (66, 79) and polymer of spermine (8) have been shown to effectively inhibit polyamine transport. Simple lysine-spermine conjugate (34, 238) and lipophilic lysine-spermine (26) also exhibit polyamine transport inhibition activity. 44-Ant-44, the compound shown to have anti-PCP activity in this study, is structurally similar to a spermidine dimer crosslinked by a 9,10-bis-substituted-anthraldehyde.

In a recent report, 44-Ant-44 was shown to have the highest polyamine transport inhibition activity in a Chinese hamster ovary (CHO) screen (86, 169). The screen utilized two CHO cell lines: the PAT-active wild type CHO K-1 line and the PAT-defective CHO-MG line. Comparison of conjugate cytotoxicity in these two CHO lines provided an important tool to detect selective conjugate delivery via the PAT. A conjugate with high utilization of the PAT would be very toxic to CHO cells, but less so to CHO-MG cells. Highly selective PAT ligands should give high (CHO-MG/CHO) IC_{50} ratios. As shown in Table 1, 44-Ant-44 and 44-Bn-44 were the most PAT-selective of the series with CHO-MG/CHO IC_{50} ratios >600. One potential explanation of why 44-Ant-44 was superior to the benzyl derivative 44-Bn-44 is cellular metabolism. For example, a benzyl-homospermidine model compound was shown to be metabolized to homospermidine in cell culture, whereas the anthryl-homospermidine was not (232). This is rationalized due to significant steric constraints near the benzylic position of the anthryl platform, which may impede the action of amine oxidases (169).

Although, inhibition of polyamine uptake with compound 44-Ant-44 showed impressive results, it did not cure the disease. This is expected as the increase of both ODC levels and uptake of exogenous polyamines account for the increased polyamine levels during PCP. Studies using both the ODC inhibitor DFMO and polyamine transport ligand 44-Ant-44 to treat PCP are being conducted. This combination therapy is expected

to be a more effective PCP treatment as a synergistic effect has been shown in cancer therapy (26, 34). Because of the limited supply of the compound, only one dosage and one treatment condition were tested in the current study. Additional dosages remain to be tested to determine whether a lower dose also works or whether a higher dose of the compound would be more effective. Other methods of drug delivery, such as placing the drug in drinking water, also need to be explored. Successful development of combination therapy may have a great impact on cancer therapy, as cancers also have increased polyamine synthesis and uptake (61, 182).

FUTURE STUDIES

Based on results of this study, the following studies should be conducted to further characterize polyamine-mediated apoptosis of AMs and to develop polyamine transport as a target for treatment of PCP.

1. Investigate the mechanisms by which *Pneumocystis* induces AZI over-expression. The possibility that *Pneumocystis* β-glucan stimulates AMs to increase AZI expression needs to be confirmed. Other *Pneumocystis* components such as MSG, mannan, and chitin that may also be involved in *Pneumocystis*-induced AZI over-expression should be identified, and the receptors that transmit the signal leading to AZI over-expression need to be determined. The transcription factors that cause AZI over-expression in AMs during PCP should also be investigated.

2. Investigate blocking polyamine transport as a target for treatment of PCP. The PAT inhibitor 44-Ant-44 shows promise as a therapy for PCP, based upon the observation that it prolonged the survival of animals with PCP. In order to evaluate its potential usefulness, the optimal dosage, delivery route, and frequency of 44-Ant-44 administration need to be determined. Additional PAT inhibitors or derivatives of 44-Ant-44 need to be developed and tested to identify the most effective PAT inhibitor for therapy of PCP. Treatment of PCP with PAT inhibitor(s) alone and in combination with the polyamine synthesis inhibitor DFMO or the conventional therapy of TMP/SMZ for therapeutic efficacy against PCP in animal models should be conducted.

3. Investigate polyamine metabolism as a target for treatment of PCP. PAO expression and activity are increased in AMs during PCP, leading to production of excess H_2O_2 that triggers AMs to undergo apoptosis. The possibility that inhibiting PAO activity will prevent AMs from undergoing apoptosis and prolong the survival of infected animals need to be examined.

REFERENCES

1. **Alhonen-Hongisto, L., P. Seppanen, and J. Janne.** 1980. Intracellular putrescine and spermidine deprivation induces increased uptake of the natural polyamines and methylglyoxal bis(guanylhydrazone). Biochem J **192:**941-5.
2. **Aliouat, E. M., E. Dei-Cas, L. Dujardin, J. P. Tissier, P. Billaut, and D. Camus.** 1996. High infectivity of Pneumocystis carinii cultivated on L2 rat alveolar epithelial cells. J Eukaryot Microbiol **43:**22S.
3. **Almrud, J. J., M. A. Oliveira, A. D. Kern, N. V. Grishin, M. A. Phillips, and M. L. Hackert.** 2000. Crystal structure of human ornithine decarboxylase at 2.1 A resolution: structural insights to antizyme binding. J Mol Biol **295:**7-16.
4. **Aouida, M., A. Leduc, R. Poulin, and D. Ramotar.** 2005. AGP2 encodes the major permease for high affinity polyamine import in Saccharomyces cerevisiae. J Biol Chem **280:**24267-76.
5. **Atochina, E. N., J. M. Beck, A. M. Preston, A. Haczku, Y. Tomer, S. T. Scanlon, T. Fusaro, J. Casey, S. Hawgood, A. J. Gow, and M. F. Beers.** 2004. Enhanced lung injury and delayed clearance of Pneumocystis carinii in surfactant protein A-deficient mice: attenuation of cytokine responses and reactive oxygen-nitrogen species. Infect Immun **72:**6002-11.
6. **Atochina, E. N., J. M. Beck, S. T. Scanlon, A. M. Preston, and M. F. Beers.** 2001. Pneumocystis carinii pneumonia alters expression and distribution of lung collectins SP-A and SP-D. J Lab Clin Med **137:**429-39.

7. **Atzori, C., E. M. Aliouat, M. S. Bartlett, L. Dujardin, A. Cargnel, and E. Dei-Cas.** 1998. Current in vitro culture systems for Pneumocystis. FEMS Immunol Med Microbiol **22:**169-72.

8. **Aziz, S. M., M. P. Gosland, P. A. Crooks, J. W. Olson, and M. N. Gillespie.** 1995. A novel polymeric spermine conjugate inhibits polyamine transport in pulmonary artery smooth muscle cells. J Pharmacol Exp Ther **274:**181-6.

9. **Aziz, S. M., M. Yatin, D. R. Worthen, D. W. Lipke, and P. A. Crooks.** 1998. A novel technique for visualizing the intracellular localization and distribution of transported polyamines in cultured pulmonary artery smooth muscle cells. J Pharm Biomed Anal **17:**307-20.

10. **Bacchi, C. J., H. C. Nathan, S. H. Hutner, P. P. McCann, and A. Sjoerdsma.** 1980. Polyamine metabolism: a potential therapeutic target in trypanosomes. Science **210:**332-4.

11. **Bacchi, C. J., and N. Yarlett.** 2002. Polyamine metabolism as chemotherapeutic target in protozoan parasites. Mini Rev Med Chem **2:**553-63.

12. **Bartlett, M. S., J. A. Fishman, S. F. Queener, M. M. Durkin, M. A. Jay, and J. W. Smith.** 1988. New rat model of Pneumocystis carinii infection. J Clin Microbiol **26:**1100-2.

13. **Bartolome, J. V., S. Wang, N. L. Greer, and S. M. Schanberg.** 1999. Glucocorticoid regulation of ornithine decarboxylase in the postnatal rat lung. Life Sci **64:**895-904.

14. **Beck, J. M., H. D. Liggitt, E. N. Brunette, H. J. Fuchs, J. E. Shellito, and R. J. Debs.** 1991. Reduction in intensity of Pneumocystis carinii pneumonia in mice by aerosol administration of gamma interferon. Infect Immun **59:**3859-62.

15. **Beck, J. M., R. L. Newbury, B. E. Palmer, M. L. Warnock, P. K. Byrd, and H. B. Kaltreider.** 1996. Role of CD8+ lymphocytes in host defense against Pneumocystis carinii in mice. J Lab Clin Med **128:**477-87.

16. **Beck, J. M., A. M. Preston, J. G. Wagner, S. E. Wilcoxen, P. Hossler, S. R. Meshnick, and R. Paine, 3rd.** 1998. Interaction of rat Pneumocystis carinii and rat alveolar epithelial cells in vitro. Am J Physiol **275:**L118-25.

17. **Benfield, T. L., B. Lundgren, S. J. Levine, G. Kronborg, J. H. Shelhamer, and J. D. Lundgren.** 1997. The major surface glycoprotein of Pneumocystis carinii induces release and gene expression of interleukin-8 and tumor necrosis factor alpha in monocytes. Infect Immun **65:**4790-4.

18. **Benfield, T. L., B. Lundgren, J. H. Shelhamer, and J. D. Lundgren.** 1999. Pneumocystis carinii major surface glycoprotein induces interleukin-8 and monocyte chemoattractant protein-1 release from a human alveolar epithelial cell line. Eur J Clin Invest **29:**717-22.

19. **Benfield, T. L., P. Prento, J. Junge, J. Vestbo, and J. D. Lundgren.** 1997. Alveolar damage in AIDS-related Pneumocystis carinii pneumonia. Chest **111:**1193-9.

20. **Benfield, T. L., J. Vestbo, J. Junge, T. L. Nielsen, A. B. Jensen, and J. D. Lundgren.** 1995. Prognostic value of interleukin-8 in AIDS-associated Pneumocystis carinii pneumonia. Am J Respir Crit Care Med **151:**1058-62.

21. **Bercovich, Z., and C. Kahana.** 2004. Degradation of antizyme inhibitor, an ornithine decarboxylase homologous protein, is ubiquitin-dependent and is inhibited by antizyme. J Biol Chem **279:**54097-102.

22. **Bey, P., F. N. Bolkenius, N. Seiler, and P. Casara.** 1985. N-2,3-Butadienyl-1,4-butanediamine derivatives: potent irreversible inactivators of mammalian polyamine oxidase. J Med Chem **28:**1-2.

23. **Brown, G. D.** 2006. Dectin-1: a signalling non-TLR pattern-recognition receptor. Nat Rev Immunol **6:**33-43.

24. **Brown, G. D., and S. Gordon.** 2001. Immune recognition. A new receptor for beta-glucans. Nature **413:**36-7.

25. **Burgess, J. W., T. J. Kottom, and A. H. Limper.** 2008. Pneumocystis carinii exhibits a conserved meiotic control pathway. Infect Immun **76:**417-25.

26. **Burns, M. R., G. F. Graminski, R. S. Weeks, Y. Chen, and T. G. O'Brien.** 2009. Lipophilic lysine-spermine conjugates are potent polyamine transport inhibitors for use in combination with a polyamine biosynthesis inhibitor. J Med Chem **52:**1983-93.

27. **Carinii, A.** 1910. Formas de eschizogonia do Trypanozoma lewisi. Comm. Soc. Med. Sao Paolo **16:**204.

28. **Carmona, E. M., R. Vassallo, Z. Vuk-Pavlovic, J. E. Standing, T. J. Kottom, and A. H. Limper.** 2006. Pneumocystis cell wall beta-glucans induce dendritic cell costimulatory molecule expression and inflammatory activation through a Fas-Fas ligand mechanism. J Immunol **177:**459-67.

29. **Casanova-Cardiel, L., and M. J. Leibowitz.** 1997. Presence of Pneumocystis carinii DNA in pond water. J Eukaryot Microbiol **44:**28S.

30. **Chagas, C.** 1909. Nova tripanozomiata humana. Mem. Inst. Oswaldo Cruz **94:**159-218.

31. **Chaturvedi, R., M. Asim, N. D. Lewis, H. M. Algood, T. L. Cover, P. Y. Kim, and K. T. Wilson.** 2007. L-arginine availability regulates inducible nitric oxide synthase-dependent host defense against Helicobacter pylori. Infect Immun **75:**4305-15.

32. **Chaturvedi, R., Y. Cheng, M. Asim, F. I. Bussiere, H. Xu, A. P. Gobert, A. Hacker, R. A. Casero, Jr., and K. T. Wilson.** 2004. Induction of polyamine oxidase 1 by Helicobacter pylori causes macrophage apoptosis by hydrogen peroxide release and mitochondrial membrane depolarization. J Biol Chem **279:**40161-73.

33. **Chen, W., E. A. Havell, and A. G. Harmsen.** 1992. Importance of endogenous tumor necrosis factor alpha and gamma interferon in host resistance against Pneumocystis carinii infection. Infect Immun **60:**1279-84.

34. **Chen, Y., R. S. Weeks, M. R. Burns, D. W. Boorman, A. Klein-Szanto, and T. G. O'Brien.** 2006. Combination therapy with 2-difluoromethylornithine and a polyamine transport inhibitor against murine squamous cell carcinoma. Int J Cancer **118:**2344-9.

35. **Choi, K. S., Y. H. Suh, W. H. Kim, T. H. Lee, and M. H. Jung.** 2005. Stable siRNA-mediated silencing of antizyme inhibitor: regulation of ornithine decarboxylase activity. Biochem Biophys Res Commun **328:**206-12.

36. **Clarkson, A. B., Jr., D. E. Williams, and C. Rosenberg.** 1988. Efficacy of DL-alpha-difluoromethylornithine in a rat model of Pneumocystis carinii pneumonia. Antimicrob Agents Chemother **32:**1158-63.

37. **Coleman, C. S., and A. E. Pegg.** 2001. Polyamine analogues inhibit the ubiquitination of spermidine/spermine N1-acetyltransferase and prevent its targeting to the proteasome for degradation. Biochem J **358:**137-45.

38. **Coleman, C. S., and A. E. Pegg.** 1997. Proteasomal degradation of spermidine/spermine N1-acetyltransferase requires the carboxyl-terminal glutamic acid residues. J Biol Chem **272:**12164-9.

39. **Covassin, L., M. Desjardins, D. Soulet, R. Charest-Gaudreault, M. Audette, and R. Poulin.** 2003. Xylylated dimers of putrescine and polyamines: influence of the polyamine backbone on spermidine transport inhibition. Bioorg Med Chem Lett **13:**3267-71.

40. **Crabtree, G. R., and E. N. Olson.** 2002. NFAT signaling: choreographing the social lives of cells. Cell **109 Suppl:**S67-79.

41. **Cullis, P. M., R. E. Green, L. Merson-Davies, and N. Travis.** 1999. Probing the mechanism of transport and compartmentalisation of polyamines in mammalian cells. Chem Biol **6:**717-29.

42. **Cushion, M. T., M. S. Collins, and M. J. Linke.** 2009. Biofilm formation by Pneumocystis spp. Eukaryot Cell **8:**197-206.

43. **Delanoe, P., M. Delanoe.** 1912. Sur les rapports des kystes de Carinii du poumon des rats avec le trypanosoma Lewisii. CR Acad Sci (Paris) **155:**658-60.

44. **DeLorenzo, L. J., C. T. Huang, G. P. Maguire, and D. J. Stone.** 1987. Roentgenographic patterns of Pneumocystis carinii pneumonia in 104 patients with AIDS. Chest **91:**323-7.

45. **Dennehy, K. M., G. Ferwerda, I. Faro-Trindade, E. Pyz, J. A. Willment, P. R. Taylor, A. Kerrigan, S. V. Tsoni, S. Gordon, F. Meyer-Wentrup, G. J. Adema, B. J. Kullberg, E. Schweighoffer, V. Tybulewicz, H. M. Mora-Montes, N. A. Gow, D. L. Williams, M. G. Netea, and G. D. Brown.** 2008. Syk kinase is required for collaborative cytokine production induced through Dectin-1 and Toll-like receptors. Eur J Immunol **38:**500-6.

46. **Ding, K., A. Shibui, Y. Wang, M. Takamoto, T. Matsuguchi, and K. Sugane.** 2005. Impaired recognition by Toll-like receptor 4 is responsible for exacerbated murine Pneumocystis pneumonia. Microbes Infect **7:**195-203.

47. **Douglas, C. M.** 2001. Fungal beta(1,3)-D-glucan synthesis. Med Mycol **39 Suppl 1:**55-66.

48. **Downing, J. F., D. L. Kachel, R. Pasula, and W. J. Martin, 2nd.** 1999. Gamma interferon stimulates rat alveolar macrophages to kill Pneumocystis carinii by L-arginine- and tumor necrosis factor-dependent mechanisms. Infect Immun **67:**1347-52.

49. **Edman, J. C., J. A. Kovacs, H. Masur, D. V. Santi, H. J. Elwood, and M. L. Sogin.** 1988. Ribosomal RNA sequence shows Pneumocystis carinii to be a member of the fungi. Nature **334:**519-22.

50. **Evans, S. E., P. Y. Hahn, F. McCann, T. J. Kottom, Z. V. Pavlovic, and A. H. Limper.** 2005. Pneumocystis cell wall beta-glucans stimulate alveolar epithelial cell chemokine generation through nuclear factor-kappaB-dependent mechanisms. Am J Respir Cell Mol Biol **32:**490-7.

51. **Ezekowitz, R. A. B., D. J. Williams, H. Koziel, M. Y. Armstrong, A. Warner, F. F. Richards, and R. M. Rose.** 1991. Uptake of Pneumocystis carinii mediated by the macrophage mannose receptor. Nature **351:**155-8.

52. **Fischl, M. A., G. M. Dickinson, and L. La Voie.** 1988. Safety and efficacy of sulfamethoxazole and trimethoprim chemoprophylaxis for Pneumocystis carinii pneumonia in AIDS. JAMA **259:**1185-9.

53. **Fishman, E. K., D. Magid, and J. E. Kuhlman.** 1990. Pneumocystis carinii involvement of the liver and spleen: CT demonstration. J Comput Assist Tomogr **14:**146-8.

54. **Fleury, J., E. Escudier, M. J. Pocholle, C. Carre, and J. F. Bernaudin.** 1985. Cell population obtained by bronchoalveolar lavage in Pneumocystis carinii pneumonitis. Acta Cytol **29:**721-6.

55. **Fraser, I. P., K. Takahashi, H. Koziel, B. Fardin, A. Harmsen, and R. A. Ezekowitz.** 2000. Pneumocystis carinii enhances soluble mannose receptor production by macrophages. Microbes Infect **2:**1305-10.

56. **Fuller, G. L., J. A. Williams, M. G. Tomlinson, J. A. Eble, S. L. Hanna, S. Pohlmann, K. Suzuki-Inoue, Y. Ozaki, S. P. Watson, and A. C. Pearce.** 2007. The C-type lectin receptors CLEC-2 and Dectin-1, but not DC-SIGN, signal via a novel YXXL-dependent signaling cascade. J Biol Chem **282:**12397-409.

57. **Gandre, S., Z. Bercovich, and C. Kahana.** 2002. Ornithine decarboxylase-antizyme is rapidly degraded through a mechanism that requires functional ubiquitin-dependent proteolytic activity. Eur J Biochem **269:**1316-22.

58. **Gantner, B. N., R. M. Simmons, S. J. Canavera, S. Akira, and D. M. Underhill.** 2003. Collaborative induction of inflammatory responses by dectin-1 and Toll-like receptor 2. J Exp Med **197:**1107-17.

59. **Gay, N. J., and M. Gangloff.** 2007. Structure and function of Toll receptors and their ligands. Annu Rev Biochem **76:**141-65.

60. **Gerner, E. W., and P. S. Mamont.** 1986. Restoration of the polyamine contents in rat hepatoma tissue-culture cells after inhibition of polyamine biosynthesis. Relationship with cell proliferation. Eur J Biochem **156:**31-5.

61. **Gerner, E. W., and F. L. Meyskens, Jr.** 2004. Polyamines and cancer: old molecules, new understanding. Nat Rev Cancer **4:**781-92.

62. **Gigliotti, F., A. G. Harmsen, C. G. Haidaris, and P. J. Haidaris.** 1993. Pneumocystis carinii is not universally transmissible between mammalian species. Infect Immun **61:**2886-90.

63. **Gillin, F. D., D. S. Reiner, and P. P. McCann.** 1984. Inhibition of growth of Giardia lamblia by difluoromethylornithine, a specific inhibitor of polyamine biosynthesis. J Protozool **31:**161-3.

64. **Goodridge, H. S., T. Shimada, A. J. Wolf, Y. M. Hsu, C. A. Becker, X. Lin, and D. M. Underhill.** 2009. Differential use of CARD9 by dectin-1 in macrophages and dendritic cells. J Immunol **182:**1146-54.

65. **Goodridge, H. S., R. M. Simmons, and D. M. Underhill.** 2007. Dectin-1 stimulation by Candida albicans yeast or zymosan triggers NFAT activation in macrophages and dendritic cells. J Immunol **178:**3107-15.

66. **Graminski, G. F., C. L. Carlson, J. R. Ziemer, F. Cai, N. M. Vermeulen, S. M. Vanderwerf, and M. R. Burns.** 2002. Synthesis of bis-spermine dimers that are potent polyamine transport inhibitors. Bioorg Med Chem Lett **12:**35-40.

67. **Gringhuis, S. I., J. den Dunnen, M. Litjens, M. van der Vlist, B. Wevers, S. C. Bruijns, and T. B. Geijtenbeek.** 2009. Dectin-1 directs T helper cell differentiation by controlling noncanonical NF-kappaB activation through Raf-1 and Syk. Nat Immunol **10:**203-13.

68. **Hahn, P. Y., S. E. Evans, T. J. Kottom, J. E. Standing, R. E. Pagano, and A. H. Limper.** 2003. Pneumocystis carinii cell wall beta-glucan induces release of macrophage inflammatory protein-2 from alveolar epithelial cells via a lactosylceramide-mediated mechanism. J Biol Chem **278:**2043-50.

69. **Hanson, W. L., M. M. Bradford, W. L. Chapman, Jr., V. B. Waits, P. P. McCann, and A. Sjoerdsma.** 1982. alpha-Difluoromethylornithine: a promising lead for preventive chemotherapy for coccidiosis. Am J Vet Res **43:**1651-3.

70. **Hay, J. W., D. H. Osmond, and M. A. Jacobson.** 1988. Projecting the medical costs of AIDS and ARC in the United States. J Acquir Immune Defic Syndr **1:**466-85.

71. **Hayashi, S., Y. Murakami, and S. Matsufuji.** 1996. Ornithine decarboxylase antizyme: a novel type of regulatory protein. Trends Biochem Sci **21:**27-30.

72. **Heiskala, M., J. Zhang, S. Hayashi, E. Holtta, and L. C. Andersson.** 1999. Translocation of ornithine decarboxylase to the surface membrane during cell activation and transformation. EMBO J **18:**1214-22.

73. **Helweg-Larsen, J., T. L. Benfield, J. Eugen-Olsen, J. D. Lundgren, and B. Lundgren.** 1999. Effects of mutations in Pneumocystis carinii dihydropteroate synthase gene on outcome of AIDS-associated P. carinii pneumonia. Lancet **354:**1347-51.

74. **Heston, W. D., D. Kadmon, D. F. Covey, and W. R. Fair.** 1984. Differential effect of alpha-difluoromethylornithine on the in vivo uptake of 14C-labeled polyamines and methylglyoxal bis(guanylhydrazone) by a rat prostate-derived tumor. Cancer Res **44:**1034-40.

75. **Hoffman, O. A., J. E. Standing, and A. H. Limper.** 1993. Pneumocystis carinii stimulates tumor necrosis factor-alpha release from alveolar macrophages through a beta-glucan-mediated mechanism. J Immunol **150:**3932-40.

76. **Hollifield, M., E. Bou Ghanem, W. J. de Villiers, and B. A. Garvy.** 2007. Scavenger receptor A dampens induction of inflammation in response to the fungal pathogen Pneumocystis carinii. Infect Immun **75:**3999-4005.

77. **Huang, L., K. Crothers, C. Atzori, T. Benfield, R. Miller, M. Rabodonirina, and J. Helweg-Larsen.** 2004. Dihydropteroate synthase gene mutations in Pneumocystis and sulfa resistance. Emerg Infect Dis **10:**1721-8.

78. **Huang, L., A. Morris, A. H. Limper, and J. M. Beck.** 2006. An Official ATS Workshop Summary: Recent advances and future directions in pneumocystis pneumonia (PCP). Proc Am Thorac Soc **3:**655-64.

79. **Huber, M., J. G. Pelletier, K. Torossian, P. Dionne, I. Gamache, R. Charest-Gaudreault, M. Audette, and R. Poulin.** 1996. 2,2'-Dithiobis(N-ethyl-spermine-5-carboxamide) is a high affinity, membrane-impermeant antagonist of the mammalian polyamine transport system. J Biol Chem **271:**27556-63.

80. **Hughes, W. T.** 1982. Natural mode of acquisition for de novo infection with Pneumocystis carinii. J Infect Dis **145:**842-8.

81. **Hyvonen, M. T., A. Uimari, T. A. Keinanen, S. Heikkinen, R. Pellinen, T. Wahlfors, A. Korhonen, A. Narvanen, J. Wahlfors, L. Alhonen, and J. Janne.** 2006. Polyamine-regulated unproductive splicing and translation of spermidine/spermine N1-acetyltransferase. RNA **12:**1569-82.

82. **Igarashi, K., and K. Kashiwagi.** 1999. Polyamine transport in bacteria and yeast. Biochem J **344 Pt 3:**633-42.

83. **Jung, M. H., S. C. Kim, G. A. Jeon, S. H. Kim, Y. Kim, K. S. Choi, S. I. Park, M. K. Joe, and K. Kimm.** 2000. Identification of differentially expressed genes in normal and tumor human gastric tissue. Genomics **69:**281-6.

84. **Kang, P. B., A. K. Azad, J. B. Torrelles, T. M. Kaufman, A. Beharka, E. Tibesar, L. E. DesJardin, and L. S. Schlesinger.** 2005. The human macrophage mannose receptor directs Mycobacterium tuberculosis lipoarabinomannan-mediated phagosome biogenesis. J Exp Med **202:**987-99.

85. **Kaplan, J. E., D. Hanson, M. S. Dworkin, T. Frederick, J. Bertolli, M. L. Lindegren, S. Holmberg, and J. L. Jones.** 2000. Epidemiology of human immunodeficiency virus-associated opportunistic infections in the United States in the era of highly active antiretroviral therapy. Clin Infect Dis **30 Suppl 1:**S5-14.

86. **Kaur, N., J. G. Delcros, J. Imran, A. Khaled, M. Chehtane, N. Tschammer, B. Martin, and O. Phanstiel, IV.** 2008. A comparison of chloroambucil- and xylene-containing polyamines leads to improved ligands for accessing the polyamine transport system. J Med Chem **51:**1393-401.

87. **Kazanjian, P., W. Armstrong, P. A. Hossler, W. Burman, J. Richardson, C. H. Lee, L. Crane, J. Katz, and S. R. Meshnick.** 2000. Pneumocystis carinii mutations are associated with duration of sulfa or sulfone prophylaxis exposure in AIDS patients. J Infect Dis **182:**551-7.

88. **Keren-Paz, A., Z. Bercovich, Z. Porat, O. Erez, O. Brener, and C. Kahana.** 2006. Overexpression of antizyme-inhibitor in NIH3T3 fibroblasts provides growth advantage through neutralization of antizyme functions. Oncogene **25:**5163-72.

89. **Kessl, J. J., P. Hill, B. B. Lange, S. R. Meshnick, B. Meunier, and B. L. Trumpower.** 2004. Molecular basis for atovaquone resistance in Pneumocystis jirovecii modeled in the cytochrome bc(1) complex of Saccharomyces cerevisiae. J Biol Chem **279:**2817-24.

90. **Kim, K., J. H. Ryu, J. W. Park, M. S. Kim, and Y. S. Chun.** 2005. Induction of a SSAT isoform in response to hypoxia or iron deficiency and its protective effects on cell death. Biochem Biophys Res Commun **331:**78-85.

91. **Klein, R. D., T. G. Geary, A. S. Gibson, M. A. Favreau, C. A. Winterrowd, S. J. Upton, J. S. Keithly, G. Zhu, R. L. Malmberg, M. P. Martinez, and N. Yarlett.** 1999. Reconstitution of a bacterial/plant polyamine biosynthesis pathway in Saccharomyces cerevisiae. Microbiology **145 (Pt 2):**301-7.

92. **Kolls, J. K., S. Habetz, M. K. Shean, C. Vazquez, J. A. Brown, D. Lei, P. Schwarzenberger, P. Ye, S. Nelson, W. R. Summer, and J. E. Shellito.** 1999. IFN-gamma and CD8+ T cells restore host defenses against Pneumocystis carinii in mice depleted of CD4+ T cells. J Immunol **162:**2890-4.

93. **Kolls, J. K., D. Lei, C. Vazquez, G. Odom, W. R. Summer, S. Nelson, and J. Shellito.** 1997. Exacerbation of murine Pneumocystis carinii infection by adenoviral-mediated gene transfer of a TNF inhibitor. Am J Respir Cell Mol Biol **16:**112-8.

94. **Kouvela, E. C., A. D. Petropoulos, and D. L. Kalpaxis.** 2006. Unraveling new features of clindamycin interaction with functional ribosomes and dependence of the drug potency on polyamines. J Biol Chem **281:**23103-10.

95. **Kovacs, J. A., V. J. Gill, S. Meshnick, and H. Masur.** 2001. New insights into transmission, diagnosis, and drug treatment of Pneumocystis carinii pneumonia. JAMA **286:**2450-60.

96. **Koziel, H., Q. Eichbaum, B. A. Kruskal, P. Pinkston, R. A. Rogers, M. Y. Armstrong, F. F. Richards, R. M. Rose, and R. A. Ezekowitz.** 1998. Reduced binding and phagocytosis of Pneumocystis carinii by alveolar macrophages from persons infected with HIV-1 correlates with mannose receptor downregulation. J Clin Invest **102:**1332-44.

97. **Koziel, H., B. A. Kruskal, R. A. Ezekowitz, and R. M. Rose.** 1993. HIV impairs alveolar macrophage mannose receptor function against Pneumocystis carinii. Chest **103:**111S-112S.

98. **Koziel, H., X. Li, M. Y. Armstrong, F. F. Richards, and R. M. Rose.** 2000. Alveolar macrophages from human immunodeficiency virus-infected persons demonstrate impaired oxidative burst response to Pneumocystis carinii in vitro. Am J Respir Cell Mol Biol **23:**452-9.

99. **Krajicek, B. J., A. H. Limper, and C. F. Thomas, Jr.** 2008. Advances in the biology, pathogenesis and identification of Pneumocystis pneumonia. Curr Opin Pulm Med **14:**228-34.

100. **Kutty, G., B. Hernandez-Novoa, M. Czapiga, and J. A. Kovacs.** 2008. Pneumocystis encodes a functional S-adenosylmethionine synthetase gene. Eukaryot Cell **7:**258-67.

101. **Lasbury, M. E., P. J. Durant, M. S. Bartlett, J. W. Smith, and C. H. Lee.** 2003. Correlation of organism burden and alveolar macrophage counts during infection with Pneumocystis carinii and recovery. Clin Diagn Lab Immunol **10:**293-302.

102. **Lasbury, M. E., P. J. Durant, and C. H. Lee.** 2003. Decrease in alveolar macrophage number during Pneumocystis carinii infection. J Eukaryot Microbiol **50 Suppl:**630-1.

103. **Lasbury, M. E., P. J. Durant, C. A. Ray, D. Tschang, R. Schwendener, and C. H. Lee.** 2006. Suppression of alveolar macrophage apoptosis prolongs survival of rats and mice with pneumocystis pneumonia. J Immunol **176:**6443-53.

104. **Lasbury, M. E., P. J. Durant, S. H. Wang, C. Zhang, C. P. Liao, D. Tschang, and C. H. Lee.** 2006. GM-CSF expression in the lung during Pneumocystis pneumonia. J Eukaryot Microbiol **53 Suppl 1:**S124-6.

105. **Lasbury, M. E., S. Merali, P. J. Durant, D. Tschang, C. A. Ray, and C. H. Lee.** 2007. Polyamine-mediated apoptosis of alveolar macrophages during Pneumocystis pneumonia. J Biol Chem **282:**11009-20.

106. **Lasbury, M. E., X. Tang, P. J. Durant, and C. H. Lee.** 2003. Effect of transcription factor GATA-2 on phagocytic activity of alveolar macrophages from Pneumocystis carinii-infected hosts. Infect Immun **71:**4943-52.

107. **Lebron, F., R. Vassallo, V. Puri, and A. H. Limper.** 2003. Pneumocystis carinii cell wall beta-glucans initiate macrophage inflammatory responses through NF-kappaB activation. J Biol Chem **278:**25001-8.

108. **Lee, C. H., N. L. Bauer, M. M. Shaw, M. M. Durkin, M. S. Bartlett, S. F. Queener, and J. W. Smith.** 1993. Proliferation of rat Pneumocystis carinii on cells sheeted on microcarrier beads in spinner flasks. J Clin Microbiol **31:**1659-62.

109. **Lee, C. H., J. Helweg-Larsen, X. Tang, S. Jin, B. Li, M. S. Bartlett, J. J. Lu, B. Lundgren, J. D. Lundgren, M. Olsson, S. B. Lucas, P. Roux, A. Cargnel, C. Atzori, O. Matos, and J. W. Smith.** 1998. Update on Pneumocystis carinii f. sp. hominis typing based on nucleotide sequence variations in internal transcribed spacer regions of rRNA genes. J Clin Microbiol **36:**734-41.

110. **Lee, S. J., N. Y. Zheng, M. Clavijo, and M. C. Nussenzweig.** 2003. Normal host defense during systemic candidiasis in mannose receptor-deficient mice. Infect Immun **71:**437-45.

111. **LeibundGut-Landmann, S., O. Gross, M. J. Robinson, F. Osorio, E. C. Slack, S. V. Tsoni, E. Schweighoffer, V. Tybulewicz, G. D. Brown, J. Ruland, and C. Reis e Sousa.** 2007. Syk- and CARD9-dependent coupling of innate immunity to the induction of T helper cells that produce interleukin 17. Nat Immunol **8:**630-8.

112. **Lemaitre, B., E. Nicolas, L. Michaut, J. M. Reichhart, and J. A. Hoffmann.** 1996. The dorsoventral regulatory gene cassette spatzle/Toll/cactus controls the potent antifungal response in Drosophila adults. Cell **86:**973-83.

113. **Leppert, B. J., J. M. Mansfield, and D. M. Paulnock.** 2007. The soluble variant surface glycoprotein of African trypanosomes is recognized by a macrophage scavenger receptor and induces I kappa B alpha degradation independently of TRAF6-mediated TLR signaling. J Immunol **179:**548-56.

114. **Levin, V. A., K. R. Hess, A. Choucair, P. J. Flynn, K. A. Jaeckle, A. P. Kyritsis, W. K. Yung, M. D. Prados, J. M. Bruner, S. Ictech, M. J. Gleason, and H. W. Kim.** 2003. Phase III randomized study of postradiotherapy chemotherapy with combination alpha-difluoromethylornithine-PCV versus PCV for anaplastic gliomas. Clin Cancer Res **9:**981-90.

115. **Liao, C. P., M. E. Lasbury, S. H. Wang, C. Zhang, P. J. Durant, Y. Murakami, S. Matsufuji, and C. H. Lee.** 2009. Pneumocystis mediates overexpression of antizyme inhibitor resulting in increased polyamine levels and apoptosis in alveolar macrophages. J Biol Chem **284:**8174-84.

116. **Limper, A. H., M. Edens, R. A. Anders, and E. B. Leof.** 1998. Pneumocystis carinii inhibits cyclin-dependent kinase activity in lung epithelial cells. J Clin Invest **101:**1148-55.

117. **Limper, A. H., J. S. Hoyte, and J. E. Standing.** 1997. The role of alveolar macrophages in Pneumocystis carinii degradation and clearance from the lung. J Clin Invest **99:**2110-7.

118. **Limper, A. H., K. P. Offord, T. F. Smith, and W. J. Martin, 2nd.** 1989. Pneumocystis carinii pneumonia. Differences in lung parasite number and inflammation in patients with and without AIDS. Am Rev Respir Dis **140:**1204-9.

119. **Limper, A. H., J. E. Standing, O. A. Hoffman, M. Castro, and L. W. Neese.** 1993. Vitronectin binds to Pneumocystis carinii and mediates organism attachment to cultured lung epithelial cells. Infect Immun **61:**4302-9.

120. **Lipschik, G. Y., H. Masur, and J. A. Kovacs.** 1991. Polyamine metabolism in Pneumocystis carinii. J Infect Dis **163:**1121-7.

121. **Lu, J. J., M. S. Bartlett, M. M. Shaw, S. F. Queener, J. W. Smith, M. Ortiz-Rivera, M. J. Leibowitz, and C. H. Lee.** 1994. Typing of Pneumocystis carinii strains that infect humans based on nucleotide sequence variations of internal transcribed spacers of rRNA genes. J Clin Microbiol **32:**2904-12.

122. **Lund, F. E., K. Schuer, M. Hollifield, T. D. Randall, and B. A. Garvy.** 2003. Clearance of Pneumocystis carinii in mice is dependent on B cells but not on P carinii-specific antibody. J Immunol **171:**1423-30.

123. **Lundgren, B., K. Elvin, L. P. Rothman, I. Ljungstrom, C. Lidman, and J. D. Lundgren.** 1997. Transmission of Pneumocystis carinii from patients to hospital staff. Thorax **52:**422-4.

124. **Lyons, H. A., K. Vinijchaikul, and G. R. Hennigar.** 1961. Pneumocystis carinii pneumonia unassociated with other disease. Clinical and pathological studies. Arch Intern Med **108:**929-36.

125. **Macian, F.** 2005. NFAT proteins: key regulators of T-cell development and function. Nat Rev Immunol **5:**472-84.

126. **Mamont, P. S., P. Bohlen, P. P. McCann, P. Bey, F. Schuber, and C. Tardif.** 1976. Alpha-methyl ornithine, a potent competitive inhibitor of ornithine decarboxylase, blocks proliferation of rat hepatoma cells in culture. Proc Natl Acad Sci U S A **73:**1626-30.

127. **Mangold, U.** 2005. The antizyme family: polyamines and beyond. IUBMB Life **57:**671-6.

128. **Mangold, U., and E. Leberer.** 2005. Regulation of all members of the antizyme family by antizyme inhibitor. Biochem J **385:**21-8.

129. **Marodi, L., H. M. Korchak, and R. B. Johnston, Jr.** 1991. Mechanisms of host defense against Candida species. I. Phagocytosis by monocytes and monocyte-derived macrophages. J Immunol **146:**2783-9.

130. **Masur, H., M. A. Michelis, J. B. Greene, I. Onorato, R. A. Stouwe, R. S. Holzman, G. Wormser, L. Brettman, M. Lange, H. W. Murray, and S. Cunningham-Rundles.** 1981. An outbreak of community-acquired Pneumocystis carinii pneumonia: initial manifestation of cellular immune dysfunction. N Engl J Med **305:**1431-8.

131. **Matsufuji, S., T. Matsufuji, N. M. Wills, R. F. Gesteland, and J. F. Atkins.** 1996. Reading two bases twice: mammalian antizyme frameshifting in yeast. EMBO J **15:**1360-70.

132. **Medzhitov, R., P. Preston-Hurlburt, and C. A. Janeway, Jr.** 1997. A human homologue of the Drosophila Toll protein signals activation of adaptive immunity. Nature **388:**394-7.

133. **Meissner, N. N., F. E. Lund, S. Han, and A. Harmsen.** 2005. CD8 T cell-mediated lung damage in response to the extracellular pathogen pneumocystis is dependent on MHC class I expression by radiation-resistant lung cells. J Immunol **175:**8271-9.

134. **Merali, S.** 1999. Pneumocystis carinii polyamine catabolism. J Biol Chem **274:**21017-22.

135. **Merali, S., and A. B. Clarkson, Jr.** 1996. Polyamine content of Pneumocystis carinii and response to the ornithine decarboxylase inhibitor DL-alpha-difluoromethylornithine. Antimicrob Agents Chemother **40:**973-8.

136. **Merali, S., U. Frevert, J. H. Williams, K. Chin, R. Bryan, and A. B. Clarkson, Jr.** 1999. Continuous axenic cultivation of Pneumocystis carinii. Proc Natl Acad Sci U S A **96:**2402-7.

137. **Merali, S., D. Vargas, M. Franklin, and A. B. Clarkson, Jr.** 2000. S-adenosylmethionine and Pneumocystis carinii. J Biol Chem **275:**14958-63.

138. **Meshnick, S. R.** 1999. Drug-resistant Pneumocystis carinii. Lancet **354:**1318-9.

139. **Meyskens, F. L., Jr., and E. W. Gerner.** 1999. Development of difluoromethylornithine (DFMO) as a chemoprevention agent. Clin Cancer Res **5:**945-51.

140. **Miller, R. F., H. E. Ambrose, and A. E. Wakefield.** 2001. Pneumocystis carinii f. sp. hominis DNA in immunocompetent health care workers in contact with patients with P. carinii pneumonia. J Clin Microbiol **39:**3877-82.

141. **Milord, F., J. Pepin, L. Loko, L. Ethier, and B. Mpia.** 1992. Efficacy and toxicity of eflornithine for treatment of Trypanosoma brucei gambiense sleeping sickness. Lancet **340:**652-5.

142. **Mita, K., K. Fukuchi, K. Hamana, S. Ichimura, and M. Nenoi.** 2004. Accumulation of spermidine/spermine N1-acetyltransferase and alternatively spliced mRNAs as a delayed response of HeLa S3 cells following X-ray irradiation. Int J Radiat Biol **80:**369-75.

143. **Mitchell, J. L., G. G. Judd, A. Bareyal-Leyser, and S. Y. Ling.** 1994. Feedback repression of polyamine transport is mediated by antizyme in mammalian tissue-culture cells. Biochem J **299 (Pt 1):**19-22.

144. **Morris, A., J. D. Lundgren, H. Masur, P. D. Walzer, D. L. Hanson, T. Frederick, L. Huang, C. B. Beard, and J. E. Kaplan.** 2004. Current epidemiology of Pneumocystis pneumonia. Emerg Infect Dis **10:**1713-20.

145. **Morris, A., K. Wei, K. Afshar, and L. Huang.** 2008. Epidemiology and clinical significance of pneumocystis colonization. J Infect Dis **197:**10-7.

146. **Muller, I. B., R. Das Gupta, K. Luersen, C. Wrenger, and R. D. Walter.** 2008. Assessing the polyamine metabolism of Plasmodium falciparum as chemotherapeutic target. Mol Biochem Parasitol **160:**1-7.

147. **Murakami, Y., T. Ichiba, S. Matsufuji, and S. Hayashi.** 1996. Cloning of antizyme inhibitor, a highly homologous protein to ornithine decarboxylase. J Biol Chem **271:**3340-2.

148. **Murray-Stewart, T., Y. Wang, W. Devereux, and R. A. Casero, Jr.** 2002. Cloning and characterization of multiple human polyamine oxidase splice variants that code for isoenzymes with different biochemical characteristics. Biochem J **368:**673-7.

149. **Napper, C. E., K. Drickamer, and M. E. Taylor.** 2006. Collagen binding by the mannose receptor mediated through the fibronectin type II domain. Biochem J **395:**579-86.

150. **Navin, T. R., C. B. Beard, L. Huang, C. del Rio, S. Lee, N. J. Pieniazek, J. L. Carter, T. Le, A. Hightower, and D. Rimland.** 2001. Effect of mutations in Pneumocystis carinii dihydropteroate synthase gene on outcome of P carinii pneumonia in patients with HIV-1: a prospective study. Lancet **358:**545-9.

151. **Nightingale, S. L.** 1991. From the Food and Drug Administration. JAMA **265:**1229.

152. **Nikiforova, N. N., T. V. Velikodvorskaja, A. V. Kachko, L. G. Nikolaev, G. S. Monastyrskaya, S. A. Lukyanov, S. N. Konovalova, E. V. Protopopova, V. A. Svyatchenko, N. N. Kiselev, V. B. Loktev, and E. D. Sverdlov.** 2002. Induction of alternatively spliced spermidine/spermine N1-acetyltransferase mRNA in the human kidney cells infected by venezuelan equine encephalitis and tick-borne encephalitis viruses. Virology **297:**163-71.

153. **Nilsson, J., B. Grahn, and O. Heby.** 2000. Antizyme inhibitor is rapidly induced in growth-stimulated mouse fibroblasts and releases ornithine decarboxylase from antizyme suppression. Biochem J **346 Pt 3:**699-704.

154. **Ninomiya-Tsuji, J., K. Kishimoto, A. Hiyama, J. Inoue, Z. Cao, and K. Matsumoto.** 1999. The kinase TAK1 can activate the NIK-I kappaB as well as the MAP kinase cascade in the IL-1 signalling pathway. Nature **398:**252-6.

155. **O'Brien, J. G., B. J. Dong, R. L. Coleman, L. Gee, and K. B. Balano.** 1997. A 5-year retrospective review of adverse drug reactions and their risk factors in human immunodeficiency virus-infected patients who were receiving intravenous pentamidine therapy for Pneumocystis carinii pneumonia. Clin Infect Dis **24:**854-9.

156. **O'Neill, L. A., and A. G. Bowie.** 2007. The family of five: TIR-domain-containing adaptors in Toll-like receptor signalling. Nat Rev Immunol **7:**353-64.

157. **O'Riordan, D. M., J. E. Standing, K. Y. Kwon, D. Chang, E. C. Crouch, and A. H. Limper.** 1995. Surfactant protein D interacts with Pneumocystis carinii and mediates organism adherence to alveolar macrophages. J Clin Invest **95:**2699-710.

158. **O'Riordan, D. M., J. E. Standing, and A. H. Limper.** 1995. Pneumocystis carinii glycoprotein A binds macrophage mannose receptors. Infect Immun **63:**779-84.

159. **O'Shaughnessy, J. A., L. M. Demers, S. E. Jones, J. Arseneau, P. Khandelwal, T. George, R. Gersh, D. Mauger, and A. Manni.** 1999. Alpha-difluoromethylornithine as treatment for metastatic breast cancer patients. Clin Cancer Res **5:**3438-44.

160. **Oredsson, S. M.** 2003. Polyamine dependence of normal cell-cycle progression. Biochem Soc Trans **31:**366-70.

161. **Packham, G., and J. L. Cleveland.** 1997. Induction of ornithine decarboxylase by IL-3 is mediated by sequential c-Myc-independent and c-Myc-dependent pathways. Oncogene **15:**1219-32.

162. **Palanimurugan, R., H. Scheel, K. Hofmann, and R. J. Dohmen.** 2004. Polyamines regulate their synthesis by inducing expression and blocking degradation of ODC antizyme. EMBO J **23:**4857-67.

163. **Palsson-McDermott, E. M., and L. A. O'Neill.** 2007. Building an immune system from nine domains. Biochem Soc Trans **35:**1437-44.

164. **Parry, L., R. Balana Fouce, and A. E. Pegg.** 1995. Post-transcriptional regulation of the content of spermidine/spermine N1-acetyltransferase by N1N12-bis(ethyl)spermine. Biochem J **305 (Pt 2):**451-8.

165. **Peiser, L., S. Mukhopadhyay, and S. Gordon.** 2002. Scavenger receptors in innate immunity. Curr Opin Immunol **14:**123-8.

166. **Pendeville, H., N. Carpino, J. C. Marine, Y. Takahashi, M. Muller, J. A. Martial, and J. L. Cleveland.** 2001. The ornithine decarboxylase gene is essential for cell survival during early murine development. Mol Cell Biol **21:**6549-58.

167. **Pesanti, E. L., M. S. Bartlett, and J. W. Smith.** 1988. Lack of detectable activity of ornithine decarboxylase in Pneumocystis carinii. J Infect Dis **158:**1137-8.

168. **Phair, J., A. Munoz, R. Detels, R. Kaslow, C. Rinaldo, and A. Saah.** 1990. The risk of Pneumocystis carinii pneumonia among men infected with human immunodeficiency virus type 1. Multicenter AIDS Cohort Study Group. N Engl J Med **322:**161-5.

169. **Phanstiel, O., IV., N. Kaur, and J. G. Delcros.** 2007. Structure-activity investigations of polyamine-anthracene conjugates and their uptake via the polyamine transporter. Amino Acids **33:**305-13.

170. **Pifer, L. L., D. Woods, and W. T. Hughes.** 1978. Propagation of Pneumocystis carinii in Vero cell culture. Infect Immun **20:**66-8.

171. **Pignatti, C., B. Tantini, C. Stefanelli, and F. Flamigni.** 2004. Signal transduction pathways linking polyamines to apoptosis. Amino Acids **27:**359-65.

172. **Pottratz, S. T., S. Reese, and J. L. Sheldon.** 1998. Pneumocystis carinii induces interleukin 6 production by an alveolar epithelial cell line. Eur J Clin Invest **28:**424-9.

173. **Poulin, R., L. Lu, B. Ackermann, P. Bey, and A. E. Pegg.** 1992. Mechanism of the irreversible inactivation of mouse ornithine decarboxylase by alpha-difluoromethylornithine. Characterization of sequences at the inhibitor and coenzyme binding sites. J Biol Chem **267:**150-8.

174. **Procop, G. W., S. Haddad, J. Quinn, M. L. Wilson, N. G. Henshaw, L. B. Reller, R. L. Artymyshyn, M. T. Katanik, and M. P. Weinstein.** 2004. Detection of Pneumocystis jiroveci in respiratory specimens by four staining methods. J Clin Microbiol **42:**3333-5.

175. **Pryhuber, G. S., H. L. Huyck, S. Bhagwat, M. A. O'Reilly, J. N. Finkelstein, F. Gigliotti, and T. W. Wright.** 2008. Parenchymal cell TNF receptors contribute to inflammatory cell recruitment and respiratory failure in Pneumocystis carinii-induced pneumonia. J Immunol **181:**1409-19.

176. **Qin, C., I. Samudio, S. Ngwenya, and S. Safe.** 2004. Estrogen-dependent regulation of ornithine decarboxylase in breast cancer cells through activation of nongenomic cAMP-dependent pathways. Mol Carcinog **40:**160-70.

177. **Rao, N. A., P. L. Zimmerman, D. Boyer, J. Biswas, D. Causey, J. Beniz, and P. W. Nichols.** 1989. A clinical, histopathologic, and electron microscopic study of Pneumocystis carinii choroiditis. Am J Ophthalmol **107:**218-28.

178. **Rapaka, R. R., E. S. Goetzman, M. Zheng, J. Vockley, L. McKinley, J. K. Kolls, and C. Steele.** 2007. Enhanced defense against Pneumocystis carinii mediated by a novel dectin-1 receptor Fc fusion protein. J Immunol **178:**3702-12.

179. **Ray, R. M., S. A. McCormack, and L. R. Johnson.** 2001. Polyamine depletion arrests growth of IEC-6 and Caco-2 cells by different mechanisms. Am J Physiol Gastrointest Liver Physiol **281:**G37-43.

180. **Riebold, D., C. Fritzsche, M. Lademann, A. Bier, and E. C. Reisinger.** 2006. Pneumocystis jiroveci dihydropteroate synthase gene mutations at codon 171 but not at codons 55 or 57 detected in Germany. Clin Infect Dis **42:**582-3.

181. **Rock, F. L., G. Hardiman, J. C. Timans, R. A. Kastelein, and J. F. Bazan.** 1998. A family of human receptors structurally related to Drosophila Toll. Proc Natl Acad Sci U S A **95:**588-93.

182. **Roy, U. K., N. S. Rial, K. L. Kachel, and E. W. Gerner.** 2008. Activated K-RAS increases polyamine uptake in human colon cancer cells through modulation of caveolar endocytosis. Mol Carcinog **47:**538-53.

183. **Rudmann, D. G., A. M. Preston, M. W. Moore, and J. M. Beck.** 1998. Susceptibility to Pneumocystis carinii in mice is dependent on simultaneous deletion of IFN-gamma and type 1 and 2 TNF receptor genes. J Immunol **161:**360-6.

184. **Saijo, S., N. Fujikado, T. Furuta, S. H. Chung, H. Kotaki, K. Seki, K. Sudo, S. Akira, Y. Adachi, N. Ohno, T. Kinjo, K. Nakamura, K. Kawakami, and Y. Iwakura.** 2007. Dectin-1 is required for host defense against Pneumocystis carinii but not against Candida albicans. Nat Immunol **8:**39-46.

185. **Saric, M., and A. B. Clarkson, Jr.** 1994. Ornithine decarboxylase in Pneumocystis carinii and implications for therapy. Antimicrob Agents Chemother **38:**2545-52.

186. **Schipper, R. G., V. M. Cuijpers, L. H. De Groot, M. Thio, and A. A. Verhofstad.** 2004. Intracellular localization of ornithine decarboxylase and its regulatory protein, antizyme-1. J Histochem Cytochem **52:**1259-66.

187. **Schipper, R. G., L. C. Penning, and A. A. Verhofstad.** 2000. Involvement of polyamines in apoptosis. Facts and controversies: effectors or protectors? Semin Cancer Biol **10:**55-68.

188. **Seiler, N.** 1995. Polyamine oxidase, properties and functions. Prog Brain Res **106:**333-44.

189. **Seiler, N., and F. Raul.** 2005. Polyamines and apoptosis. J Cell Mol Med **9:**623-42.

190. **Sepkowitz, K. A.** 2002. Opportunistic infections in patients with and patients without Acquired Immunodeficiency Syndrome. Clin Infect Dis **34:**1098-107.

191. **Slatore, C. G., and S. A. Tilles.** 2004. Sulfonamide hypersensitivity. Immunol Allergy Clin North Am **24:**477-90, vii.

192. **Smego, R. A., Jr., S. Nagar, B. Maloba, and M. Popara.** 2001. A meta-analysis of salvage therapy for Pneumocystis carinii pneumonia. Arch Intern Med **161:**1529-33.

193. **Steele, C., L. Marrero, S. Swain, A. G. Harmsen, M. Zheng, G. D. Brown, S. Gordon, J. E. Shellito, and J. K. Kolls.** 2003. Alveolar macrophage-mediated killing of Pneumocystis carinii f. sp. muris involves molecular recognition by the Dectin-1 beta-glucan receptor. J Exp Med **198:**1677-88.

194. **Steele, C., M. Zheng, E. Young, L. Marrero, J. E. Shellito, and J. K. Kolls.** 2002. Increased host resistance against Pneumocystis carinii pneumonia in gammadelta T-cell-deficient mice: protective role of gamma interferon and CD8(+) T cells. Infect Immun **70:**5208-15.

195. **Stringer, J. R., C. B. Beard, R. F. Miller, and A. E. Wakefield.** 2002. A new name (Pneumocystis jiroveci) for Pneumocystis from humans. Emerg Infect Dis **8:**891-6.

196. **Stringer, J. R., and M. T. Cushion.** 1998. The genome of Pneumocystis carinii. FEMS Immunol Med Microbiol **22:**15-26.

197. **Stringer, J. R., M. T. Cushion, and A. E. Wakefield.** 2001. New nomenclature for the genus Pneumocystis. J Eukaryot Microbiol **Suppl:**184S-189S.

198. **Stringer, J. R., and S. P. Keely.** 2001. Genetics of surface antigen expression in Pneumocystis carinii. Infect Immun **69:**627-39.

199. **Sunkin, S. M., and J. R. Stringer.** 1996. Translocation of surface antigen genes to a unique telomeric expression site in Pneumocystis carinii. Mol Microbiol **19:**283-95.

200. **Suzuki, H., Y. Kurihara, M. Takeya, N. Kamada, M. Kataoka, K. Jishage, O. Ueda, H. Sakaguchi, T. Higashi, T. Suzuki, Y. Takashima, Y. Kawabe, O. Cynshi, Y. Wada, M. Honda, H. Kurihara, H. Aburatani, T. Doi, A. Matsumoto, S. Azuma, T. Noda, Y. Toyoda, H. Itakura, Y. Yazaki, T. Kodama, and et al.** 1997. A role for macrophage scavenger receptors in atherosclerosis and susceptibility to infection. Nature **386:**292-6.

201. **Suzuki, N., S. Suzuki, G. S. Duncan, D. G. Millar, T. Wada, C. Mirtsos, H. Takada, A. Wakeham, A. Itie, S. Li, J. M. Penninger, H. Wesche, P. S. Ohashi, T. W. Mak, and W. C. Yeh.** 2002. Severe impairment of interleukin-1 and Toll-like receptor signalling in mice lacking IRAK-4. Nature **416:**750-6.

202. **Suzuki, O., T. Matsumoto, and Y. Katsumata.** 1984. Determination of polyamine oxidase activities in human tissues. Experientia **40:**838-9.

203. **Swain, S. D., S. J. Lee, M. C. Nussenzweig, and A. G. Harmsen.** 2003. Absence of the macrophage mannose receptor in mice does not increase susceptibility to Pneumocystis carinii infection in vivo. Infect Immun **71:**6213-21.

204. **Swain, S. D., T. W. Wright, P. M. Degel, F. Gigliotti, and A. G. Harmsen.** 2004. Neither neutrophils nor reactive oxygen species contribute to tissue damage during Pneumocystis pneumonia in mice. Infect Immun **72:**5722-32.

205. **Tachado, S. D., J. Zhang, J. Zhu, N. Patel, M. Cushion, and H. Koziel.** 2007. Pneumocystis-mediated IL-8 release by macrophages requires coexpression of mannose receptors and TLR2. J Leukoc Biol **81:**205-11.

206. **Tang, X., M. E. Lasbury, D. D. Davidson, M. S. Bartlett, J. W. Smith, and C. H. Lee.** 2000. Down-regulation of GATA-2 transcription during Pneumocystis carinii infection. Infect Immun **68:**4720-4.

207. **Tasaka, S., N. Hasegawa, S. Kobayashi, W. Yamada, T. Nishimura, T. Takeuchi, and A. Ishizaka.** 2007. Serum indicators for the diagnosis of pneumocystis pneumonia. Chest **131:**1173-80.

208. **Taylor, P. R., G. D. Brown, D. M. Reid, J. A. Willment, L. Martinez-Pomares, S. Gordon, and S. Y. Wong.** 2002. The beta-glucan receptor, dectin-1, is predominantly expressed on the surface of cells of the monocyte/macrophage and neutrophil lineages. J Immunol **169:**3876-82.

209. **Taylor, P. R., S. Gordon, and L. Martinez-Pomares.** 2005. The mannose receptor: linking homeostasis and immunity through sugar recognition. Trends Immunol **26:**104-10.

210. **Thomas, C. F., Jr., and A. H. Limper.** 2004. Pneumocystis pneumonia. N Engl J Med **350:**2487-98.

211. **Toma, E., A. Thorne, J. Singer, J. Raboud, C. Lemieux, S. Trottier, M. G. Bergeron, C. Tsoukas, J. Falutz, R. Lalonde, C. Gaudreau, and R. Therrien.** 1998. Clindamycin with primaquine vs. Trimethoprim-sulfamethoxazole therapy for mild and moderately severe Pneumocystis carinii pneumonia in patients with AIDS: a multicenter, double-blind, randomized trial (CTN 004). CTN-PCP Study Group. Clin Infect Dis **27:**524-30.

212. **Uematsu, S., and S. Akira.** 2008. Toll-Like receptors (TLRs) and their ligands. Handb Exp Pharmacol**:**1-20.

213. **Uemura, T., K. Kashiwagi, and K. Igarashi.** 2007. Polyamine uptake by DUR3 and SAM3 in Saccharomyces cerevisiae. J Biol Chem **282:**7733-41.

214. **Uemura, T., K. Kashiwagi, and K. Igarashi.** 2005. Uptake of putrescine and spermidine by Gap1p on the plasma membrane in Saccharomyces cerevisiae. Biochem Biophys Res Commun **328:**1028-33.

215. **Underhill, D. M., E. Rossnagle, C. A. Lowell, and R. M. Simmons.** 2005. Dectin-1 activates Syk tyrosine kinase in a dynamic subset of macrophages for reactive oxygen production. Blood **106:**2543-50.

216. **Underwood, A. P., E. J. Louis, R. H. Borts, J. R. Stringer, and A. E. Wakefield.** 1996. Pneumocystis carinii telomere repeats are composed of TTAGGG and the subtelomeric sequence contains a gene encoding the major surface glycoprotein. Mol Microbiol **19:**273-81.

217. **Valera, I., N. Fernandez, A. G. Trinidad, S. Alonso, G. D. Brown, A. Alonso, and M. S. Crespo.** 2008. Costimulation of dectin-1 and DC-SIGN triggers the arachidonic acid cascade in human monocyte-derived dendritic cells. J Immunol **180:**5727-36.

218. **Valerio, A., E. Tronconi, F. Mazza, A. Cargnel, G. Fantoni, and C. Atzori.** 2006. DHPS-mutated isolates of Pneumocystis jirovecii from HIV-infected individuals: analysis of related ITS genotypes. J Eukaryot Microbiol **53 Suppl 1:**S108-9.

219. **Vargas, S. L., W. T. Hughes, M. E. Santolaya, A. V. Ulloa, C. A. Ponce, C. E. Cabrera, F. Cumsille, and F. Gigliotti.** 2001. Search for primary infection by Pneumocystis carinii in a cohort of normal, healthy infants. Clin Infect Dis **32:**855-61.

220. **Vargas, S. L., C. A. Ponce, F. Gigliotti, A. V. Ulloa, S. Prieto, M. P. Munoz, and W. T. Hughes.** 2000. Transmission of Pneumocystis carinii DNA from a patient with P. carinii pneumonia to immunocompetent contact health care workers. J Clin Microbiol **38:**1536-8.

221. **Vassallo, R., T. J. Kottom, J. E. Standing, and A. H. Limper.** 2001. Vitronectin and fibronectin function as glucan binding proteins augmenting macrophage responses to Pneumocystis carinii. Am J Respir Cell Mol Biol **25:**203-11.

222. **Vassallo, R., J. E. Standing, and A. H. Limper.** 2000. Isolated Pneumocystis carinii cell wall glucan provokes lower respiratory tract inflammatory responses. J Immunol **164:**3755-63.

223. **Verma, D. S., and P. S. Sunkara.** 1982. An essential role for polyamine biosynthesis during human granulopoietic differentiation. Cancer Res **42:**3046-9.

224. **Vlastos, A. T., L. A. West, E. N. Atkinson, I. Boiko, A. Malpica, W. K. Hong, and M. Follen.** 2005. Results of a phase II double-blinded randomized clinical trial of difluoromethylornithine for cervical intraepithelial neoplasia grades 2 to 3. Clin Cancer Res **11:**390-6.

225. **Vuk-Pavlovic, Z., E. K. Mo, C. R. Icenhour, J. E. Standing, J. H. Fisher, and A. H. Limper.** 2006. Surfactant protein D enhances Pneumocystis infection in immune-suppressed mice. Am J Physiol Lung Cell Mol Physiol **290:**L442-9.

226. **Wada, M., S. M. Sunkin, J. R. Stringer, and Y. Nakamura.** 1995. Antigenic variation by positional control of major surface glycoprotein gene expression in Pneumocystis carinii. J Infect Dis **171:**1563-8.

227. **Wakefield, A. E., C. C. Fritscher, A. S. Malin, L. Gwanzura, W. T. Hughes, and R. F. Miller.** 1994. Genetic diversity in human-derived Pneumocystis carinii isolates from four geographical locations shown by analysis of mitochondrial rRNA gene sequences. J Clin Microbiol **32:**2959-61.

228. **Walzer, P. D.** 1986. Attachment of microbes to host cells: relevance of Pneumocystis carinii. Lab Invest **54:**589-92.

229. **Walzer, P. D., C. K. Kim, J. Foy, M. J. Linke, and M. T. Cushion.** 1988. Cationic antitrypanosomal and other antimicrobial agents in the therapy of experimental Pneumocystis carinii pneumonia. Antimicrob Agents Chemother **32:**896-905.

230. **Wang, C., J. G. Delcros, J. Biggerstaff, and O. Phanstiel, IV.** 2003. Molecular requirements for targeting the polyamine transport system. Synthesis and biological evaluation of polyamine-anthracene conjugates. J Med Chem **46:**2672-82.

231. **Wang, C., J. G. Delcros, J. Biggerstaff, and O. Phanstiel, IV.** 2003. Synthesis and biological evaluation of N1-(anthracen-9-ylmethyl)triamines as molecular recognition elements for the polyamine transporter. J Med Chem **46:**2663-71.

232. **Wang, C., J. G. Delcros, L. Cannon, F. Konate, H. Carias, J. Biggerstaff, R. A. Gardner, and O. Phanstiel, IV.** 2003. Defining the molecular requirements for the selective delivery of polyamine conjugates into cells containing active polyamine transporters. J Med Chem **46:**5129-38.

233. **Wang, J., F. Gigliotti, S. P. Bhagwat, S. B. Maggirwar, and T. W. Wright.** 2007. Pneumocystis stimulates MCP-1 production by alveolar epithelial cells through a JNK-dependent mechanism. Am J Physiol Lung Cell Mol Physiol **292:**L1495-505.

234. **Wang, S. H., C. Zhang, M. E. Lasbury, C. P. Liao, P. J. Durant, D. Tschang, and C. H. Lee.** 2008. Decreased inflammatory response in Toll-like receptor 2 knockout mice is associated with exacerbated Pneumocystis pneumonia. Microbes Infect **10:**334-41.

235. **Wang, Y., W. Devereux, T. M. Stewart, and R. A. Casero, Jr.** 1999. Cloning and characterization of human polyamine-modulated factor-1, a transcriptional cofactor that regulates the transcription of the spermidine/spermine N(1)-acetyltransferase gene. J Biol Chem **274:**22095-101.

236. **Wang, Y., S. Doucette, Q. Qian, and J. E. Kirby.** 2007. Yield of primary and repeat induced sputum testing for Pneumocystis jiroveci in human immunodeficiency virus-positive and -negative patients. Arch Pathol Lab Med **131:**1582-4.

237. **Wang, Y., L. Xiao, A. Thiagalingam, B. D. Nelkin, and R. A. Casero, Jr.** 1998. The identification of a cis-element and a trans-acting factor involved in the response to polyamines and polyamine analogues in the regulation of the human spermidine/spermine N1-acetyltransferase gene transcription. J Biol Chem **273:**34623-30.

238. **Weeks, R. S., S. M. Vanderwerf, C. L. Carlson, M. R. Burns, C. L. O'Day, F. Cai, B. H. Devens, and H. K. Webb.** 2000. Novel lysine-spermine conjugate inhibits polyamine transport and inhibits cell growth when given with DFMO. Exp Cell Res **261:**293-302.

239. **Williams, M. D., J. R. Wright, K. L. March, and W. J. Martin, 2nd.** 1996. Human surfactant protein A enhances attachment of Pneumocystis carinii to rat alveolar macrophages. Am J Respir Cell Mol Biol **14:**232-8.

240. **Wright, T. W., R. H. Notter, Z. Wang, A. G. Harmsen, and F. Gigliotti.** 2001. Pulmonary inflammation disrupts surfactant function during Pneumocystis carinii pneumonia. Infect Immun **69:**758-64.

241. **Wyder, M. A., E. M. Rasch, and E. S. Kaneshiro.** 1998. Quantitation of absolute Pneumocystis carinii nuclear DNA content. Trophic and cystic forms isolated from infected rat lungs are haploid organisms. J Eukaryot Microbiol **45:**233-9.

242. **Xie, X., R. J. Gillies, and E. W. Gerner.** 1997. Characterization of a diamine exporter in Chinese hamster ovary cells and identification of specific polyamine substrates. J Biol Chem **272:**20484-9.

243. **Xu, H., R. Chaturvedi, Y. Cheng, F. I. Bussiere, M. Asim, M. D. Yao, D. Potosky, S. J. Meltzer, J. G. Rhee, S. S. Kim, S. F. Moss, A. Hacker, Y. Wang, R. A. Casero, Jr., and K. T. Wilson.** 2004. Spermine oxidation induced by Helicobacter pylori results in apoptosis and DNA damage: implications for gastric carcinogenesis. Cancer Res **64:**8521-5.

244. **Yarlett, N., and C. J. Bacchi.** 1988. Effect of DL-alpha-difluoromethylornithine on polyamine synthesis and interconversion in Trichomonas vaginalis grown in a semi-defined medium. Mol Biochem Parasitol **31:**1-9.

245. **Yong, S. J., Z. Vuk-Pavlovic, J. E. Standing, E. C. Crouch, and A. H. Limper.** 2003. Surfactant protein D-mediated aggregation of Pneumocystis carinii impairs phagocytosis by alveolar macrophages. Infect Immun **71:**1662-71.

246. **Zavascki, A. P., A. L. Maia, and L. Z. Goldani.** 2007. Pneumocystis jiroveci thyroiditis: report of 15 cases in the literature. Mycoses **50:**443-6.

247. **Zhang, C., S. H. Wang, M. E. Lasbury, D. Tschang, C. P. Liao, P. J. Durant, and C. H. Lee.** 2006. Toll-like receptor 2 mediates alveolar macrophage response to Pneumocystis murina. Infect Immun **74:**1857-64.

248. **Zhang, C., S. H. Wang, C. P. Liao, M. E. Lasbury, P. J. Durant, D. Tschang, and C. H. Lee.** 2006. Toll-like receptor 2 knockout reduces lung inflammation during Pneumocystis pneumonia but has no effect on phagocytosis of Pneumocystis organisms by alveolar macrophages. J Eukaryot Microbiol **53 Suppl 1:**S132-3.

249. **Zhang, J., J. Zhu, X. Bu, M. Cushion, T. B. Kinane, H. Avraham, and H. Koziel.** 2005. Cdc42 and RhoB activation are required for mannose receptor-mediated phagocytosis by human alveolar macrophages. Mol Biol Cell **16:**824-34.

250. **Zhang, J., J. Zhu, A. Imrich, M. Cushion, T. B. Kinane, and H. Koziel.** 2004. Pneumocystis activates human alveolar macrophage NF-kappaB signaling through mannose receptors. Infect Immun **72:**3147-60.

251. **Zhang, M., A. I. MacDonald, M. A. Hoyt, and P. Coffino.** 2004. Proteasomes begin ornithine decarboxylase digestion at the C terminus. J Biol Chem **279:**20959-65.

252. **Zhang, M., C. M. Pickart, and P. Coffino.** 2003. Determinants of proteasome recognition of ornithine decarboxylase, a ubiquitin-independent substrate. EMBO J **22:**1488-96.

253. **Zhang, Y., A. Bell, P. S. Perlman, and M. J. Leibowitz.** 2000. Pentamidine inhibits mitochondrial intron splicing and translation in Saccharomyces cerevisiae. RNA **6:**937-51.

254. **Zhao, B., and A. P. Butler.** 2001. Core promoter involvement in the induction of rat ornithine decarboxylase by phorbol esters. Mol Carcinog **32:**92-9.

255. **Zimmerman, P. E., D. R. Voelker, F. X. McCormack, J. R. Paulsrud, and W. J. Martin, 2nd.** 1992. 120-kD surface glycoprotein of Pneumocystis carinii is a ligand for surfactant protein A. J Clin Invest **89:**143-9.

CURRICULUM VITAE

Chung-Ping Liao

Education

2004 - 2009 Ph.D., Pathology
Indiana University, Indianapolis, IN, USA

1999 - 2001 M.S., Microbiology and Immunology
National Yang-Ming University, Taipei, Taiwan

1995 - 1999 B.S., Medical Technology
Chang Gung University, Taoyuan, Taiwan

Honors

2008 Student Travel Award for X International Workshops on Opportunistic Protists

2006 Student Travel Award for International Conference on the Role of Polyamines and Their Analogs in Cancer and Other Diseases

2004 Graduate Fellowship of Indiana University

Professional Experience

2005 - 2009 Teaching Assistant
Molecular Biology Workshop, Indiana University

2001 - 2004 Research Assistant
Department of Pediatrics, Taipei Veterans General Hospital, Taiwan

Conference Abstracts

2008 **Liao, C. P.**, M. E. Lasbury, S. H. Wang, C. Zhang, P. J. Durant, and C. H. Lee. Antizyme Inhibitor Mediates Increased Polyamine Uptake in Alveolar Macrophages during *Pneumocystis* Pneumonia. Boston, MA.

2006 **Liao, C. P.**, M. E. Lasbury, P. J. Durant, S Merali, and C. H. Lee. Polyamines and Apoptosis of Alveolar Macrophages during *Pneumocystis* Pneumonia. Rome, Italy.

Conference Presentation

2008 Polyamines and Apoptosis of Alveolar Macrophages during *Pneumocystis* Pneumonia. Rome, Italy.

Publications

1. **Liao, C. P.**, M. E. Lasbury, S. H. Wang, C. Zhang, P. J. Durant, Y. Murakami, S. Matsufuji, and C. H. Lee. 2009. *Pneumocystis* mediates overexpression of antizyme inhibitor resulting in increased polyamine levels and apoptosis in alveolar macrophages. *J Biol Chem 284:8174-8184.*

2. Lasbury, M. E., P. J. Durant, **C. P. Liao**, and C. H. Lee. 2009. Effects of decreased calmodulin protein on the survival mechanisms of alveolar macrophages during *Pneumocystis* pneumonia. *Infect Immun 77:3344-3354.*

3. Wang, S. H., C. Zhang, M. E. Lasbury, **C. P. Liao**, P. J. Durant, D. Tschang, and C. H. Lee. 2008. Decreased inflammatory response in Toll-like receptor 2 knockout mice is associated with exacerbated *Pneumocystis* pneumonia. *Microbes Infect 10:334-341*.

4. **Liao, C. P.**, M. E. Lasbury, S. H. Wang, C. Zhang, P. J. Durant, D. Tschang, and C. H. Lee. 2006. Inflammatory cells are sources of polyamines that induce alveolar macrophage to undergo apoptosis during *Pneumocystis* pneumonia. *J Eukaryot Microbiol 53 Suppl 1:S134-135.*

5. Zhang, C., S. H. Wang, **C. P. Liao**, M. E. Lasbury, P. J. Durant, D. Tschang, and C. H. Lee. 2006. Toll-like receptor 2 knockout reduces lung inflammation during *Pneumocystis* pneumonia but has no effect on phagocytosis of *Pneumocystis* organisms by alveolar macrophages. *J Eukaryot Microbiol 53 Suppl 1:S132-133.*

6. Wang, S. H., C. Zhang, **C. P. Liao**, M. E. Lasbury, P. J. Durant, D. Tschang, and C. H. Lee. 2006. Syndecan-1 expression in the lung during *Pneumocystis* infection. *J Eukaryot Microbiol 53 Suppl 1:S122-123.*

7. Lasbury, M. E., S. H. Wang, C. Zhang, **C. P. Liao**, P. J. Durant, D. Tschang, and C. H. Lee. 2006. Caspase-9 as a target for *Pneumocystis* pneumonia therapy. *J Eukaryot Microbiol 53 Suppl 1:S138-139.*

8. Zhang, C., S. H. Wang, M. E. Lasbury, D. Tschang, **C. P. Liao**, P. J. Durant, and C. H. Lee. 2006. Toll-like receptor 2 mediates alveolar macrophage response to *Pneumocystis* murina. *Infect Immun 74:1857-1864.*

9. Lasbury, M. E., P. J. Durant, S. H. Wang, C. Zhang, **C. P. Liao**, D. Tschang, and C. H. Lee. 2006. Alterations in surfactant protein A form and clearance during *Pneumocystis* pneumonia. *J Eukaryot Microbiol 53 Suppl 1:S119-121*.

10. Lasbury, M. E., P. J. Durant, S. H. Wang, C. Zhang, **C. P. Liao**, D. Tschang, and C. H. Lee. 2006. GM-CSF expression in the lung during *Pneumocystis* pneumonia. *J Eukaryot Microbiol 53 Suppl 1:S124-126.*

11. Lasbury, M. E., C. A. Ray, P. J. Durant, S. H. Wang, C. Zhang, **C. P. Liao**, D. Tschang, and C. H. Lee. 2006. Survival pathway signal transduction is reduced in alveolar macrophages during *Pneumocystis* pneumonia. *J Eukaryot Microbiol 53 Suppl 1:S130-131*.

12. Lasbury, M. E., P. J. Durant, D. Tschang, S. H. Wang, C. Zhang, **C. P. Liao**, and C. H. Lee. 2006. Expression and activation of complement protein and alveolar damage during *Pneumocystis* pneumonia. *J Eukaryot Microbiol 53 Suppl 1:S136-137.*

13. Ray, C. A., M. E. Lasbury, P. J. Durant, S. H. Wang, C. Zhang, **C. P. Liao**, D. Tschang, and C. H. Lee. 2006. Transforming growth factor-beta activation and signaling in the alveolar environment during *Pneumocystis* pneumonia. *J Eukaryot Microbiol 53 Suppl 1:S127-129.*

14. **Liao, C. P.**, and W. J. Syu. 2002. Analysis of the baseplate region of phage AR1 that specifically infects *Escherichia coli* O157:H7. *J Microbiol Immunol Infect 35:269-271*.